Complex Exponential Dynamics

Robert L. Devaney *
Boston University

August 9, 2006

*Please address all correspondence to Robert L. Devaney, Department of Mathematics, Boston University, 111 Cummington Street, Boston MA 02215, or e-mail bob@bu.edu.

1 Introduction

Our goal in this paper is give a somewhat quirky introduction to the field of complex dynamics. Usually, in the many introductions to this field that have appeared in the past twenty years or so, the main emphasis is on polynomial (in fact, quadratic polynomial) or rational dynamics. In this paper, we will take a slightly different tack; while we will of course discuss the polynomial case (and, yes, the Mandelbrot set), our main emphasis will be on entire functions and, most often, the complex exponential function.

There are several reasons for taking this approach. First, as mentioned above, there are many other papers and books where the emphasis is on polynomials ([Bea], [Bl], [CG], [McM], [Mil], [Ste]). Second, the dynamics of entire functions has experienced a tremendous surge of interest in recent years. And third, there are many very interesting connections between transcendental dynamics and planar topology. Indeed, one of our main subthemes in this paper is to highlight many of the very interesting types of sets from a topological point of view that arise as the Julia sets of entire functions.

In this paper, we asume that the reader is familiar with the basic ideas of discrete dynamical systems, general topology, and complex analysis. We will then use these fields as the foundation for our discussion of complex dynamics. This paper should be readable by people who have a background in discrete dynamics. Readers familiar with the basic ideas of complex dynamics dealing with polynomials or rational functions should also get something out of this paper, as we shall empahsize many of the topics that are differnt when entire functions are considered.

We will not provide all of the proofs: these can be found in the books cited above or in the research literature. We will, however, provide at least one proof in each section (or, at least, a somewhat detailed sketch), just to give the reader a sampling of how things are worked out in complex dynamics as well as the interplay between the background fields.

It is a pleasure to thank Ki$\ell\ell$er Devaney, who digested this entire article and returned many highly stylized comments; all errors that remain are due to her.

2 Basic Notions

Our goal in this section is to introduce some of the basic definitions and tools used in complex dynamics. These are drawn from the fields of discrete dynamical systems theory and complex analysis. In later sections we will specialize the discussion to entire transcendental functions.

2.1 Preliminaries from Dynamics

Suppose that $F : \mathbb{C} \to \mathbb{C}$ is complex analytic. As in discrete dynamics, we are interested in the dynamics of F, so we are concerned with iteration of F. Given $z_0 \in \mathbb{C}$, the *orbit of* z_0 is the sequence

$$z_0,\ F(z_0),\ F(F(z_0)), \ldots$$

For simplicity, we write F^n for the n-fold composition of F with itself. Then the main question in dynamics is: can we predict the fate of orbits. That is, what happens to the sequence $\{F^n(z_0)\}$ as n tends to ∞?

There are many different types of orbits for a typical function. Perhaps the most important are the *fixed points* z_0 for which $F(z_0) = z_0$. Next in importance are the *periodic points of period* n (also called cycles of period n or n-cycles): they are points that satisfy $F^n(z_0) = z_0$. The *period* of the cycle is the least $n \geq 1$ for which $F^n(z_0) = z_0$. The point z_0 is an eventual fixed point (or cycle) if z_0 is not itself fixed (or periodic), but $F^n(z_0)$ is fixed (or periodic) for some $n \geq 1$. Other important orbits are those that tend to a fixed point or periodic orbit, or those that tend to ∞.

Example. Let $D(z) = z^2$. The orbits of 0 and 1 are fixed. The orbits of -1 and $\pm i$ are eventually fixed since these orbits land on the fixed point at 1 after several iterations. If $|z_0| > 1$, then $D^n(z_0) \to \infty$ as $n \to \infty$. If $|z_0| < 1$ then $D^n(z_0) \to 0$ as $n \to \infty$. The points $z_1 = e^{2\pi i/3}$ and $z_2 = e^{4\pi/3}$ lie on a cycle of period 2 for D. In fact, $e^{2\pi i(p/q)}$ is periodic if both p and q are integers with q odd. If z_0 lies on the unit circle, then the entire orbit of z_0 remains on this circle.

Example. Let $E(z) = (1/e)e^z$. We have $E(1) = 1$ and $E'(1) = 1$. If $x \in \mathbb{R}$ and $x < 1$, then $E^n(x_0)$ tends to the fixed point at 1. If $x_0 > 1$, then $E^n(x_0) \to \infty$ as $n \to \infty$. This can be shown using the web diagram as shown in Figure 1.

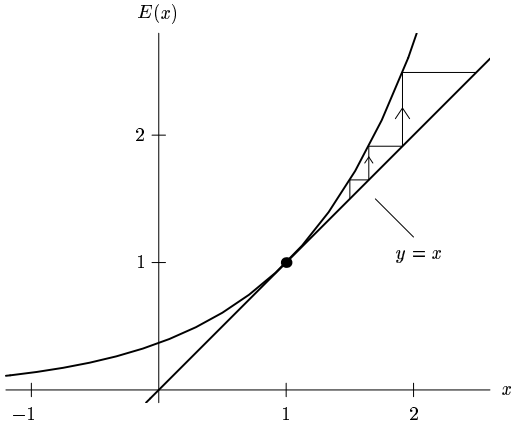

Figure 1: The graph of $E(x) = (1/e)e^x$.

Example. Let $S(z) = \sin z$. Then 0 is a fixed point for S. If $x_0 \in \mathbb{R}$, then either $S(x_0) = 0$ (so the orbit is eventually fixed), or $S^n(x_0) \to 0$. On the other hand, points on the imaginary axis have orbits that tend to ∞ since $\sin(iy) = i \sinh(y)$.

Example. Let $C(z) = \cos z$. Then C has a real fixed point at $x_0 = 0.7390\ldots$ and the orbit of any $x \in \mathbb{R}$ either lands on or tends to x_0.

2.2 Types of fixed or periodic points

In this section we will assume that z_0 is a fixed point for F. If z_0 lies on an n-cycle, then everything below goes through using F^n instead of F.

Definition 2.1 *The fixed point z_0 is:*

1. *attracting if $0 < |F'(z_0)| < 1$;*
2. *superattracting if $F'(z_0) = 0$;*
3. *repelling if $|F'(z_0)| > 1$;*
4. *neutral or indifferent if $F'(z_0) = e^{2\pi i\theta_0}$. If θ_0 is rational, then z_0 is rationally indifferent or parabolic, otherwise z_0 is irrationally indifferent.*

Note that there are no fixed points of saddle type for complex functions as we have just one "eigenvalue" for the derivative, namely $F'(z_0)$, not two distinct eigenvalues.

The dynamical behavior of F near attracting, repelling or superattracting fixed points is completely understood, as we discuss below. In the neutral case, the behavior near certain irrationally indifferent fixed points is still not completely understood.

Suppose F and G are two analytic functions. We say that F is (analytically) conjugate to G if there is an (analytic) homeomorphism $h : \mathbb{C} \to \mathbb{C}$ such that $h \circ F = G \circ h$. We also define local conjugacy on subsets of $\mathbb{C}$ in the natural manner.

The reason why analytic functions are easy to understand near attracting fixed points is given by the following theorem.

Theorem 2.2 Linearization Theorem. *Suppose z_0 is an attracting fixed point for F and $F'(z_0) = \lambda$ with $0 < |\lambda| < 1$. Then there is a neighborhood U of z_0 and an analytic map $h : U \to \{z \,|\, |z| < 1\}$ such that $h \circ F(z) = \lambda \cdot h(z)$. That is, F is analytically conjugate to the linear map $z \to \lambda z$ on U.*

In the repelling case, we use the Inverse Function Theorem to conjugate the branch of the inverse of F that fixes z_0 to a linear map of the form $z \to \lambda^{-1} z$ with $|\lambda| > 1$. Then F is locally conjugate to $z \to \lambda z$.

Finally, if z_0 is superattracting, then there is a neighborhood U of z_0 and $n > 1$ such that F is analytically conjugate to $z \to z^n$ on U, where h takes values in some disk $\{z \,|\, |z| < r < 1\}$.

As we mentioned above, the dynamics near neutral fixed points is extremely complicated, and we will not go into details here. But there are two cases that are completely understood. The first is the case of a rationally indifferent fixed point. In this case the Fatou Flower Theorem [Mil] asserts that, for some $k > 0$, there are k attracting and k repelling petals meeting at z_0. Roughly speaking, an attracting petal is an open set U bounded by a simple closed curve γ passing through z_0 that has the property that

1. $F(\overline{U}) \subset U \cup \{z_0\}$
2. $F(\gamma) \cap \gamma = \{z_0\}$

It can be shown that all orbits within U tend to z_0 under iteration.

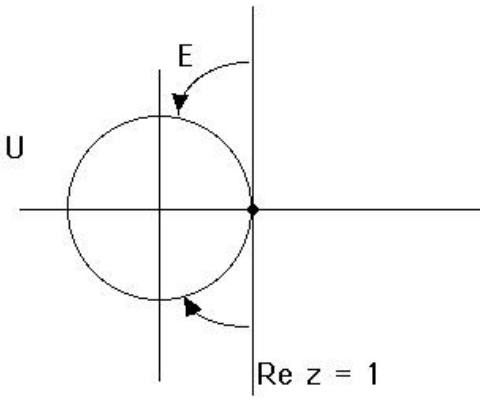

Figure 2: The plane $\operatorname{Re} z \leq 1$ is an attracting petal for $E(z) = (1/e)e^z$.

Example. Let $E(z) = (1/e)e^z$. Then $z_0 = 1$ is a neutral fixed point with $E'(z_0) = 1$. Consider the vertical line segment $\operatorname{Re} z = 1$. Let $U = \{z \mid \operatorname{Re} z < 1\}$. Then U is an attracting petal for E (not worrying too much about the fact that the boundary of U is not a closed curve, though it is if we consider the Riemann sphere). Indeed, E maps U to the interior of the unit circle in $\mathbb{C}$ and so $E(\overline{U})$ meets $\operatorname{Re} z = 1$ only at $z_0 = 1$. Thus it follows that all orbits of E in the half plane $\operatorname{Re} z < 1$ tend to 1 under iteration. See Figure 2.

A repelling petal is simply an attracting petal for F^{-1}, which exists locally near z_0 since $F'(z_0) \neq 0$. In the above example, the preimage of the circle of radius 1 centered at $x = 2$ on the real axis (under the branch of the inverse of E that fixes $z_0 = 1$) and its interior form a repelling petal. Note that any orbit in the repelling petal must eventually leave the petal (except, of course, the neutral fixed point). See Figure 3.

Example. Let $S(z) = \sin z$. Then 0 is a rationally indifferent fixed point. There are now two attracting petals, both straddling the real axis. Orbits on the imaginary axis leave a neighborhood of 0. Indeed, on the imaginary axis, as we saw earlier, we have $\sin(iy) = i \sinh(y)$, so orbits tend to ∞ along this axis. See Figure 4.

Now suppose that z_0 is an irrationally indifferent fixed point with $F'(z_0) = e^{2\pi i \theta_0}$. We will deal only with the case that θ_0 is a Brjuno number. To define these irrationals, we make a brief digression to consider continued fractions.

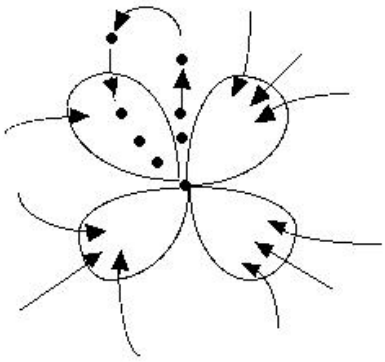

Figure 3: Four Fatou flowers for a rationally indifferent fixed point.

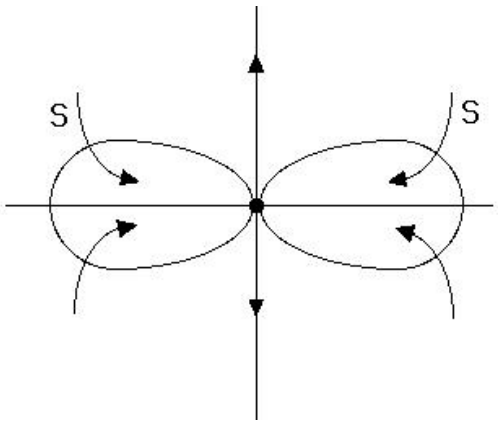

Figure 4: There are two attracting petals $\mathcal{S}$ for $\sin z$ and two repelling directions.

Since θ_0 is irrational, it has an infinite continued fraction expansion of the form

$$\theta_0 = a_0 + \cfrac{1}{a_1 + \cfrac{1}{a_2 + \cfrac{1}{\ddots}}}$$

where each a_j is a positive integer (and a_0 may be 0). The convergents of θ_0 are defined to be the rational numbers

$$\frac{p_n}{q_n} = a_0 + \cfrac{1}{a_1 + \cfrac{1}{\ddots + a_n}}$$

It is known that the convergents of θ_0 are the closest rational approximants of θ_0 (in the sense that there are no rationals p/q between θ_0 and p_n/q_n with $q < q_n$).

The rational number θ_0 is said to be a *Brjuno number* if the series

$$\sum_{n=1}^{\infty} \frac{\log(q_{n+1})}{q_n}$$

converges. For example, all diophantine numbers are Brjuno, so the Brjunos are dense in the reals. Recall that θ is diophantine if θ is "far" from rationals in the sense that there are constants $c > 0, k \geq 2$ such that

$$\left|\theta - \frac{p}{q}\right| > \frac{c}{q^k}$$

for all rationals p/q. Unfortunately for dynamical systems, the complement of the Brjunos in the irrationals is also dense. The Brjuno numbers form a set of full measure however.

The natural question is when is a nonlinear function conjugate to an irrational rotation. As stated, this question clearly cannot depend on the rotation angle θ_0, as we can always conjugate the irrational rotation $z \to e^{2\pi i\theta_0}z$ by an analytic function to obtain a nonlinear function that acts like an irrational rotation. So the question is: are there any irrationals θ_0 for which every nonlinear function of the form

$$z \to e^{2\pi i\theta_0}z + a_2z^2 + \dots$$

for a given θ is conjugate to an irrational rotation? The following theorem answers this question.

Theorem 2.3 Yoccoz' Theorem. *The function* $z \to e^{2\pi i\theta}z + a_2z^2 + \ldots$ *is locally conjugate to* $z \to e^{2\pi i\theta}z$ *(independent of any higher order terms) if* θ *is a Brjuno number. If* θ *is not a Brjuno number, then the quadratic polynomial*

$$z \mapsto e^{2\pi i\theta}z + z^2$$

has a fixed point at the origin which is not linearizable.

Suppose $F'(z_0) = e^{2\pi i\theta_0}$ where θ_0 is Brjuno. By Yoccoz' Theorem, there is a neighborhood U of z_0 such that each orbit in $U - \{z_0\}$ is dense on an invariant simple closed curve surrounding z_0. The maximal simply connected open set about z_0 with this property is called a Siegel disk after C. L. Siegel who first proved that maps of the form

$$z \to e^{2\pi i\theta}z + a_2z^2 + \ldots$$

are linearizable if θ is diophantine.

2.3 Preliminaries from Complex Analysis

The main reason that one dimensional complex analytic dynamics is so special is that all of the tools of complex analysis are available. In this section we review some of the most basic results from this field that we will use over and over again.

One of the most important tools is the:

Theorem 2.4 Riemann Mapping Theorem. *Let* U *be an open, simply connected subset of* $\mathbb{C}$ *and suppose that* U *is not equal to* $\mathbb{C}$ *itself. Let* $z_0 \in U$. *Then there is an analytic map* ϕ *taking* U *onto the unit disk* $\mathbb{D}$ *in one-to-one fashion and satisfying* $\phi(z_0) = 0$. *Moreover, if we normalize so that* $\phi'(z_0) > 0$, *then the map* ϕ *is unique.*

The importance of this result is that, whenever we encounter some dynamical behavior on an open simply connected set, we may transfer the dynamics to the unit disk $\mathbb{D}$ via the Riemann map ϕ. Many of the important theorems in complex analysis are stated in terms of maps of the disk. A principal example of this is the:

Theorem 2.5 Schwarz Lemma. *Suppose* $F : \mathbb{D} \to \mathbb{D}$ *is analytic and* $F(0) = 0$. *Then* $|F'(0)| \leq 1$ *and, moreover, either* $|F(z)| < |z|$ *for all* $z \neq 0$, *or else* $F(z) = e^{i\theta} \cdot z$ *for some* $\theta \in \mathbb{R}$.

Note that, if F is not a rotation, the condition $|F(z)| < |z|$ guarantees that all points in $\mathbb{D}$ move closer to 0 at each application of F and so all orbits in $\mathbb{D}$ tend to 0 under iteration of F. Therefore the importance of this result is the fact that either $F : \mathbb{D} \to \mathbb{D}$ is either a rotation, or else all orbits in $\mathbb{D}$ tend to the fixed point at 0.

We will often invoke the following modification of this result.

Corollary 2.6 *Suppose U is a simply connected open set not equal to $\mathbb{C}$ itself. Suppose further that $F(\overline{U}) \subset U$. Then F has a fixed point in U and, moreover, all orbits of F tend to this fixed point.*

This is true since there is a fixed point in U by the Brouwer Fixed Point Theorem. Then we can conjugate F to a map of the disk via the Riemann map ϕ, and we may assume that the fixed point is sent to 0. Since the map $\phi \circ F \circ \phi^{-1}$ is analytic on $\mathbb{D}$ and fixes 0, the Schwarz Lemma applies. Since $F(\overline{U}) \subset U$, it follows that $\phi \circ F \circ \phi^{-1}$ cannot be a rotation, and so F must have a globally attracting fixed point.

This is one of the principal differences between real and complex dynamics. In real dynamics we can have all sorts of dynamics inside a simply connected region. For example, the classical horseshoe map may be defined inside a simply connected region. For complex maps however, this is never the case. We may only have a globally attracting fixed point or a rotation domain in such a region. This is one of the reasons that complex dynamical systems are so well understood.

There is another way to view this. On $\mathbb{D}$, there is a very special metric called the *Poincaré metric*. If $F : \mathbb{D} \to \mathbb{D}$ is analytic, then it turns out that either F is a strict contraction in the Poincaré metric, or else F is an isometry. This is often referred to as the Schwarz-Pick Lemma. Thus, by the Riemann Mapping Theorem, we can transfer the Poincaré metric to any simply connected domain in (but not equal to all of) $\mathbb{C}$.

Perhaps the most important types of orbits are those that lie in the *Julia set* which is named for the French mathematician Gaston Julia who first studied these orbits around 1918. To define the Julia set, we need to make a digression into the theory of normal families of functions. Let $\{G_i\}$ be a family of analytic functions in $\mathbb{C}$. Often, but not always, the G_i will be the iterates of a given function.

Definition 2.7 *The family of functions $\{G_i\}$ is a normal family on an open set $U \subset \mathbb{C}$ if every sequence of the G_i's has a subsequence that either*

1. *converges uniformly on compact subsets of U, or*

2. *converges uniformly to ∞ on compact subsets of U.*

Recall that, in case 1, the subsequence converges to a function on U that necessarily is analytic. By the Arzela-Ascoli theorem, the G_i form a normal family on U if the G_i are equicontinuous (in the spherical metric) on compact subsets of U. Another main tool from complex analysis is:

Theorem 2.8 Montel's Theorem. *Suppose the $\{G_i\}$ are a family of analytic functions on $\mathbb{C}$ and that there are two distinct values z_1 and z_2 in $\mathbb{C}$ that are never assumed by the G_i. Then $\{G_i\}$ is a normal family of functions.*

Example. Let $D(z) = z^2$. Then the family of iterates of D, $\{D^n\}$ is

1. normal on any open subset of $\{z \,|\, |z| < 1\}$;

2. normal on any open subset of $\{z \,|\, |z| > 1\}$;

3. not normal on any open set that intersects the unit circle.

Indeed, in case 1, the D^n converge uniformly on compact subsets to 0. In case 2, the D^n converge uniformly on compact subsets to ∞. But in case 3, there are open sets in U on which the D^n converge either to 0 or to ∞, and hence this sequence does not converge to an analytic function.

Definition 2.9 *A function $E : \mathbb{C} \to \mathbb{C}$ is entire if $E(z) \neq \infty$ for any $z \in \mathbb{C}$ and E is not a polynomial. Sometimes such functions are called entire transcendental functions.*

Our main goal in this paper is to study the dynamics of entire functions, but we will occasionally deal with polynomials in order to contrast these two cases. With the exception of Section 10, we will not treat meromorphic functions, i.e., functions with poles.

One of the main differences between polynomials and entire functions is the behavior at ∞. For a polynomial P, we may extend P to the entire Riemann sphere by defining $P(\infty) = \infty$. We have $P'(\infty) = 0$, so that ∞ is a superattracting fixed point. This can be seen by conjugating P via $\phi(z) = 1/z$. The fixed point at ∞ is sent to 0 and then one calculates that $(\phi \circ P \circ \phi^{-1})'(0) = 0$.

For an entire function E, we cannot extend E to ∞ continuously, never mind analytically. Indeed, the behavior of E near ∞ is quite complicated. This is illustrated by the:

Theorem 2.10 Great Picard Theorem. *In any neighborhood of ∞ an entire function assumes all values in $\mathbb{C}$ infinitely often with the possible exception of one value.*

Example. Let $E(z) = e^z$. A neighborhood of ∞ contains a region of the form $\{z| \ |z| > r\}$ for some r. This region contains infinitely many strips of the form $k\pi \leq \text{Im } z < (k+2)\pi$, and each of these strips is mapped in one-to-one fashion onto $\mathbb{C} - \{0\}$.

For the record, ∞ is called an *essential singularity* of the entire function.

2.4 Role of the Singular Values

For entire functions, there are two types of *singular values* that play an important role in determining the dynamics. These are the critical and asymptotic values. A *critical value* is an image of a critical point, i.e., $F(z_0)$ where $F'(z_0) = 0$.

Definition 2.11 *The point $z_0 \in \mathbb{C}$ is an asymptotic value of E if there is a curve $\gamma(t)$ satisfying $\lim_{t\to\infty} \gamma(t) = \infty$ and $\lim_{t\to\infty} E(\gamma(t)) = z_0$.*

Example. The omitted value 0 is an asymptotic value for $E_\lambda(z) = \lambda e^z$ since any curve $\gamma(t)$ that satisfies $\lim_{t\to\infty}$ Re $(\gamma(t)) = -\infty$ also satisfies $\lim_{t\to\infty} E(\gamma(t)) = 0$. Also, the point at ∞ is also an asymptotic value.

One of the main reasons that singular values are important is the fact that any attracting fixed point must have a singular value in its immediate basin of attraction; indeed, this is one of the major features that distinguishes complex dynamics from other branches of discrete dynamical systems. The *basin of attraction* of z_0 is the set of all points whose orbit tends to z_0. The *immediate* basin of attraction of z_0 is the component of the basin that contains z_0. Basins of attraction for attracting n-cycles are defined using F^n instead of F.

Theorem 2.12 Role of the Singular Values Theorem. *Suppose the analytic function F has an attracting fixed point or cycle. Then there is at least one singular value in the immediate basin of attraction of this point.*

Proof. To see why the immediate basin of the fixed point z_0 contains a singular value, we argue by contradiction. We may assume that $F'(z_0) \neq 0$ for otherwise we are done. Let U_0 be a bounded neighborhood of z_0 contained in the immediate basin of z_0 and satisfying $F(U_0) \subset U_0$. We can find such a U_0 using the linearization result for attracting fixed points.

We may assume also that F is one-to-one on U_0. Now we pull back by a branch of F^{-1}: let U_1 be the preimage of U_0 that contains U_0. Now if U_1 is unbounded, we may find a curve $\gamma(t) \subset U_1$ with $\gamma(t) \to \infty$ as $t \to \infty$ and $F(\gamma(t))$ approaching a limit in U_0. This yields an asymptotic value in U_0, so it follows that U_1 must be bounded. Also, $F \,|\, U_1$ must be one-to-one for otherwise there would be a critical point in U_1 and therefore a critical value in U_0.

Continuing in this fashion we construct $U_{n+1} \supset U_n$ for each $n \geq 1$ with U_{n+1} bounded and $F : U_{n+1} \to U_n$. Let W be the union of the U_n. W is an open set in $\mathbb{C}$ and we have $F : W \to W$ is one-to-one. Hence $F^{-1} : W \to W$ is well-defined and analytic.

Now $W \neq \mathbb{C}$ for otherwise F would be a Möbius transformation and hence not entire. Also, there are (many more than) two points not in W, since the other preimages of U_0 do not lie in W. As a consequence, the family of functions $\{F^{-n}\}$ is a normal family on W. Therefore the F^{-n} has a subsequence that converges to an analytic function on W. But each F^{-n} fixes z_0 whereas $F^{-n}(z)$ tends to the boundary of W as $n \to \infty$. As a consequence, the limit function is not even continuous. This contradiction establishes the result.

□

Corollary 2.13 *Suppose F has at most n singular values. Then F can have at most n attracting cycles.*

Example. The exponential function $E_\lambda(z) = \lambda e^z$ has no critical values and only one asymptotic value, 0. Hence E_λ can have at most one attracting cycle. If $0 < \lambda < 1/e$, the graph of E_λ lies below that of $E_{1/e}$, and so E_λ has a real attracting fixed point. Figure 5 shows that 0 is attracted to this attracting fixed point.

Example. The sine family $S_\lambda(z) = \lambda \sin z$ has no asymptotic values and infinitely many critical points but only 2 critical values, $\pm\lambda$. When $|\lambda| < 1$ the origin is an attracting fixed point which must attract one critical value. Since S_λ is odd, in fact 0 attracts both critical values, and so for these λ-values, 0 is the only attracting cycle.

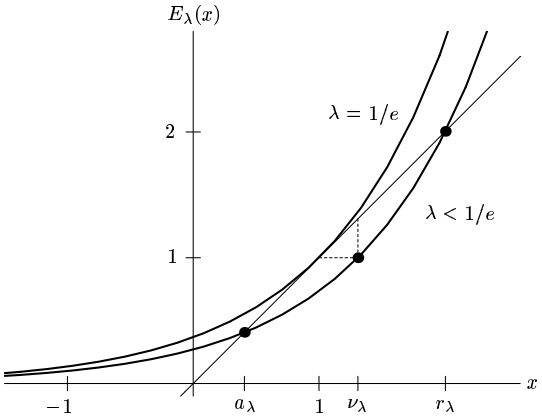

Figure 5: The graphs of E_λ for $\lambda = 1/e$ and $\lambda < 1/e$.

2.5 The Julia Set

The most important orbits in a complex dynamical system lie in the *Julia set*, named for Gaston Julia, who initiated the study of these sets in 1918.

Definition 2.14 *Let $F : \mathbb{C} \to \mathbb{C}$ be complex analytic. The Julia set of F, denoted $J(F)$, is the set of points at which the family of iterates $\{F^n\}$ fails to be a normal family.*

Points in $J(F)$ have orbits that are sensitive to initial conditions. If $z \in J(F)$ and U is any neighborhood of z, then by Montel's Theorem, $\cup F^n(U)$ contains all points in $\mathbb{C}$, with at most one exception. We think of this as meaning that the Julia set is the chaotic regime for F, because orbits here are extremely sensitive to initial conditions.

Example. For $D(z) = z^2$, $J(D)$ is the unit circle. If U is a neighborhood of z with $|z| = 1$, then we may always find a smaller neighborhood U' of U satisfying

$$U' = \{z \,|\, \theta_1 < \text{Arg} z < \theta_2, 0 < r_1 < |z| < r_2\}$$

It is then easy to see that $\bigcup D^n(U')$ covers $\mathbb{C} - \{0\}$.

Note that repelling cycles always lie in the Julia set. To see this suppose that $F^n(z_0) = z_0$ and $|(F^n)'(z_0)| = \lambda > 1$. Then the sequence of analytic

functions F^{kn} cannot converge to ∞ in any neighborhood of z_0 since each F^{kn} fixes z_0. Also, F^{kn} cannot converge to an analytic function on any neighborhood of z_0 since $|(F^{kn})'(z_0)| = \lambda^{kn} \to \infty$ as $k \to \infty$. So any limit function would be nondifferentiable at z_0.

Rationally indifferent periodic points also lie in the Julia set. Inside the attracting petals, iterates of the map tend toward the cycle, but in the repelling petals orbits move away. Hence we cannot have uniform convergence of iterates in any neighborhood of the periodic point.

Example. The fixed point $z_0 = 1$ for $E(z) = (1/e)e^z$ is neutral with $E'(z_0) = 1$. The web diagram shows that if $x < 1$, the orbit of x tends to 1, but if $x > 1$, the orbit tends to ∞. Hence $1 \in J(E)$. See Figure 1.

Example. The fixed point 0 for $S(z) = \sin z$ also satisfies $S'(0) = 1$. Orbits on the real axis tend to 0 (or are eventually fixed at 0), but nonzero orbits on the imaginary axis tend to ∞. Again, we cannot have uniform convergence in any neighborhood of 0.

Theorem 2.15 Properties of the Julia Set. *The Julia set is*

1. *closed;*
2. *nonempty;*
3. *forward invariant (i.e., if $z \in J(F)$, then $F(z) \in J(F)$);*
4. *backward invariant;*
5. *equal to the closure of the set of repelling cycles of F.*

The fact that $J(F)$ is nonempty is surprisingly not so easy to show, at least as far as I am aware. Properties 1, 3, and 4 are straightforward exercises. Property 5 gives a more dynamical definition of the Julia set, so let's prove this part. We will prove this under the simplifying assumption that F has a repelling periodic point. Every example considered in this paper has such a point, and indeed every analytic function has infinitely many such points.

Proof: By definition, the family of functions $\{F^n\}$ is not normal at any point in $J(F)$. So we will show that there is a repelling periodic point in any neighborhood of a point where $\{F^n\}$ fails to be normal. Toward that end,

suppose $\{F^n\}$ is not normal at p and let W be a neighborhood of p. We will produce a repelling periodic point in W.

Under our assumption, there exists a repelling periodic point z_0 somewhere. We may assume that z_0 is a fixed point for F. Using the linearization around this fixed point, there is a neighborhood U_0 of z_0 such that $F : U_0 \to \mathbb{C}$ is a diffeomorphism onto its image which we may assume contains U_0. Hence F^{-1} is well-defined on U_0 and maps U_0 inside itself. Let $U_i = F^{-i}(U_0)$ and note that $U_{i+1} \subset U_i$ and $\cap U_i = \{z_0\}$.

Since $\{F^n\}$ is not normal at p, there is a point $z_1 \in W$ and an integer n such that $F^n(z_1) = z_0$[1]. Similarly, since $\{F^n\}$ is not normal at z_0, there is a point $z_2 \in U_0$ and an integer m such that $F^m(z_2) = z_1$. Hence $F^{m+n}(z_2) = z_0$.

We now make the simplifying assumption that $(F^{m+n})'(z_2) \neq 0$. If z_2 is a critical point for F^{m+n}, then some modifications to the following argument are necessary. We leave these details to the reader. Since $(F^{m+n})'(z_2) \neq 0$, there is a neighborhood V of z_2 which is contained in U_0 and that is mapped diffeomorphically onto a neighborhood of z_0 by F^{m+n}. By adjusting V, we may assume that $F^m(V) \subset W$ and that F^{m+n} maps V diffeomorphically onto U_j for some j. It follows that F^{m+n+j} is a diffeomorphism mapping V onto U_0. Consequently, this map has an inverse which contracts U_0 onto V. There is a fixed point for F^{m+n+j} in V which, by the Schwarz lemma, must be repelling. The orbit of this repelling periodic point enters W, since $F^m(V) \subset W$. This completes the proof.

□

One of the most interesting topological facts about Julia sets is the following:

Proposition 2.16 *Either the Julia set of F is nowhere dense in the plane, or else $J(F) = \mathbb{C}$.*

Indeed, if $J(F)$ contains an open set U, then $\cup F^n(U)$ covers the whole plane (except at most one point) and, by forward invariance, this set is contained in J. We can exclude that nasty "except one point" too since $J(F)$ is closed.

As a remark, if F is a polynomial, then $J(F)$ can never be the entire plane since all orbits in a neighborhood of ∞ tend to ∞ (so $\{F^n\}$ is normal there). But we will see that there are many examples of entire functions for

[1] z_0 cannot be the "exceptional point" (that is, the point not hit by F) since it is easy to see that such a point has no preimages and so is a superattracting fixed point.

which $J = \mathbb{C}$. Indeed, one of the most interesting aspects of entire dynamics is the abrupt transition from nowhere dense Julia sets to Julia sets that are the whole plane.

2.6 The Fatou Set

The complement of the Julia set is called the *Fatou set* (or *stable set*). Attracting cycles and their basins of attraction always lie in the Fatou set since iterates here tend to the cycle and thus form a normal family.

If z_0 is a fixed point (or cycle) for which we have a Siegel disk, then z_0 (and any point in the rotation domain) also lies in the Fatou set. To see this, recall that F^n is conjugate in a neighborhood U of z_0 to $z \to e^{2\pi i n\theta_0}$ for some irrational θ_0. A subsequence F^{n_i} is then conjugate in U to irrational rotation by $2\pi n_i\theta_0$. We think of $2\pi n_i\theta_0$ as a sequence of points on the unit circle. As such, this sequence must have a limit point. Then the corresponding F^n tend to a map that is conjugate to rotation by this limiting angle.

Another type of region that lies in the Fatou set is a wandering domain. This set is a component of the Fatou set that is never periodic or eventually periodic, that is, this domain wanders forever.

Example. Let $G_\lambda(z) = z + \lambda \sin z$ where λ is chosen as follows. The real graph of $G_\lambda(x)$ has infinitely many critical values, and we may choose λ so that there is an orbit that consists entirely of critical points and tends to ∞ as shown in Figure 6. If x_0 lies on this orbit of critical points, then we may choose a disk U about x_0 so that $G_\lambda(U) \subset U + 2\pi$. It follows that the orbit of any point in U tends to ∞. Thus U is a wandering domain provided $G_\lambda^n(U)$ lies in a different component of the Julia set for each n. This follows from the following exercise.

Exercise. The vertical lines $\operatorname{Re} z = 2k\pi$ for $z \in \mathbb{Z}$ lie in the Julia set of G_λ.

Another type or region in the Fatou set is a *Baker domain* or *domain at* ∞. This is a set that is forward invariant and in which all orbits tend to ∞.

Example. Let $H(z) = z + 2 + e^{-z}$. Then any point in the half plane $\operatorname{Re} z > 0$ has orbit tending to ∞. This is true since $z + 2$ moves z two units to the right, but adding e^{-z} moves $z + 2$ at most one unit in any direction. Hence $\operatorname{Re} H(z) > \operatorname{Re} z + 1$ for $\operatorname{Re} z > 0$. Therefore $\operatorname{Re} z > 0$ is a domain at ∞.

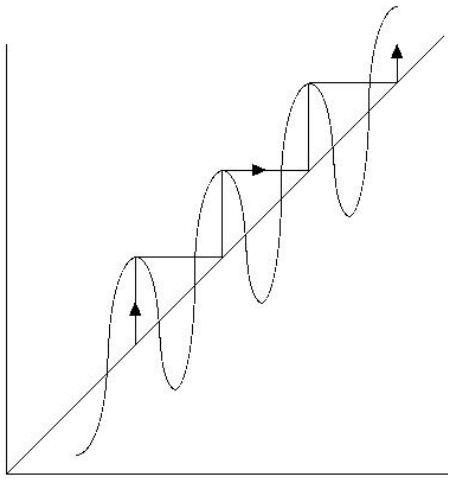

Figure 6: The graph of $G_\lambda(z) = z + \lambda \sin z$.

Note that each example of a wandering domain and Baker domain features a function with infinitely many singular values.

Finally, basins of attraction of parabolic periodic points also lie in the Fatou set. These basins consist of all points whose orbits eventually enter an attracting petal.

Example. For $E(z) = (1/e)e^z$, we have seen that the half plane Re $z < 1$ is mapped inside itself and that 1 is a neutral fixed point. Consequently, this region (and all its preimages) lies in the basin of attraction of 1.

We now describe one of the fundamental theorems in complex dynamics, the "No Wandering Domains" Theorem, due to Dennis Sullivan [Su]. The version we will use is an extension to the entire case due independently to Goldberg and Keen [GK] and Eremenko and Lyubich [EL]. This theorem really should be called the:

Theorem 2.17 Classification of Stable Domains. *Suppose E is an entire function that has only finitely many singular values. Then every component of the Fatou set is eventually periodic. Moreover, if U is a component of the Fatou set that is periodic, then U is one of the following:*

1. *the basin of attraction of an attracting or superattracting cycle;*

2. *the basin of attraction of a rationally indifferent cycle;*

3. a Siegel disk.

And that's it! There are no wandering domains, domains at infinity, or any other type of Fatou set for entire functions with finitely many singular values. Clearly, these kinds of maps deserve a name.

Definition 2.18 *An entire function that has only finitely many singular values is called critically finite.*

Luckily, everyone's favorite entire functions are critically finite. This includes the exponential (λe^z), sine ($\lambda \sin z$), and cosine ($\lambda \cos z$) families, where $\lambda \in \mathbb{C}$.

3 Quadratic Dynamics

In this chapter we present a review of some well known (and a few not-so-well-known) results involving the family of quadratic polynomials $Q_c(z) = z^2 + c$. Our primary goal is to introduce the external rays in both the dynamical and parameter planes and to show how these can be used to understand some of the complicated structures that live in these planes. We will see the "remnants" of these rays, the so-called hairs, when we look at Julia sets and parameter planes for entire functions.

3.1 The Filled Julia set

For the quadratic family, the only singular value is the critical value $c = Q_c(0)$ since 0 is the only critical point. Polynomials never have (finite) asymptotic values.

Definition 3.1 *The filled Julia set of Q_c, denoted K_c, is the set of points whose orbits are bounded.*

It is easy to check that the boundary of K_c in $\mathbb{C}$ is the Julia set $J(Q_c)$. Furthermore, ∞ is a superattracting fixed point for Q_c, so K_c is compact and we can use the linearization theorem to show that Q_c is conjugate to $Q_0(z) = z^2$ in a neighborhood of ∞. That is, we can find a closed disk U about ∞ in $\overline{\mathbb{C}}$ and an $r > 1$ together with an analytic homeomorphism

$$\phi_c : U \to \{z \,|\, |z| \geq r\}$$

such that $\phi_c \circ Q_c = (\phi_c(z))^2$.

Now suppose that the orbit of 0 under Q_c is bounded. Then we can extend the conjugacy ϕ_c to the entire exterior of K_c. Here is how to do this. Each point in U has exactly two preimages in $Q_c^{-1}(U)$. Similarly, each point in $\{z \,|\, |z| > r\}$ has exactly two preimages under z^2 (in $\{z \,|\, |z| \geq \sqrt{r}\}$). Using continuity, we can extend ϕ_c analytically to $Q_c^{-1}(U)$ in a unique fashion. The only impediment to this would be if $c \in U$. Then there would be only one preimage of the critical value c and therefore no way to extend ϕ_c as a function.

So, as long as c lies in the filled Julia set we can continue this procedure infinitely often and thus we have a conjugacy with z^2 defined on the exterior of K_c and taking values in $\{z \,|\, |z| > 1\}$.

3.2 The Fundamental Dichotomy

These facts allow us to prove the following important result for quadratic maps.

Theorem 3.2 The Fundamental Dichotomy. *Suppose* $0 \in K_c$. *Then* K_c *is connected. If* $0 \notin K_c$, *then* K_c *is a Cantor set.*

For the connectedness portion of this result, we have that, for each n, $Q_c^{-n}(U)$ is a closed disk in the Riemann sphere. Its complement is therefore an open, simply connected subset of $\mathbb{C}$. The closure of these subsets are nested as n increases and hence their intersection is a closed, connected set. Clearly, this intersection is K_c.

Now suppose $Q_c^n(0) \to \infty$. We may assume (by pulling our original U back enough times), that c lies on the boundary of U. Now we pull back once more. Every point in U (with the exception of c) has two preimages symmetrically located about 0. The critical value has only one preimage, namely 0, so the boundary of the complement of $Q_c^{-1}(U)$ is topologically a closed figure eight curve.

Now the complement of $Q_c^{-1}(U)$ consists of two open, simply connected regions which we denote by I_0 and I_1. Each I_j is mapped in one-to-one fashion by Q_c onto the complement of U which we call V. Hence $Q_c(I_j) = V \supset (I_0 \cup I_j)$ in its interior.

It follows that if $z \in K_c$, then the entire orbit of z lies in $I_0 \cup I_1$. Thus we can assign a sequence of symbols 0 and 1 to each z in the usual way:

$$S(z) = s_0 s_1 s_2 \ldots$$

where each s_j is 0 or 1 and $s_j = 0$ if $Q_c^j(z) \in I_0$, $s_j = 1$ if $Q_c^j(z) \in I_1$.

Another way to say this is as follows. Let P_j be the inverse of Q_c on V that takes its values in I_j. So P_0 maps V onto I_0 and P_1 maps V onto I_1. We may then say that

$$S(z) = s_0 s_1 s_2 \dots$$

if

$$z \in \bigcap_{n=0}^{\infty} P_{s_0} \circ P_{s_1} \circ \dots \circ P_{s_n}(V).$$

In fact, $z = \bigcap_{n=0}^{\infty} P_{s_0} \circ \dots \circ P_{s_n}(V)$ since each P_j is a strict contraction in the Poincaré metric on V.

This then gives a one-to-one mapping from K_c onto the space of sequences of 0's and 1's. Standard arguments show that this map is continuous with continuous inverse. Since the space of sequences is homeomorphic to a Cantor set, we're done.

3.3 The Mandelbrot Set

The Fundamental Dichotomy is really quite amazing. It tells us that, for quadratic maps, there are only two types of filled Julia sets: those that are connected and those that are totally disconnected. There are no Julia sets that consist of 2 or 20 or 200 disjoint pieces. Moreover, it is the orbit of the critical value that determines which case we have. This leads to the definition of the well-known Mandelbrot set.

Definition 3.3 *The Mandelbrot set $\mathcal{M}$ is the set of all c-values for which the orbit of 0 under Q_c does not tend to ∞. Equivalently, $\mathcal{M}$ is the set of c-values for which the Julia set of Q_c is connected.*

The image of the Mandelbrot set has become somewhat of an icon in complex dynamics. See Figure 7.

The visible bulbs in $\mathcal{M}$ correspond to c-values for which Q_c has an attracting cycle of some given period. For example, the main central cardioid in $\mathcal{M}$ consists of c-values for which Q_c has an attracting fixed point. This can be seen by solving for the fixed points

$$z^2 + c = z$$

that are attracting

$$|Q_c'(z)| = |2z| < 1.$$

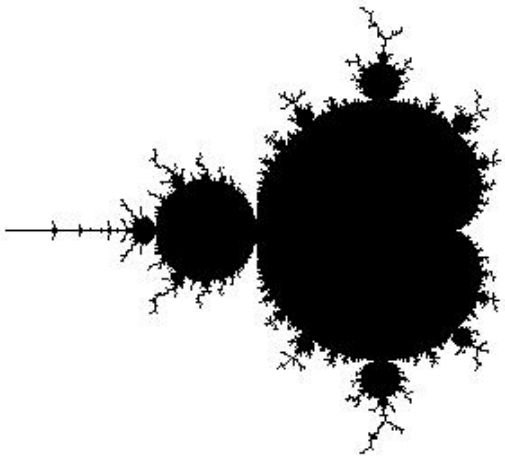

Figure 7: The Mandelbrot set.

Solving these two equations simultaneously, we see that the boundary of this region is given by

$$c = z - z^2$$

where $z = \frac{1}{2}e^{2\pi i\theta}$. That is, the function

$$c(\theta) = \frac{1}{2}e^{2\pi i\theta} - \frac{1}{4}e^{4\pi i\theta}$$

parametrizes the boundary of the cardioid. At $c(\theta)$, $Q_{c(\theta)}$ has a fixed point that is neutral; the derivative of $Q_{c(\theta)}$ at this fixed point is $e^{2\pi i\theta}$.

For each rational value of θ, there is a bulb tangent to the main cardioid at $c(\theta)$. For c-values in the bulb attached to the cardioid at $c(p/q)$, Q_c has an attracting cycle of period q. We call this bulb the p/q bulb attached to the main cardioid and denote it by $B_{p/q}$.

It is known that, as c passes from the main cardioid, through $c(p/q)$, and into $B_{p/q}$, Q_c undergoes a p/q-bifurcation. By this we mean: when c lies in the main cardioid near $c(p/q), Q_c$ has an attracting fixed point with a nearby repelling cycle of period q. At $c(p/q)$ the attracting fixed point and repelling cycle merge to produce the neutral fixed point with derivative $e^{2\pi ip/q}$. When c lies in $B_{p/q}$, Q_c now has an attracting cycle of period q and a repelling fixed

point. We will discuss these bulbs in more detail below, but first we pause to take up one of the most important subjects in complex dynamics.

3.4 External Rays

Suppose K_c is connected. We now have a conjugacy ϕ_c from the exterior of K_c to the exterior of the unit disk. In the language of the Riemann Mapping Theorem, this map is the *exterior Riemann map*. The map ϕ_c conjugates Q_c in the exterior of K_c to $Q_0(z) = z^2$ in $\{z \mid |z| > 1\}$. In particular, since z^2 preserves the straight rays $\theta =$ constant, it follows that Q_c preserves the preimages of these rays.

Definition 3.4 *The external ray of angle θ is the preimage of the straight ray $re^{2\pi i\theta}$ with $r > 1$ under ϕ_c.*

Thus we see that the action of Q_c in the exterior of K_c is the same as the action of doubling on the straight rays outside the unit circle. Of course, we understand doubling completely (if not, see the Appendix to this section), so the conjugacy implies that we understand the dynamics of Q_c completely as well, at least outside of K_c.

Certain of the external rays "land" on the boundary of K_c. That is, for certain θ values

$$\lim_{r\to\infty} \phi_c^{-1}(re^{2\pi i\theta})$$

exists. We call this point in $J(Q_c)$ the *landing point* of the external ray with angle θ.

It is known that if $J(Q_c)$ is locally connected, then all rays actually land. (This is a consequence of Carathéodory theory, since Q_c actually gives the uniformization of the exterior of K_c.) In this case, the conjugacy with z^2 shows that $Q_c \mid J(Q_c)$ is effectively a quotient of the squaring map.

The major importance of the external rays, however, does not lie in the "dynamical plane." Rather, the amazing results of Douady and Hubbard allow us to extend the exterior Riemann map to the exterior of the Mandelbrot set. Define $\Phi(c) = \phi_c(c)$ for $c \notin \mathcal{M}$. Then it is known [DH] that Φ is an analytic map that takes the exterior of the Mandelbrot set onto the exterior of the unit disk in one-to-one fashion. In particular, the preimages of the straight rays under Φ are the external rays for $\mathcal{M}$. We will discuss how these rays land in a subsequent section.

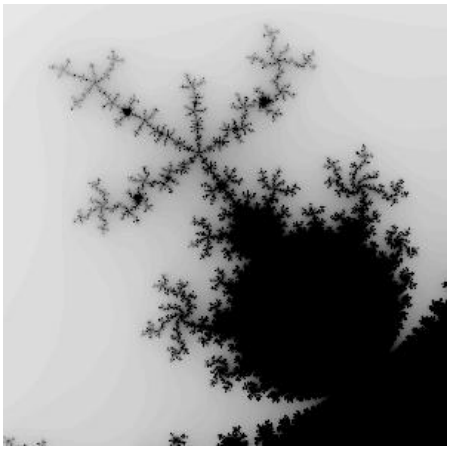

Figure 8: The 2/5 bulb.

3.5 Some Folk Theorems.

Now let's pause to have some fun. Strictly speaking, the following sections have nothing to do with our main topic, but they do at least illustrate the power of the external rays of $\mathcal{M}$. One of our major thrusts later will be to develop a similar theory for the more difficult exponential case.

As we described above, the Mandelbrot set consists of a basic cardioid shape (the attracting fixed point region) from which hang numerous "bulbs" or "decorations." The bulbs directly attached to the cardioid are the p/q bulbs $B(p/q)$.

One of the surprising folk theorems we discuss below is that we can recognize the p/q-bulb from the geometry of the bulb itself. That is, we can read off dynamical information from the geometric information contained in the Mandelbrot set.

For example, the 2/5 bulb is displayed in Figure 8. For any c-value in the largest disk in this figure, Q_c has an attracting cycle with rotation number 2/5 about a central repelling fixed point. Note that the 2/5 bulb possesses an antenna-like structure that features a junction point from which five spokes emanate. One of these spokes is attached directly to the 2/5 bulb; we call this spoke the principal spoke. Now look at the "smallest" of the non-principal spokes. Note that this spoke is located, roughly speaking, 2/5 of a turn in the counterclockwise direction from the principal spoke. This is how we

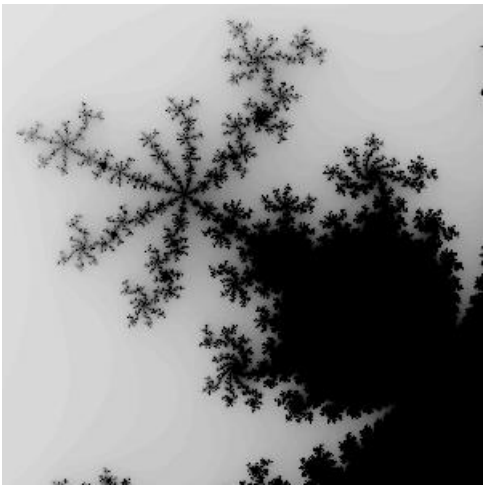

Figure 9: The 3/7 bulb.

geometrically identify this bulb as the 2/5-bulb.

As another example, in Figure 9 we display the 3/7 bulb. Note that this bulb has 7 spokes emanating from the junction point, and the smallest is located 3/7 of a turn in the counterclockwise direction from the principal spoke. This then is the folk theorem: You can recognize the p/q bulb by locating the "smallest" spoke in the antenna and determining its location relative to the principal spoke. Of course, the word "smallest" needs some clarification here; later in this section we will make this notion precise. As an additional disclaimer, this folk theorem is only about 80% true using the Euclidean notion of "smallness" or Lebesgue measure. Our goal is to provide a somewhat different framework in which this result is always true.

There is more to the story of interplay between the geometry of the Mandelbrot set and the corresponding dynamics. In Figure 10, we display the 1/2 and 1/3 bulbs. The 1/2 bulb is the large bulb to the left; the 1/3 bulb is the topmost bulb. In between these two bulbs are infinitely many smaller bulbs, but the largest we recognize as the 2/5 bulb. Now note that 2/5 can be obtained from 1/2 and 1/3 by "Farey addition":

$$\frac{1}{2} \oplus \frac{1}{3} = \frac{2}{5}.$$

That is, to obtain the largest bulb between two given bulbs (in a particular ordering), we simply add the corresponding fractions just the way we always

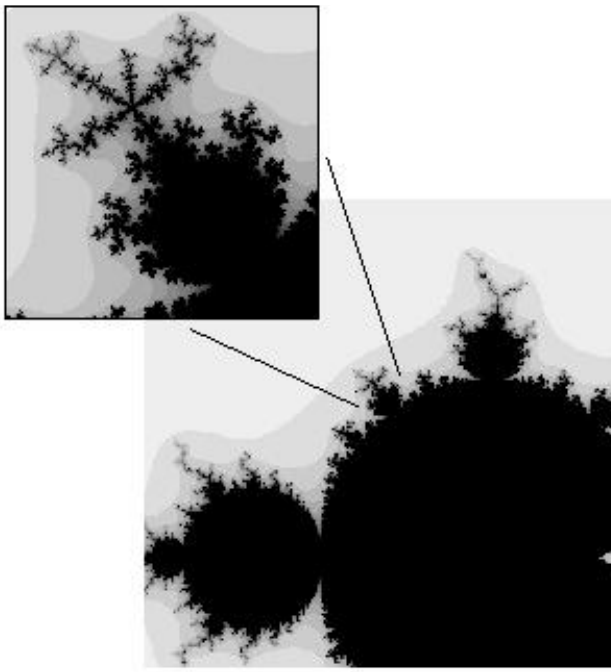

Figure 10: $\frac{1}{2} \oplus \frac{1}{3} = \frac{2}{5}$.

wanted to add them, namely by adding the numerators and adding the denominators. This is the second of the folk theorems we discuss below. In particular it follows that the size of bulbs is determined by the Farey tree. For a discussion of the basic properties of the Farey tree, see the appendix in this section.

As a second example, note that

$$\frac{2}{5} \oplus \frac{3}{7} = \frac{5}{12}$$

and that the 5/12 bulb is the largest between the 2/5 and 3/7 bulbs. See Figure 11.

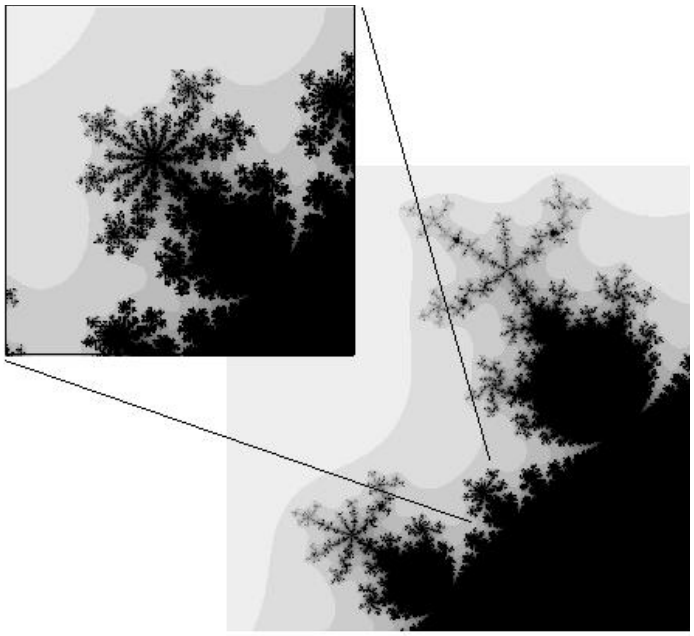

Figure 11: $\frac{2}{5} \oplus \frac{3}{7} = \frac{5}{12}$.

While we will not give complete proofs of each of these folk theorems in this paper, we will indicate some of the combinatorial arguments involved in making the statements precise. For more folk theorems and complete proofs, we refer to [DM1].

3.6 Landing Points of External Rays

Now we can begin to make precise the folk theorems mentioned above. In order to do this, we will use some well known facts about both the Farey tree and angle doubling mod 1. See the appendix to this section for more details about these prerequisites.

Let $\mathcal{O}$ denote the exterior of the unit circle in the plane, i.e.,

$$\mathcal{O} = \{z \mid |z| > 1\}.$$

As mentioned above, there is a unique analytic homeomorphism Φ mapping the exterior of the Mandelbrot set to $\mathcal{O}$. The mapping Φ takes positive reals to positive reals. This mapping is the uniformization of the exterior of the Mandelbrot set, or the exterior Riemann map.

The importance of Φ stems from the fact that the image under Φ^{-1} of the straight rays $\theta =$ constant in $\mathcal{O}$ have dynamical significance. In the Mandelbrot set, we define the external ray with external angle θ_0 to be the image of $\theta = \theta_0$ under Φ^{-1}. It is known that an external ray whose angle θ_0 is rational actually "lands" on $\mathcal{M}$. That is

$$\lim_{r \to 1} \Phi^{-1}(re^{2\pi i\theta_0})$$

exists and is a unique point on the boundary of $\mathcal{M}$. This c-value is called the landing point of the ray with angle θ_0.

For example, the ray with angle 0 lies on the real axis and lands on $\mathcal{M}$ at the cusp of the main cardioid, namely the parameter $c = 1/4$. Also, the ray with angle $1/2$ lies on the negative real axis and lands on $\mathcal{M}$ at the tip of the "tail" of $\mathcal{M}$ which can be shown to be $c = -2$.

Consider now the interior of $\mathcal{M}$. The interior consists of infinitely many simply connected regions. A *bulb* of $\mathcal{M}$ is a component of the interior of $\mathcal{M}$ in which each c-value corresponds to a quadratic function which admits an attracting cycle. The period of this cycle is constant over each bulb. In many cases, a bulb is attached to a component of lower period at a unique point called the *root point* of the component.

The important result of Douady and Hubbard [DH] is:

Theorem 3.5 *Suppose a bulb B consists of c-values for which the quadratic map has an attracting q-cycle. Then the root point of this bulb is the landing point of exactly 2 rays, and the angles of each of these rays have period q under doubling.*

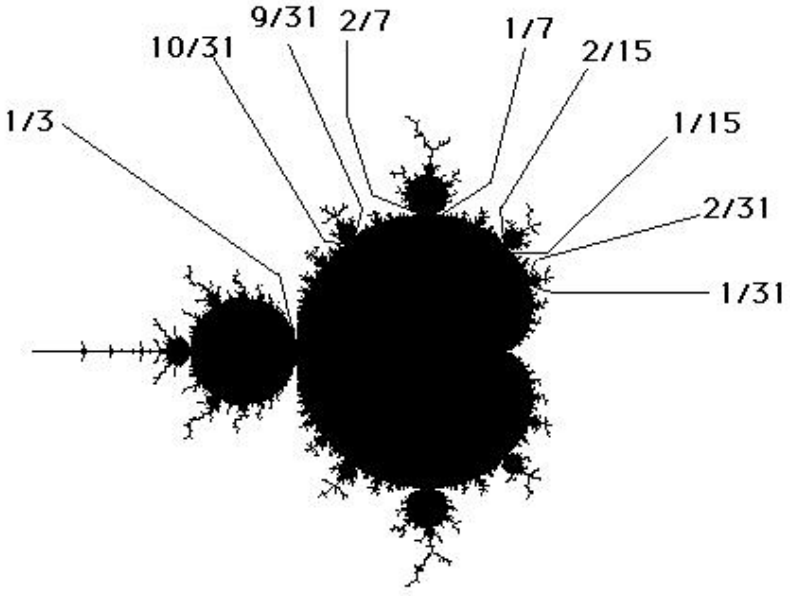

Figure 12: Rays landing on the Mandelbrot set.

Thus, how the angles of the external rays of $\mathcal{M}$ are arranged determines the ordering of the bulbs in $\mathcal{M}$. For example, the large bulb directly to the left of the main cardioid is the 1/2 bulb, so two rays with period 2 under doubling must land there. Now the only angles with period 2 under doubling are 1/3 and 2/3, so these are the angles of the rays that land at the root point of $B_{1/2}$.

Now consider the 1/3 bulb atop the main cardioid. This bulb lies "between" the rays 0 and 1/3. There are only two angles between 0 and 1/3 that have period 3 under doubling, namely 1/7 and 2/7, so these are the rays that land at the root point of $B_{1/3}$.

The 2/5 bulb lies between the 1/3 and 1/2 bulbs. Hence the rays that land at this root point must have period 5 under doubling and lie between 2/7 and 1/3. The only angles that have this property are 9/31 and 10/31, so these rays must land at the root point. See Figure 12.

These ideas allow us to measure the "largeness" or "smallness" of portions of the Mandelbrot set. Suppose we have two rays with angles θ_- and θ_+ that both land at a point c_* in the boundary of $\mathcal{M}$.

Then, by the homeomorphism Φ, all rays with angles between θ_- and θ_+ must approach the component of $M - \{c_*\}$ cut off by θ_- and θ_+. (We remark that it is not known that all such rays actually land on $\mathcal{M}$ – indeed, this is the major open conjecture about $\mathcal{M}$.) Thus it is natural to measure the size of this portion of $\mathcal{M}$ by the length of the interval $[\theta_-, \theta_+]$.

The root point of the p/q bulb of $\mathcal{M}$ divides $\mathcal{M}$ into two sets. The component containing the p/q bulbs is called the p/q *limb*. We can then measure the size of the p/q limb if we know the angles of the two external rays that land on the root point of the p/q bulb. This is the subject of the next section.

3.7 Rays landing on the p/q bulb

In order to make the notion of "large" or "small" precise in the statement of the folk theorems, we need a way to determine the angles of the rays landing at the root point of $B_{p/q}$. We denote the angles of these two rays in binary by $\overline{s_\pm(p/q)}$, where $\overline{s_-(p/q)} < \overline{s_+(p/q)}$. We call $\overline{s_-(p/q)}$ the *lower angle* of $B_{p/q}$ and $\overline{s_+(p/q)}$ the *upper angle*.

As we will see, $s_\pm(p/q)$ is a string of q digits (0 or 1) and so $\overline{s_\pm(p/q)}$ denotes the infinite repeating sequence whose basic block is $s_\pm$. Douady and Hubbard [DH] have a geometric method involving Julia sets to determine these angles. Our method is more combinatorial and resembles algorithms due to Atela [A], LaVaurs [Lav], and Lau and Schleicher [LS].

To describe this algorithm, let $R_{p/q}$ denote rotation of the unit circle through p/q turns, i.e.,

$$R_{p/q}(\theta) = e^{2\pi i(\theta + p/q)}.$$

We will consider the itineraries of points in the unit circle under R using two different partitions of the circle.

The *lower partition* of the circle is defined as follows. Let $I_0^- = \{\theta \mid 0 < \theta \le 1 - p/q\}$ and $I_1^- = \{\theta \mid 1 - p/q < \theta \le 1\}$. Note that the boundary point 0 belongs to I_1^- and $-p/q = 1 - p/q$ belongs to I_0^-. We then define $s_-(p/q)$ to be the itinerary of p/q under $R_{p/q}$ relative to this partition. We call $s_-(p/q)$ the *lower itinerary of* p/q. That is, $s_-(p/q) = s_1 \ldots s_q$ where s_j is either 0 or 1 and the digit $s_j = 0$ iff $R_{p/q}^{j-1}(p/q) \in I_0^-$. Otherwise, $s_j = 1$.

For example, $s_-(1/3) = 001$ since

$$\begin{aligned} I_0^- &= (0, 2/3] \\ I_1^- &= (2/3, 1] \end{aligned}$$

and the orbit $\frac{1}{3} \to \frac{2}{3} \to 1 \to \frac{1}{3} \cdots$ lies in I_0^-, I_0^-, I_1^-, respectively.

Similarly, $s_-(2/5) = 01001$ since

$$\begin{aligned} I_0^- &= (0, 3/5] \\ I_1^- &= (3/5, 1] \end{aligned}$$

and the orbit is $\frac{2}{5} \to \frac{4}{5} \to \frac{1}{5} \to \frac{3}{5} \to 0 \to \frac{2}{5} \ldots$.

We also define the *upper partition* I_0^+ and I_1^+ as follows

$$\begin{aligned} I_0^+ &= [0, 1 - p/q) \\ I_1^+ &= [1 - p/q, 1). \end{aligned}$$

The *upper itinerary of* p/q, $s_+(p/q)$, is then the itinerary of p/q relative to this partition. Note that I_0^+ and I_1^+ differ from I_0^- and I_0^+ only at the endpoints.

For example, $s_+(1/3) = 010$ since the orbit is $\frac{1}{3} \to \frac{2}{3} \to 0 \cdots$ and

$$\begin{aligned} I_0^+ &= [0, 2/3) \\ I_1^+ &= [2/3, 1). \end{aligned}$$

This orbit starts in I_0^+, hops to I_1^+, and then returns to I_0^+ before cycling. For $2/5$, we have

$$\begin{aligned} I_0^+ &= [0, 3/5) \\ I_1^+ &= [3/5, 1) \end{aligned}$$

and $s_+(2/5) = 01010$.

The following theorem provides the algorithm for computing the angles of rays landing at the root point of the p/q bulb. For a proof, we refer to [DH] or [DM1].

Theorem 3.6 *The two rays landing at the root point of the p/q bulb are $\overline{s_-(p/q)}$ and $\overline{s_+(p/q)}$.*

Note that $s_\pm(p/q)$ differ only in their last two digits (provided $q \geq 2$). Indeed we may write

$$\begin{aligned} s_-(p/q) &= s_1 \ldots s_{q-2} 0\ 1 \\ s_+(p/q) &= s_1 \ldots s_{q-2} 1\ 0 \end{aligned}$$

The reason for this is that the upper and lower itineraries are the same except at $R_{p/q}^{q-2}(p/q) = -p/q$ and $R_{p/q}^{q-1}(p/q) = 0$, which form the endpoints of the two partitions of the circle.

We now define the *size of the p/q limb* to be the length of the interval $[s_-(p/q), s_+(p/q)]$. That is, the size of the p/q limb is given by the "number" of external rays that approach this limb. We may compute size of these bulbs explicitly by using the fact that $s_\pm(p/q)$ differ only in the last two digits.

Theorem 3.7 *The size of the p/q limb is $1/(2^q - 1)$. That is*

$$\overline{s_+(p/q)} - \overline{s_-(p/q)} = \frac{1}{2^q - 1}.$$

To see this, just write the binary expansion of the difference in the form

$$\begin{aligned}
\overline{s_+(p/q)} - \overline{s_-(p/q)} &= \frac{1}{2^{q-1}} + \frac{1}{2^{2q-1}} + \frac{1}{2^{3q-1}} + \ldots - \left(\frac{1}{2^q} + \frac{1}{2^{2q}} + \frac{1}{2^{3q}} + \ldots\right) \\
&= \frac{1}{2^{q-1}} \cdot \frac{2^q}{2^q - 1} - \frac{1}{2^q} \cdot \frac{2^q}{2^q - 1} \\
&= \frac{1}{2^q - 1}.
\end{aligned}$$

As we see in Figure 13, the visual size of the bulbs does indeed correspond to the size as defined above.

3.8 The Size of Limbs and the Farey Tree

In this section we relate the size of a p/q limb to the size of the limbs corresponding to the Farey parents of p/q. The following Proposition relates the upper and lower itineraries of p/q and its Farey parents.

Proposition 3.8 *Suppose*

$$0 < \frac{\alpha}{\beta} < \frac{\gamma}{\delta} < 1$$

are the Farey parents of p/q. Then the lower itinerary $s_-(p/q)$ consists of the first q digits of the upper angle $\overline{s_+(\alpha/\beta)}$ of the smaller parent, and the upper itinerary $s_+(p/q)$ consists of the first q digits of the lower angle $\overline{s_-(\gamma/\delta)}$ of the larger parent.

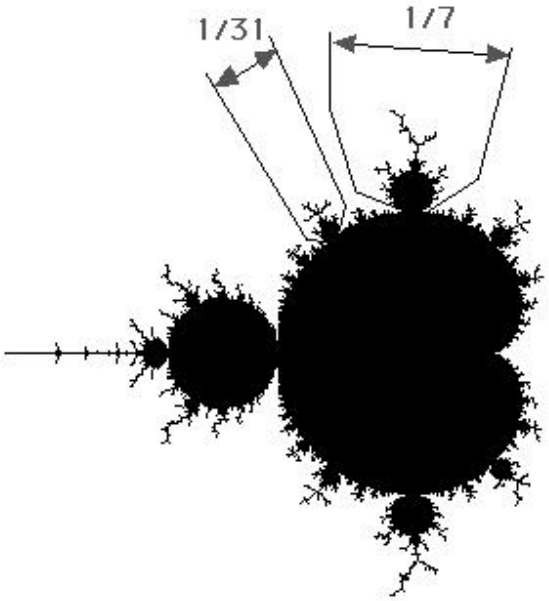

Figure 13: Size of the 2/5 and 1/3 limbs of $\mathcal{M}$.

For a proof, we refer to [DM1].

In case one of the Farey parents are 0 or 1, we must modify the above proposition.

Proposition 3.9 *Suppose that a Farey parent of p/q is 0. Then the q digits in the lower itinerary of p/q are given by*

$$s_-(p/q) = 0\ldots01.$$

If a Farey parent of p/q is 1, then we have

$$s_+(p/q) = 1\ldots10.$$

We now sketch the proof of one of the folk theorems mentioned earlier.

Theorem 3.10 *Suppose $\alpha/\beta < \gamma/\delta$ are the Farey parents of p/q. Then the size of the p/q limb is larger than the size of any other limb between the α/β and γ/δ limbs.*

Proof: Assume first that neither of the parents are 0 or 1. By the previous Proposition, we have that $\overline{s_-(p/q)}$ and $\overline{s_+(\alpha/\beta)}$ agree in their first q digits. Using these binary representations, we have

$$\overline{s_-(p/q)} - \overline{s_+(\alpha/\beta)} \leq \frac{1}{2^q}.$$

Similarly

$$\overline{s_-(\gamma/\delta)} - \overline{s_+(p/q)} \leq \frac{1}{2^q}.$$

This implies that the arc of rays between the p/q limb and either of its parents' limbs has length no larger than $1/2^q$. Thus any limb between them has size smaller than $1/2^q$.

From the previous section, we know that

$$\overline{s_+(p/q)} - \overline{s_-(p/q)} = \frac{1}{2^q - 1}.$$

As this quantity is larger than $1/2^q$, it follows that the p/q limb attracts the largest number of rays between its two parents.

In case one of the parents of $1/q$ is 0, then we have that the size of the $1/q$ bulb is $1/(2^q - 1)$ as above while the gap between 0 and $\overline{s_-(p/q)} = \overline{0\ldots01}$ is also $1/(2^q - 1)$. But then any limb between the $1/q$ limb and the cusp of the cardioid must have size strictly smaller than $1/(2^q - 1)$, again showing that the $1/q$ limb is the largest. The gap between the limbs of $1/q$ and its other Farey parent $1/(q-1)$ is handled as above. The case of Farey parent 1 is handled similarly.

3.9 Further Remarks

The technique of measuring the size of certain portions of the Mandelbrot set by the length of the interval of rays that land on that portion provides justification for other folk theorems involving the size of $\mathcal{M}$. For example, this is the same technique that is used to identify the p/q bulb using the "lengths" of the spokes in its antenna. Once we know these rays, we can easily compute the lengths of the various spokes.

As an example of this, it can be shown that the two rays that land at the junction point of the antenna adjacent to the principal spoke are given by $s_-\overline{s_+}$ and $s_+\overline{s_-}$ where we have dropped the p/q for clarity. These two rays

are therefore given by preperiodic binary sequences that begin to repeat only after the qth entry.

This fact shows that the vast majority of rays that land on the p/q limb actually approach the spokes of the antenna. For we have the following ordering of the rays landing on the p/q bulb:

$$\overline{s_-} < s_-\overline{s_+} < s_+\overline{s_-} < \overline{s_+}.$$

It is easy to check using the above techniques that the length of the arc of rays approaching the antenna between $s_-\overline{s_+}$ and $s_+\overline{s_-}$ is

$$\frac{1}{2^{q-1}} - \frac{2}{2^q(2^{q-1})}.$$

This number is much larger than the length of the arc between $\overline{s_-}$ and $s_-\overline{s_+}$ or between $\overline{s_+}$ and $s_+\overline{s_-}$, each of which has length

$$\frac{1}{2^q(2^{q-1})}.$$

We can also use these two rays separating the principal spoke from the rest of the antenna to determine a list of the q rays that land on the junction point. Then using the techniques above we can determine that the shortest is located p/q turns in the counterclockwise direction from the principal spoke. See [DM1] for details.

So the moral of the stories in this section is: there is a way, using some simple geometry and dynamics, to understand large portions of the parameter plane for quadratic polynomials. We shall see similar stories unfold for the exponential map, though the dynamics will no longer be quite so simple.

3.10 Appendix: The Farey Tree

We recall here a few facts about the *Farey tree.* The Farey tree is a tree containing all of the rationals between 0 and 1. At each stage of its construction, the Farey tree consists of a finite list of rationals. Adjacent rationals in this list are called *Farey neighbors.* The inductive step in the construction of the tree is: Each pair of Farey neighbors produces a *Farey child*, which is the rational between the two whose denominator is the smallest. Naturally, the rationals that produce a Farey child are called its *Farey parents.*

One of the most intriguing features of the Farey tree is that we obtain Farey children by Farey addition. That is, the fraction between the Farey neighbors α/β and γ/δ is given by

$$\frac{\alpha}{\beta} \oplus \frac{\gamma}{\delta} = \frac{\alpha+\gamma}{\beta+\delta}.$$

That is, to obtain the fraction between two Farey neighbors whose denominator is the smallest, we simply add the numerators and add the denominators of the parents to obtain the child.

We begin the construction of the tree with the pair of rationals 0 and 1 which we write as $0/1$ and $1/1$. Their child is $1/2$, so the second stage of the construction gives the list

$$\frac{0}{1} \quad \frac{1}{2} \quad \frac{1}{1}.$$

At the next stage we obtain two new Farey children

$$\frac{0}{1} \quad \frac{1}{3} \quad \frac{1}{2} \quad \frac{2}{3} \quad \frac{1}{1}.$$

At generation four we find

$$\frac{0}{1} \quad \frac{1}{4} \quad \frac{1}{3} \quad \frac{2}{5} \quad \frac{1}{2} \quad \frac{3}{5} \quad \frac{2}{3} \quad \frac{3}{4} \quad \frac{1}{1}.$$

It is a fact that the Farey tree contains all rationals. See [GT] or [F] for more details.

One other fact about the Farey tree is that α/β and γ/δ are Farey neighbors if and only if $\alpha\delta - \gamma\beta = \pm 1$. Consequently, we have

$$|\frac{\alpha}{\beta} - \frac{\gamma}{\delta}| = \frac{1}{\beta\delta}.$$

This is easily proved by induction.

3.11 Appendix: Angle Doubling

In order to use the fundamental results of Douady and Hubbard [DH] regarding the Mandelbrot set we recall in this appendix some facts about the doubling function. The doubling function is defined on the circle considered as the reals modulo one and is given by $D(\theta) = 2\theta \bmod 1$.

We need two facts about D:

Fact 1: The angle θ is periodic under D iff θ is a rational of the form p/q (in lowest terms) with q odd.

For example, the D-orbit of $1/3$ is

$$\frac{1}{3} \to \frac{2}{3} \to \frac{1}{3} \cdots$$

which has period 2. The rational $1/7$ has period 3 under doubling:

$$\frac{1}{7} \to \frac{2}{7} \to \frac{4}{7} \to \frac{1}{7} \cdots$$

while $1/5$ has period 4:

$$\frac{1}{5} \to \frac{2}{5} \to \frac{4}{5} \to \frac{3}{5} \to \frac{1}{5} \cdots$$

The rationals with even denominator are eventually periodic but not periodic. For example, $1/6$ lies on an eventual 2-cycle

$$\frac{1}{6} \to \frac{1}{3} \to \frac{2}{3} \to \frac{1}{3} \cdots$$

and $1/8$ is eventually fixed:

$$\frac{1}{8} \to \frac{1}{4} \to \frac{1}{2} \to 1 \to 1 \cdots$$

A second important fact about doubling is that we can read off the binary expansion of θ by noting the *itinerary* of θ in the circle relative to D. To define the itinerary, we denote the upper semicircle $0 \leq \theta < 1/2$ by I_0 and the lower semicircle $1/2 \leq \theta < 1$ by I_1. Given θ, we attach an infinite string of 0's and 1's to θ as follows: The itinerary of θ is $B(\theta) = (s_0 s_1 s_2 \ldots)$ where s_j is either 0 or 1 and $s_j = 0$ if $D^j(\theta) \in I_0$, $s_j = 1$ if $D^j(0) \in I_1$. That is, we simply watch the orbit of θ in the circle under doubling and assign 0 or 1 to the itinerary whenever $D^j(\theta)$ lands in the arc I_0 or I_1.

Fact 2: The itinerary $B(\theta)$ is the binary expansion of θ.

For example, if $\theta = 1/3$, then $\theta \in I_0$, while $D(\theta) \in I_1$ and $D^2(\theta) = \theta$. Hence $B(1/3)$ is the repeating sequence $\overline{01}$, which of course is the binary expansion of $1/3$. Similarly, $B(1/7) = \overline{001}$ while $B(1/5) = \overline{0011}$.

4 Exponential Dynamics

In this chapter we begin the study of the most important entire function, the complex exponential $E_\lambda(z) = \lambda e^z$. Our goal is to begin to paint the picture of the parameter plane or *bifurcation diagram* for this family, the analogue of the Mandelbrot set for the quadratic family. First seen around 1984 [BR], [D3], [EL], this set and the Mandelbrot set are very different.

4.1 Computing the Julia set

One of the principal differences between quadratic and exponential dynamics deals with orbits that tend to ∞. For polynomials, any orbit that tends to ∞ is necessarily in the Fatou set as the point at ∞ is a superattracting fixed point. This is not the case for E_λ:

Theorem 4.1 *Suppose $E_\lambda^n(z) \to \infty$. Then $z \in J(E_\lambda)$. In fact, $J(E_\lambda)$ is the closure of the set of points that escape to ∞.*

Proof. If the orbit of z lies in the Fatou set, then the classification of stable domains says that the orbit of z must eventually enter an attracting basin or a Siegel disk. Thus, escaping orbits do not lie in the Fatou set.

Now there must be at least one escaping orbit for E_λ, since, roughly speaking,many points in the far right half plane are mapped further to the right. Thus, given any $z \in J(E_\lambda)$, and any neighborhood of z, by Montel's Theorem the iterates of E_λ map this neighborhood over $\mathbb{C}-\{0\}$. In particular, there is a preimage of the escaping orbit in this neighborhood, and so the escaping points are dense in the Julia set of E_λ.

□

Remark. In general, escaping points for entire functions do not lie in the Julia set, as our earlier examples of wandering domains and domains at infinity show. But critically finite entire functions do have this property.

This fact gives us a method to compute the Julia sets for complex exponentials. If the orbit of z tends to ∞, then it must do so with $\text{Re}\, E_\lambda^n(z) \to \infty$. Hence we paint the picture of a Julia set using the following algorithm.

Algorithm

1. *Compute the orbit of z up to N iterations.*

2. *If the orbit of z enters the region $\mathrm{Re}\, z \geq 50$ at iteration $j \leq N$, then "color" z with a color corresponding to j. Then $z \in J(E_\lambda)$.*

3. *If the orbit never enters this half plane, then color z black and declare that $z \notin J(E_\lambda)$.*

It is interesting to note that this very crude algorithm actually yields quite accurate pictures of the Julia set. See [Du]. As we will see later, "most" of the points in the Julia set actually have orbits that tend to ∞. Since e^{50} is quite large, we capture at least some of these escape orbits by tracking them into the half plane $\mathrm{Re}\, z > 50$.

4.2 Explosions

The complex exponential family has only one singular value, namely the asymptotic value at 0. Just as in the quadratic case, we use the orbit of this point to paint the picture of the parameter plane for E_λ. We do not get as sharp a dichotomy in the exponential case, as the topology of the Julia sets for E_λ do not fall neatly into two distinct categories as in the quadratic case. However, the Classification of Stable Domains Theorem does allow us to say something depending upon the fate of the orbit of 0.

Theorem 4.2 *1. Suppose the orbit of 0 tends to ∞ under E_λ. Then $J(E_\lambda) = \mathbb{C}$.*

2. *Suppose the orbit of 0 under E_λ is preperiodic. Then $J(E_\lambda) = \mathbb{C}$.*

3. *Suppose that E_λ has an attracting or neutral periodic orbit. Then $J(E_\lambda)$ is a nowhere dense subset of $\mathbb{C}$. In fact, $J(E_\lambda)$ is confined to a half-plane of the form $\mathrm{Re}\, z \geq \nu$ for some $\nu \in \mathbb{R}$.*

Proof. In the first two cases, the Classification of Stable Domains shows that the Fatou set must be empty, as any stable domain must absorb a singular value. In the final case, the orbit of 0 tends to the attracting or neutral periodic orbit. Hence there is a far left half-plane that is mapped into the basin of this cycle, so $J(E_\lambda)$ must lie to the right of this plane.

□

Example. As we have seen, E_λ has an attracting fixed point if $0 < \lambda < 1/e$. When $\lambda = 1/e$, this fixed point turns rationally indifferent. When $\lambda > 1/e$,

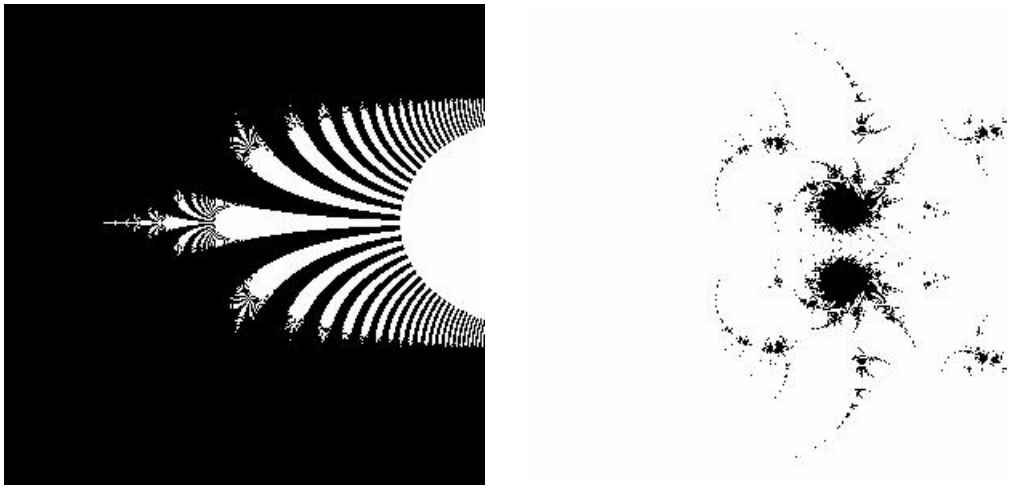

Figure 14: The Julia sets for $\lambda = 1/e$ and $\lambda = 0.4$

there are no fixed points on the real axis and the orbit of 0 tends to ∞. Hence $J(E_\lambda)$ is nowhere dense if $\lambda \leq 1/e$ while $J(E_\lambda) = \mathbb{C}$ when $\lambda > 1/e$. In fact, as we will see shortly, $J(E_\lambda)$ is contained in the half-plane $\operatorname{Re} z \geq 1$ for $0 < \lambda \leq 1/e$. So we have an *explosion* when λ passes through $1/e$: Suddenly the Julia set changes from occupying a small portion of the plane to filling the entire plane! See Figure 14. In these images, the black region is the Fatou set. (In the case of $\lambda = 0.4$ we see some black only because we iterated only 50 times to produce these images.) Also, it appears that the Julia set for $\lambda < 1/e$ contains open sets. This, of course, is not the case. We will discuss this artifact of our computing algorithm in Chapter 5.

The explosion in the Julia set is really quite remarkable. We know that repelling periodic points are dense in $J(E_\lambda)$. As λ passes through $1/e$, all repelling periodic points move continuously, and only one new repelling periodic point is born. Yet, when $\lambda \leq 1/e$, all of these periodic points occupy a (rather small subset of) the right half plane, but when $\lambda > 1/e$, they are dense in $\mathbb{C}$. Julia sets for E_λ may change in an interesting manner as λ varies.

The explosion in $J(E_\lambda)$ is a global consequence of a relatively simple complex bifurcation, the *saddle-node bifurcation*. As λ approaches $1/e$ from below, an attracting and a repelling fixed point come together and merge to form the neutral fixed point at $\lambda = 1/e$. When λ becomes larger than $1/e$, two new fixed points emerge, both of which are repelling with complex

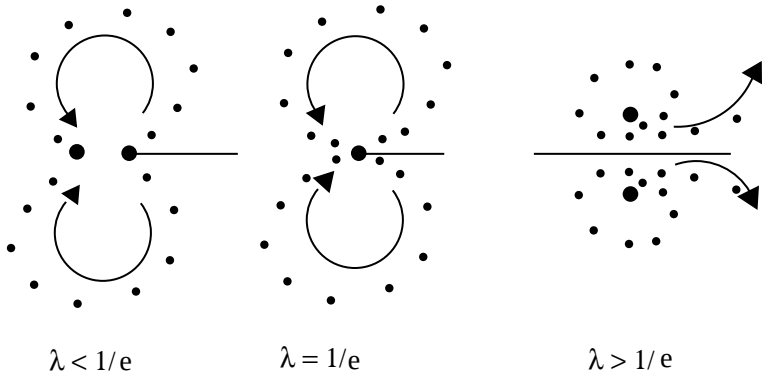

Figure 15: The local saddle-node bifurcation at $\lambda = 1/e$.

derivatives. The local picture of this bifurcation is shown in Figure 15. We will see that similar "global" bifurcations almost always accompany simple bifurcations like the saddle-node or period-doubling.

4.3 Misiurewicz Points

In case the orbit of 0 is preperiodic, $J(E_\lambda) = \mathbb{C}$ and we say that λ is a Misiurewicz point. For example, $\lambda = 2k\pi i$ is a Misiurewicz point if $k \in \mathbb{Z}$ since

$$0 \mapsto 2k\pi i \mapsto 2k\pi i \cdots.$$

Similarly, $\lambda = (2k+1)\pi i$ is also a Misiurewicz point since

$$0 \mapsto (2k+1)\pi i \mapsto -(2k+1)\pi i \mapsto -(2k+1)\pi i.$$

Misiurewicz points play the same role in the parameter plane for E_λ as the junction points in the Mandelbrot set.

4.4 Hyperbolic Components of Period 1–3

Clearly, when E_λ has an attracting cycle, there is an open set about λ in the bifurcation diagram in which all of the corresponding exponentials have an attracting cycle of the same period. The maximal such open connected region in the λ-plane is called a *hyperbolic component.*

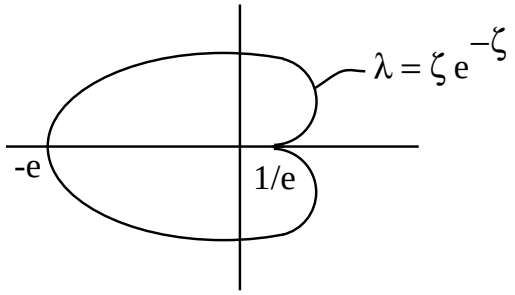

Figure 16: The attracting fixed point region C_1.

The set of λ-values for which E_λ has an attracting fixed point is, as in the case of the quadratic family, cardioid-like. For E_λ has an attracting fixed point if

$$\begin{aligned} E_\lambda(z) &= \lambda e^z = z \\ E'_\lambda(z) &= \lambda e^z = \zeta \end{aligned}$$

where $|\zeta| < 1$. These equations yield

$$\lambda = \zeta e^{-\zeta}, \ |\zeta| < 1.$$

This region is a cardioid C_1 in the plane as depicted in Figure 16.

Note that, as λ traverses the boundary of C_1, the multiplier ζ wraps once around the unit circle. Hence we expect period-n bifurcations to occur whenever ζ is an n^{th} root of unity just as in the case of the Mandelbrot set. Indeed, when $\lambda = 1/e$, $\zeta = 1$ and we have the saddle node bifurcation.

Exercise. Show that when $\lambda = -e$, the exponential family undergoes a period doubling bifurcation.

We now turn to the attracting period 2 region, C_2. This region occupies a large region in the left half plane. For each $\nu < 0, \eta > 0$, define

$$Z_{\nu,\eta} = \{\lambda \in \mathbb{C} \,|\, \mathrm{Re}\,\lambda \leq \nu, |\mathrm{Im}\,\lambda| \leq \eta\}.$$

$Z_{\nu,\eta}$ is a closed half strip in the left portion of the parameter plane.

Proposition 4.3 *For each $\eta \in \mathbb{R}^+$, there is $\nu = \nu(\eta) < 0$ such that if $\lambda \in Z_{\nu,\eta}$ then*

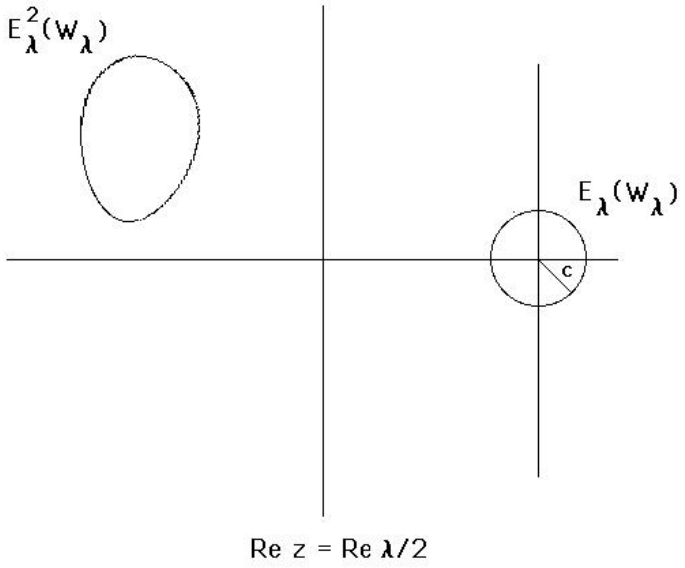

Figure 17: $E_\lambda^2(W_\lambda) \subset W_\lambda$.

1. *E_λ has an attracting two-cycle, and*
2. *$W_\lambda = \{z \mid \text{Re } z \leq \text{Re}\,(\lambda/2)\}$ is contained in the basin of attraction of the two-cycle.*

Proof. Fix $\eta > 0$ and suppose that $|\text{Im}\,\lambda| \leq \eta$. Define

$$c = c(\lambda) = |\lambda| \exp(\text{Re}\,(\lambda/2)).$$

Note that $|\lambda| c(\lambda) \to 0$ and $|\text{Re}\,\lambda| c(\lambda) \to 0$ as $\text{Re}\,\lambda \to -\infty$ since $|\text{Im}\,\lambda|$ is bounded.

We may choose $\nu = \nu(\eta)$ such that, if $\lambda \in Z_{\nu,\eta}$, then

$$|\lambda| c e^c \leq (|\text{Re}\,\lambda| + \eta) c e^c \leq |\text{Re}\,\lambda|/4$$

since $(|\text{Re}\,\lambda| + \eta) c e^c$ tends to 0 as $\text{Re}\,\lambda \to -\infty$.

We claim that E_λ^2 maps W_λ inside itself. To see this, first note that $E_\lambda(W_\lambda)$ is a punctured disk of radius c centered at 0. On this disk

$$|E_\lambda'(z)| = |E_\lambda(z)| = |\lambda| \exp(\text{Re}\,z)$$

which is at most $|\lambda|e^c$. Clearly, $E_\lambda(0) = \lambda$, so points $z \in E_\lambda(W_\lambda)$ are mapped a maximum distance of

$$\begin{aligned} |E_\lambda(z) - \lambda| &= |z - 0| \max_{z \in E_\lambda(W_\lambda)} |E'_\lambda(z)| \\ &\leq |\lambda| e^c \cdot c \\ &\leq |\text{Re } \lambda|/4. \end{aligned}$$

away from λ under E_λ, and thus well to the left of the line $\text{Re}\, z = \text{ Re } \lambda/2$. See Figure 17.

As a consequence, $E_\lambda^2(W_\lambda)$ is contained in the interior of W_λ provided $\lambda \in Z_{\nu,\lambda}$. By the Schwarz lemma, E_λ^2 has an attracting fixed point in W_λ and, moreover, each point in W_λ tends to this point under iteration of E_λ^2. This fixed point gives an attracting 2-cycle for E_λ.

□

Now we turn to the period three regions. Unlike C_1 and C_2, the set C_3 has infinitely many components.

Let $\mu = a + i\pi$ with a sufficiently large. We claim that the map E_μ has an attracting cycle of period 3. To see this, we first note that the real part of $E_\mu^i(0)$ satisfies

$$\begin{aligned} \text{Re}\, E_\mu(0) &= a \\ \text{Re}\, E_\mu^2(0) &\approx -ae^a \end{aligned}$$

Thus

$$|E_\mu^3(0)| \approx ae^{-ae^a}$$

which is very close to 0 when a is large.

Let B_δ denote the ball of radius δ centered at the origin. Then $E_\mu^j(B_\delta)$ contains a ball whose radius is on the order of $a\delta$ centered at $\mu = E_\mu(0)$ if $j = 1$; on the order of $ae^a \cdot a\delta$ centered at $E_\mu^2(0)$ if $j = 2$; and on the order of $ae^{-ae^a} \cdot ae^a \cdot a\delta$ centered at $E_\mu^3(0)$ if $j = 3$. One checks easily that this latter radius is much smaller than δ for δ on the order of $1/a$. Moreover, the distance from $E_\mu^3(0)$ to 0 is much smaller than δ. Consequently, E_μ^3 maps B_δ inside itself, and so E_μ has an attracting cycle of period 3.

Exercise. Consider $\nu = a + (2k+1)\pi i$ for a large and $k \in \mathbb{Z}$. Show that E_ν has an attracting cycle of period 3.

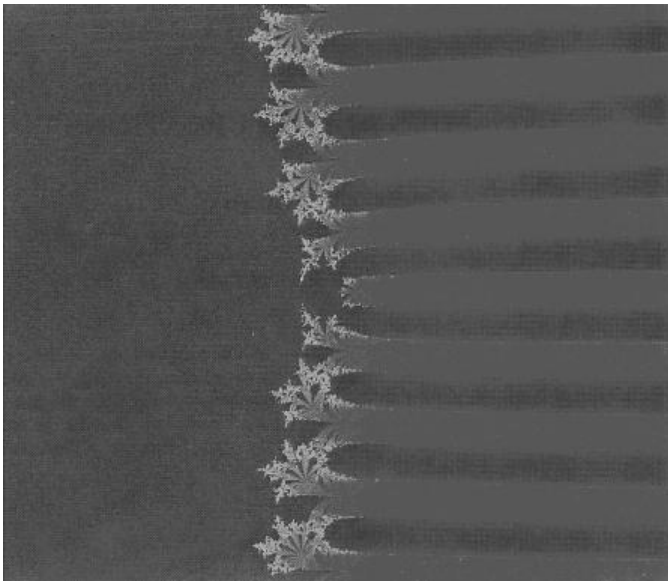

Figure 18: The parameter plane for E_λ.

Consequently, there are open sets that contain the portions of the horizontal line $\operatorname{Im} z = (2k+1)\pi$ in the far right half plane that give λ-values for which E_λ has an attracting cycle of period 3. In fact all of these sets are distinct.

Thus the bifurcation diagram or parameter plane for the exponential family is quite different from that of the quadratic map. See Figures 20 and 21. The small cardioid in the center of Figure 18 is C_1, the large region to the left is C_2; and the large horizontal black regions tending to infinity in the right half plane make up components of C_3. A portion of C_1 is magnified in Figure 19, and further zooms are in Figures 20 and 21.

4.5 Hyperbolic Components with Higher Periods

Suppose $z_0 = z_0(\lambda)$ is an attracting periodic point for E_λ. We write $z_i = E_\lambda^i(z_0)$. Let C_k denote the set of λ-values for which E_λ has an attracting cycle of period $k \geq 3$. We claim that each component of C_k is unbounded and simply connected. To prove this, we first need a lemma.

Lemma 4.4 *Let $U \subset C_k$ be open with $\overline{U}$ compact and $0 \notin \overline{U}$. Then there*

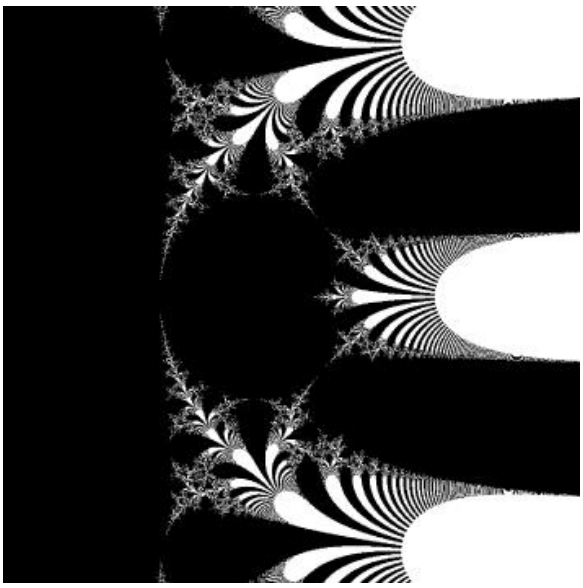

Figure 19: The cardioid C_1.

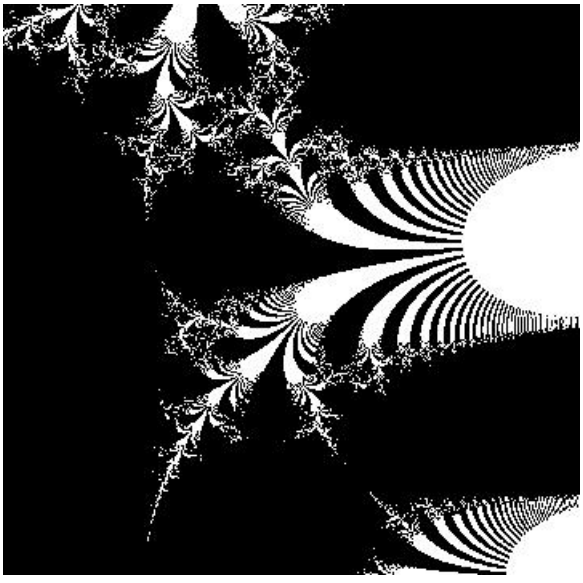

Figure 20: A zoom into the previous figure just above C_1.

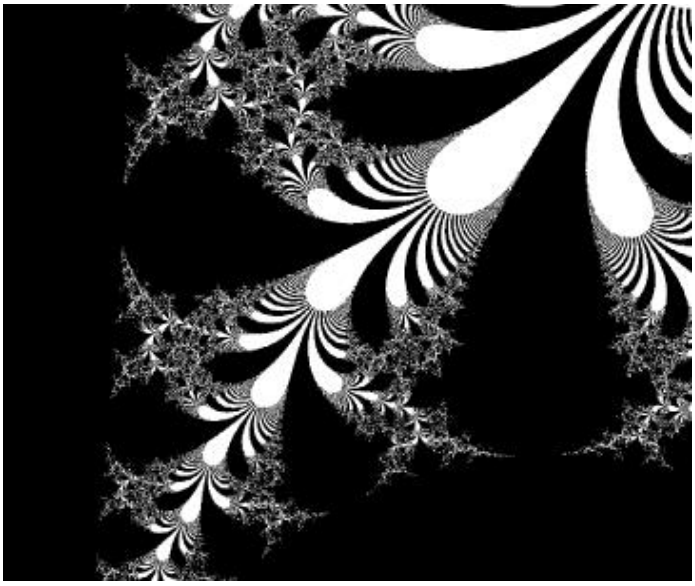

Figure 21: A further zoom.

exists constants c_1, c_2 *such that, if* $\lambda \in U$, *then* $c_1 \leq |z_j(\lambda)| \leq c_2$ *for* $j = 1, \ldots, k-1$.

Proof. Suppose some $|z_j(\lambda)| \to \infty$ as $\lambda \to \lambda_0$. Let $D_r(\lambda_0)$ denote the ball of radius r about λ_0 in the parameter plane. For each $\lambda \in D_r(\lambda_0) \cap C_k$, there is at least one $z_i(\lambda)$ for which $|z_i(\lambda)| < 1$. This follows from the Chain Rule and the fact that $E'_\lambda(z_i) = z_{i+1}$ for all i. Then

$$c_2 = \max_{s=1,\ldots,k-1} |E^s_\lambda(z_i)|$$

is the required upper bound. Similar arguments give a lower bound. □

On C_k we have the "multiplier map." This is the function $\chi : C_k \to D$ where D is the open unit disk and

$$\chi(\lambda) = E'_\lambda(z_i(\lambda)).$$

Proposition 4.5 *Each component of* C_k *is simply connected.*

Proof. Let $G_n(\lambda) = E_\lambda^n(0)$; $\{G_n\}$ is a family of entire functions. Let C be a component of C_k, $\gamma \subset C$, a simple closed curve bounding a region D, and U, a small neighborhood of γ in C. We will show that $D \subset C$.

Since $U \subset C$, the functions $\{G_{nk}\}$ converge to the periodic point $z_0(\lambda)$ on U. By the Lemma, $|z_0(\lambda)| < c_2 < \infty$ on U, so it follows that the $\{G_{nk}\}$ converge on all of D, and the limit function determines a period k periodic point $z_0(\lambda)$ for all λ. By the maximum principle, $|\chi(\lambda)| < 1$ on D, where $\chi(\lambda)$ is the multiplier.

□

Proposition 4.6 *If $k \geq 2$, each component of C_k is unbounded.*

Proof. Let C be a relatively compact component of C_k. We know that $\chi(\lambda)$ is bounded away from 0. Therefore, if $\lambda_i \to \lambda \in \overline{C} - C$, then $|\chi(\lambda)| = 1$.

In order to see that $\chi(C)$ is closed, we take a sequence of points in this set and see that they have a limit point in the set. Consider the sequence $\chi(\lambda_i)$. If we look the sequence of λ_i, it will have limit λ either in $\overline{C} - C$ or C. In the former case, we will have $z_j(\lambda_i) \to z_j'(\lambda)$. Then, $E_\lambda^k(z_j') = z_j'$. The eigenvalue map at λ cannot lie inside the unit circle (otherwise, z_j' would be attracting, and hence $\lambda \in C$). In the latter case, $\chi(\lambda)$ lies inside the unit circle. Thus, $\chi(C)$ is a relatively closed set in D.

But since χ is analytic on C, the image of C is also open. Hence $\chi(C) = D$, but $\chi(\lambda) \neq 0$ if $k \geq 2$, since $\chi(\lambda)$ is bounded away form zero.

□

We remark that the period two region is unique in that it is the only period other than one for which there is a unique component in C_k. All larger periods have infinitely many components.

Problem. Does each component of C_k have only one boundary component?

One may actually say quite a bit more about the eigenvalue map $\chi\colon C_k \to D$ when $k \geq 2$. The proof of the following Theorem involves one of the main tools in complex dynamics, the measurable Riemann Mapping Theorem [Ahl].

Theorem 4.7 *Let C be a connected component of C_k with $k \geq 2$. Let D be the open unit disk in the plane. Then $\chi\colon C \to D^* = D - \{0\}$ is a universal covering.*

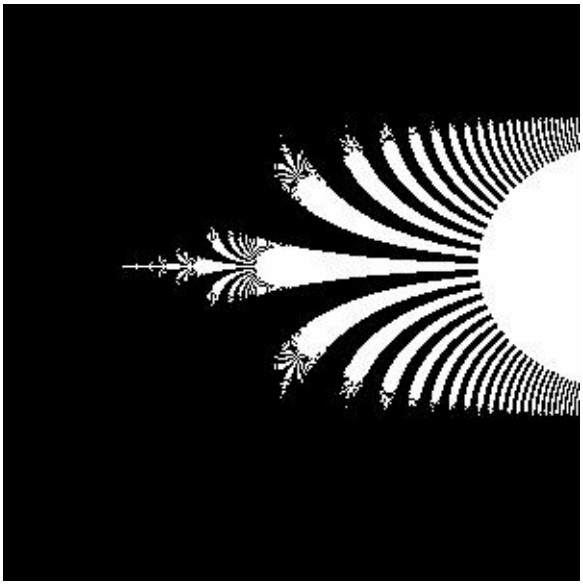

Figure 22: The Julia set for $\lambda = 1/e$.

5 Cantor Bouquets

For quadratic polynomials, as we have seen, there are basically two types of Julia sets: Cantor sets and Julia sets that are connected. For critically finite entire functions there is a similar dichotomy: either the Julia set is the entire plane or else it is nowhere dense and contains Cantor bouquets. In this section we will sketch the construction of a simple Cantor bouquet for the exponential map $E_\lambda(z) = \lambda e^z$ where λ is real and satisfies $0 < \lambda \leq 1/e$. This construction is easily extended to the case of general λ. Much of the work in this section was done in collaboration with Clara Bodelon, Michael Hayes, Michal Krych, Gareth Roberts, Lisa Goldberg, and John Hubbard [Bo1]. [Bo2].

In Figure 22, we display the Julia set for $E_{1/e}$. The complement of the Julia set is displayed in black. It appears that this Julia set contains large open sets, but this in fact is not the case. The Julia set actually consists of uncountably many curves or "hairs" extending to ∞ in the right half plane.

Each of the "fingers" in this Figure seems to have many smaller fingers protruding from them.

As we zoom in to this image, we see more and more of the self-similar

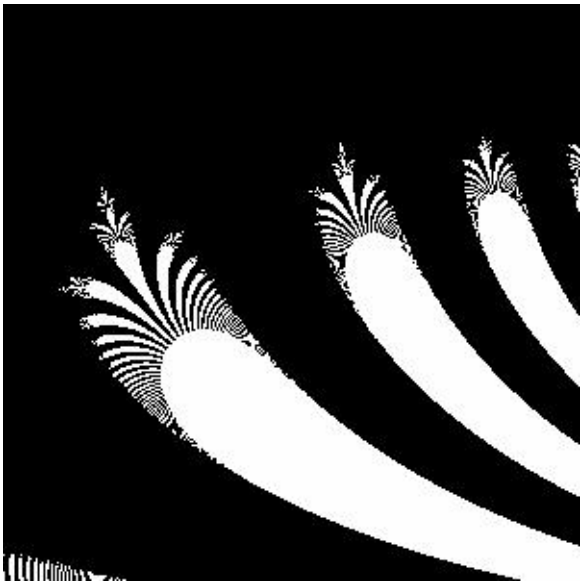

Figure 23: Magnification of the Julia set for $\lambda = 1/e$.

structure, as each finger generates more and more fingers. In fact, each of these fingers consists of a cluster of hairs that are packed together so tightly that the resulting set has Hausdorff dimension 2 [McM1].

5.1 The Idea of the Construction

Here is a rough idea of the construction of a Cantor bouquet. We will "tighten up" some of these ideas in ensuing sections.

Let $E(z) = (1/e)e^z$. As we have seen, E has a neutral fixed point at 1 on the real axis, and $E'(1) = 1$. The vertical line $\operatorname{Re} z = 1$ is mapped to the circle of radius 1 centered at the origin. In fact, E is a contraction in the half plane H to the left of this line, since

$$|E'(z)| = \frac{1}{e} \exp(\operatorname{Re} z) < 1$$

if $z \in H$. Consequently, all points in H have orbits that tend to 1. Hence this half plane lies in the Fatou set. We will try to paint the picture of the Julia set of E by painting instead its complement, the Fatou set.

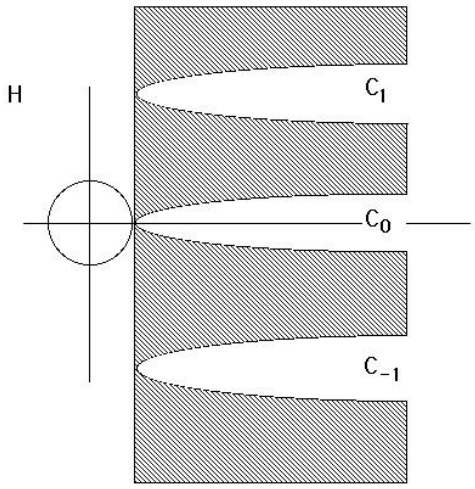

Figure 24: The preimage of H consists of H and the shaded region.

Since the half plane H is forward invariant under E, we can obtain the entire Fatou set by considering all preimages of this half plane. Now the first preimage of H certainly contains the horizontal lines Im $z = (2k+1)\pi$, Re $z \geq 1$, for each integer k, since E maps these lines to the negative real axis which lies in H. Hence there are open neighborhoods of each of these lines that lie in the Fatou set. The first preimage of H is shown in Figure 24. The complement of $E^{-1}(H)$ consists of infinitely many "fingers." The fingers are $2k\pi i$ translates of each other, and each is mapped onto the complementary half plane Re $z \geq 1$.

We denote the fingers in the complement of $E^{-1}(H)$ by C_j with $j \in \mathbb{Z}$, where C_j contains the half line Im $z = 2j\pi$, Re $z \geq 1$, which is mapped into the positive real axis. That is, the C_j are indexed by the integers in order of increasing imaginary part. Note that C_j is contained within the strip $-\frac{\pi}{2} + 2j\pi \leq$ Im $z \leq \frac{\pi}{2} + 2j\pi$.

Now each C_j is mapped in one-to-one fashion onto the entire half plane Re $z \geq 1$. Consequently each C_j contains a preimage of each other C_k. Each of these preimages forms a subfinger which extends to the right in the half plane H. See Figure 25. The complement of these subfingers necessarily lies in the Fatou set.

Now we continue inductively. Each subfinger is mapped onto one of the

Figure 25: The second preimage of H in one of the fingers C_j.

original fingers by E. Consequently, there are infinitely many sub-subfingers which are mapped to the C_j's by E^2. So at each stage we remove the complement of infinitely many subfingers from each remaining finger.

This process is reminiscent of the construction of the Cantor set in Section 3.2. There we removed the complements of pairs of disks; here we remove the complement of infinitely many fingers. As a result, after performing this operation infinitely many times, we do not end up with points. Rather, the intersection of all of these fingers is a simple curve extending to ∞.

This collection of curves forms the Julia set. E permutes these curves and each curve consists of a well-defined endpoint together with a "hair" that extends to ∞. It is tempting to think of this structure as a "Cantor set of curves," i.e., a product of the set of endpoints and the half-line. However, this is not the case as the set of endpoints is not closed.

Note that we can assign symbolic sequences to each point on these curves. We simply watch which of the C_j's these orbit of the point lies in after each iteration and assign the corresponding index j. That is, to each hair in the Julia set we attach an infinite sequence $s_0 s_1 s_2 \ldots$ where $s_j \in \mathbb{Z}$ and $s_j = k$ if the j^{th} iterate of the hair lies in C_j. The sequence $s_0 s_1 s_2 \ldots$ is called the *itinerary* of the curve.

For example, the portion of the real line $\{x \mid x \geq 1\}$ lies in the Julia set since all points (except 1) tend to ∞ under iteration, not to the fixed point, and this hair has itinerary $(000\ldots)$.

Another temptation is to say that there is a hair corresponding to ev-

ery sequence $s_0 s_1 s_2 \ldots$. This, unfortunately, is not true either, as certain sequences simply grow too quickly to correspond to orbits of E. It is known [Dev] that a sequence $(s_0 s_1 s_2 \ldots)$ is allowable in the sense that it corresponds to a point in $J(E_\lambda)$ if and only if there exists $x \in \mathbb{R}$ such that $|2\pi s_j| < E^j(x)$ for each j. Here, $E(z) = e^z$.

So this is a rough picture of $J(E)$: a "hairy" object extending toward ∞ in the right-half plane. We call this object a *Cantor bouquet*. We will see that this bouquet has some rather interesting topological properties as we investigate further.

5.2 Cantor N-Bouquets

In this section we begin the construction of a Cantor bouquet. We first construct a Cantor set on which E_λ is conjugate to the shift map on $2N+1$ symbols.

The graph of E_λ (see Figure 26) shows that E_λ has two fixed points on the real axis, an attracting fixed point at q_λ and a repelling fixed point at p_λ, with $0 < q_\lambda < p_\lambda$. Note that $q_\lambda < -\log\lambda < p_\lambda$ since

$$E'_\lambda(q_\lambda) < 1 = E'_\lambda(-\log\lambda) < E'_\lambda(p_\lambda).$$

Fix a real number ℓ_λ satisfying $-\log\lambda < \ell_\lambda < p_\lambda$ and observe that, if $\operatorname{Re} z \geq \ell_\lambda$, then

$$|E'_\lambda(z)| = \lambda e^{\operatorname{Re} z} \geq \lambda e^{\ell_\lambda} > \mu > 1$$

for some constant $\mu > 1$. Thus E_λ is "expanding" in the half plane $\operatorname{Re} z \geq \ell_\lambda$.

Note also that E_λ maps the half plane $\operatorname{Re} z < \ell_\lambda$ inside itself, in fact to the disk of radius $E_\lambda(\ell_\lambda)$ centered at 0, since $E_\lambda(\ell_\lambda) < \ell_\lambda$. Now E_λ has a fixed point in this half plane, namely q_λ. See Figure 27. It follows from the Corollary to the Schwarz lemma that all orbits in this half plane tend to q_λ, and so the Julia set of E_λ is contained in the right-half plane $\operatorname{Re} z \geq \ell_\lambda$.

We will now construct a collection of invariant Cantor sets for E_λ in the right-half plane $\operatorname{Re} z \geq \ell_\lambda$ on which E_λ is conjugate to the one-sided shift map on $2N+1$ symbols. Fix an integer $N \geq 1$. Consider the rectangle B_N bounded as follows:

1. on the left by $\operatorname{Re} z = \ell_\lambda$;

2. above and below by $\operatorname{Im} z = \pm(2N+1)\pi$;

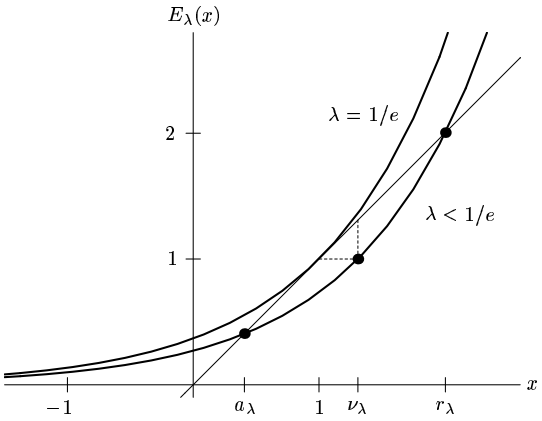

Figure 26: The graphs of E_λ for $\lambda = 1/e$ and $\lambda < 1/e$.

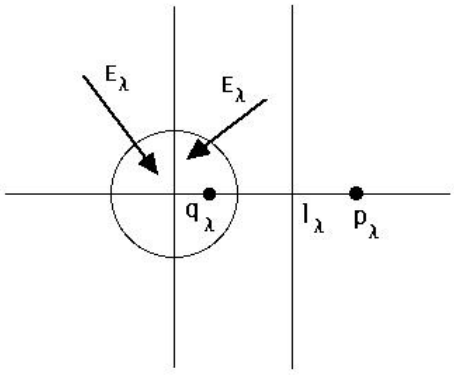

Figure 27: E_λ maps the half plane $\operatorname{Re} z < \ell_\lambda$ inside the disk.

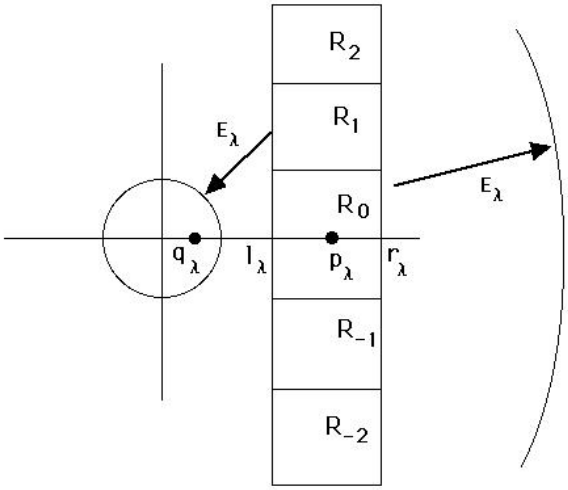

Figure 28: Construction of the R_i

3. on the right by Re $z = r_\lambda$ where r_λ satisfies $\lambda e^{r_\lambda} > r_\lambda + (2N+1)\pi$.

The inequality in part 3 guarantees that E_λ maps the right-hand edge of the rectangle to a circle of radius λe^{r_λ} centered at 0 that contains the entire rectangle B_N in its interior. Note also that E_λ maps B_N onto the annular region $\{z \,|\, \lambda e^{\ell_\lambda} \leq |z| \leq \lambda e^{r_\lambda}\}$ and that B_N is contained in the interior of this annulus.

For each integer i with $-N \leq i \leq N$, consider the subrectangle $R_i \subset B_N$ defined by $\ell_\lambda \leq$ Re $z \leq r_\lambda$ and $(2i-1)\pi \leq$ Im $z \leq (2i+1)\pi$. Note that E_λ maps each R_i onto the annular region above, and that $|E'_\lambda(z)| > \mu > 1$. Moreover, if we restrict E_λ to the interior of R_i we obtain an expanding analytic homeomorphism that maps the interior of R_i onto a region that covers all of B_N. See Figure 28. As a consequence, we may define an analytic branch of the inverse of E_λ, $L_{\lambda,i}$, that takes B_N into R_i for each i. Clearly, $L_{\lambda,i}$ is a contraction for each i. In particular, there is a constant $\nu < 1$ such that $|L'_{\lambda,i}(z)| < \nu$ for all i and all z in B_N.

Now define

$$\Lambda_N = \{z \in B_N | E^j_\lambda(z) \in B_N \text{ for } j = 0, 1, 2, \ldots\},$$

that is, Λ_N is the set of points whose orbits remain for all iterations in B_N. Let Σ_N denote the space of infinite sequences $s = (s_0 s_1 s_2 \ldots)$ where each s_j

is an integer, $-N \leq s_j \leq N$. Endow Σ_N with the product topology. For each $s \in \Sigma_N$, we identify a unique point in Λ_N via

$$\phi(s) = \lim_{n\to\infty} L_{\lambda,s_0} \circ L_{\lambda,s_1} \circ \cdots \circ L_{\lambda,s_n}(z)$$

where z is any point in B_N. The fact that $\phi(s)$ is a unique point follows from the fact that each L_{λ,s_i} is a contraction in B_N. In fact $\phi(s)$ is independent of z, and ϕ defines a homeomorphism between Σ_N and Λ_N. Moreover, ϕ gives a conjugacy between the shift map on the sequence space Σ_N and $E_\lambda|\Lambda_N$.

Since $|E'_\lambda(z)| > \mu > 1$ for all $z \in \Lambda_N$, it follows that Λ_N is a hyperbolic set. Moreover, we have an increasing sequence of these Cantor sets $\Lambda_1 \subset \Lambda_2 \subset \ldots$. Since each point in Λ_N lies in the complement of the basin of attraction of q_λ, it follows that $\Lambda_N \subset J(E_\lambda)$. We have proved:

Theorem 5.1 *Suppose $0 < \lambda < 1/e$. Then the set of points Λ_N whose orbit remains for all time in the rectangle B_N is a Cantor set in $J(E_\lambda)$. The action of E_λ on this Cantor set is conjugate to the shift map on $2N+1$ symbols.*

We next claim that each point $z_s = \phi(s)$ in one of the Λ_i comes with a unique "hair" attached. This hair is a curve associated with a natural parametrization

$$h_{\lambda,s}\colon [1,\infty) \to \mathbb{C}$$

that satisfies

1. $h_{\lambda,s}(1) = z_s$;
2. $h_{\lambda,s}$ is a homeomorphism;
3. If $t \neq 1$, then $\text{Re } E_\lambda^n(h_{\lambda,s}(t)) \to \infty$ as $n \to \infty$;
4. For each t, $h_{\lambda,s}(t)$ lies in the horizontal strip
$$(2s_0 - 1)\pi < \text{Im } z < (2s_0 + 1)\pi;$$
5. $E_\lambda(h_{\lambda,s}(t)) = h_{\lambda,\sigma(s)}(E_{1/e}(t))$ where $\sigma(s)$ denotes the shift applied to the sequence s.

By condition 3, the orbit of $h_{\lambda,s}(t)$ tends to ∞. Hence this point does not lie in the basin of attraction of q_λ and as a consequence each point on a hair also lies in the Julia set.

To define $h_{\lambda,s}$, recall that $E_{1/e}$ has a unique fixed point at 1 and that $E_{1/e}\colon [1,\infty) \to [1,\infty)$. If $t > 1$, then $E^n_{1/e}(t) \to \infty$ as $n \to \infty$. Recall that L_{λ,s_i} is the branch of the inverse of E_λ that will now take values in the horizontal strip given by

$$(2s_i - 1)\pi \leq \text{Im } z \leq (2s_i + 1)\pi.$$

Then define

$$h_{\lambda,s}(t) = \lim_{n\to\infty} L_{\lambda,s_0} \circ \ldots \circ L_{\lambda,s_{n-1}}(E^n_{1/e}(t)).$$

It can be shown that $h_{\lambda,s}$ has all of the properties listed above. See [DK].

Thus, for each $N \geq 1$, we have a map

$$H_\lambda\colon \Sigma_N \times [1,\infty) \to \mathbb{C}.$$

This map is also a homeomorphism. We call the image of H_λ a *Cantor N-bouquet* and denote it by $\mathcal{B}_{\lambda,N}$.

These Cantor N-bouquets form the skeleton of the Julia set. Indeed, every repelling periodic point has bounded itinerary, and hence lies in some $\mathcal{B}_{\lambda,N}$ for some N. In particular, such a point lies at the endpoint of a hair in some Cantor N-bouquet (and hence any M-bouquet for $M > N$). This means that the N-bouquets are dense in the Julia set. So

$$J(E_\lambda) = \text{ Closure of } \cup_{N=1}^{\infty} \mathcal{B}_{\lambda,N}.$$

We call the closure of the union of the N-bouquets a *Cantor bouquet.*

Now there are points in the Cantor bouquet that do not lie in $\mathcal{B}_{\lambda,N}$ for any N. Indeed, there are many points whose itineraries are unbounded. To understand these points, we need to introduce the notion of a straight brush. This is the topic of the following section.

5.3 Straight Brushes

To describe more completely the structure of a Cantor bouquet, we introduce the notion of a *straight brush* due to Aarts and Oversteegen [AO].

To each irrational number ζ, we assign an infinite string of integers $n_0 n_1 n_2 \ldots$ as follows. We will break up the real line into open intervals $I_{n_0 n_1 \ldots n_k}$ which have the following properties

1. $I_{n_0 \ldots n_k} \supset I_{n_0 \ldots n_{k+1}}$;

2. The endpoints of $I_{n_0 \ldots n_k}$ are rational;

3. $\zeta = \bigcap_{k=1}^{\infty} I_{n_0 \ldots n_k}$.

Now there are many ways to do this. We choose the following method based on the Farey tree. Inductively, we first define $I_k = (k, k+1)$. Given $I_{n_0 \ldots n_k}$ we define $I_{n_0 \ldots n_k j}$ as follows. Let

$$I_{n_0 \ldots n_k} = \left(\frac{\alpha}{\beta}, \frac{\gamma}{\delta} \right).$$

Let $p_0/q_0 = (\alpha + \gamma)/(\beta + \delta)$, the Farey child of α/β and γ/δ. Let p_n/q_n be the Farey child of p_{n-1}/q_{n-1} and γ/δ for $n > 0$, and let p_{n-1}/q_{n-1} be the Farey child for α/β and p_n/q_n for $n \leq 0$. We then set $I_{n_0 \ldots n_k j}$ to be the open interval $(p_j/q_j, p_{j+1}/q_{j+1})$.

Example. $I_0 = (0, 1)$. The Farey child of $0/1$ and $1/1$ is $1/2$, so $p_0/q_0 = 1/2$. Then $p_1/q_1 = \frac{1}{2} \oplus \frac{1}{1} = 2/3$, $p_2/q_2 = \frac{2}{3} \oplus \frac{1}{1} = \frac{3}{4}$, and $p_n/q_n = n+1/n+2$ for $n > 0$.

For the remaining n we have

$$\begin{aligned} p_{-1}/q_{-1} &= \frac{0}{1} \oplus \frac{1}{2} = \frac{1}{3} \\ p_{-2}/q_{-2} &= \frac{0}{1} \oplus \frac{1}{3} = \frac{1}{4} \\ p_{-n}/q_{-n} &= \frac{1}{n+2}. \end{aligned}$$

Therefore, if $n \geq 0$,

$$I_{0n} = \left(\frac{n+1}{n+2}, \frac{n+2}{n+3} \right)$$

and if $n < 0$,

$$I_{0n} = \left(\frac{1}{-n+2}, \frac{1}{-n+1} \right).$$

See Figure 29. Note that we exhaust all of the rationals via this procedure, so each irrational is contained in a unique $I_{n_0 n_1 \ldots}$.

We now define a straight brush.

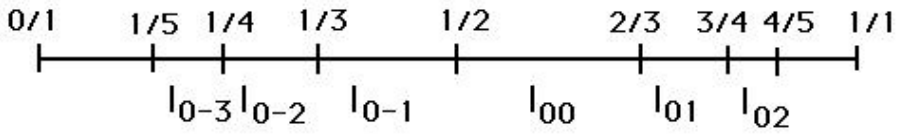

Figure 29: Construction of I_{0n}.

Definition 5.2 *A straight brush B is a subset of $[0,\infty)\times\mathcal{N}$, where $\mathcal{N}$ is a dense subset of irrationals. B has the following 3 properties.*

1. *B is "hairy" in the following sense. If $(y,\alpha)\in B$, then there exists a $y_\alpha \le y$ such that $(t,\alpha)\in B$ iff $t\ge y_\alpha$. That is, the "hair" (t,α) is contained in B where $t\ge y_\alpha$. y_α is called the endpoint of the hair corresponding to α.*

2. *Given an endpoint $(y_\alpha,\alpha)\in B$ there are sequences $\beta_n\uparrow\alpha$ and $\gamma_n\downarrow\alpha$ in $\mathcal{N}$ such that $(y_{\beta_n},\beta_n)\to(y_\alpha,\alpha)$ and $(y_{\gamma_n},\gamma_n)\to(y_\alpha,\alpha)$. That is, any endpoint of a hair in B is the limit of endpoints of other hairs from both above and below.*

3. *B is a closed subset of $\mathbb{R}^2$.*

Exercise. For any rational number v and any sequence of irrationals $\alpha_n\in\mathcal{N}$ with $\alpha_n\to v$, show that the hairs $[y_{\alpha_n},\alpha_n]$ must tend to $[\infty,v]$ in $[0,\infty)\times\mathbb{R}$.

Exercise. Show that condition 2 in the definition of a straight brush may be changed to: if (y,α) is any point in B (y need not be the endpoint of the α-hair), then there are sequences $\beta_n\uparrow\alpha$, $\gamma_n\downarrow\alpha$ so that the sequences $(y_{\beta_n},\beta_n)\to(y,\alpha)$ and $(y_{\gamma_n},\gamma_n)\to(y,\alpha)$ in B.

Exercise. Let $(y,\alpha)\in B$ and suppose y is not the endpoint y_α. Prove that (y,α) is inaccessible in $\mathbb{R}^2$ in the sense that there is no continuous curve $\gamma:[0,1]\to\mathbb{R}^2$ such that $\gamma(t)\notin B$ for $0\le t<1$ and $\gamma(1)=(y,\alpha)$.

Exercise. Prove that (y_α,α) is accessible in $\mathbb{R}^2$.

These exercises show that a straight brush is a remarkable object from the topological point of view. Let's view a straight brush as a subset of the

Riemann sphere and set $B^* = B \cup \infty$, i.e., the straight brush with the point at infinity added. Let $\mathcal{E}$ denote the set of endpoints of B, and let $\mathcal{E}^* = \mathcal{E} \cup \infty$. Then we have the following result, due to Mayer [Ma]:

Theorem 5.3 *The set $\mathcal{E}^*$ is a connected set, but $\mathcal{E}$ is totally disconnected.*

That is, the set $\mathcal{E}^*$ is a connected set, but if we remove just one point form this set, the resulting set is totally disconnected. Topology really is a weird subject!

The reason for this is that, if we draw the straight line in the plane (γ, t) where γ is a fixed rational, and then we adjoin the point at infinity, we find a disconnection of $\mathcal{E}$. This, however, is not a disconnection of $\mathcal{E}^*$. Moreover, the fact that any non-endpoint in B is inaccessible shows that we cannot disconnect $\mathcal{E}^*$ by any other curve.

Remark. Aarts and Oversteegen have shown that any two straight brushes are ambiently homeomorphic, i.e., there is a homeomorphism of $\mathbb{R}^2$ taking one brush onto the other. This leads to a formal definition of a Cantor bouquet.

Definition 5.4 *A Cantor bouquet is a subset of $\overline{\mathbb{C}}$ that is homeomorphic to a straight brush (with ∞ mapped to ∞).*

Our main goal in this section is to sketch a proof of the following result:

Theorem 5.5 *Suppose $0 < \lambda < 1/e$. Then $J(E_\lambda)$ is a Cantor bouqet.*

Proof. To construct the homeomorphism between the brush and $J(E_\lambda)$ we first introduce symbolic dynamics. Recall that E_λ has a repelling fixed point $p_\lambda > 0$ in $\mathbb{R}$ and that the half plane $\operatorname{Re} z < p_\lambda$ lies in the Fatou set. Similarly the horizontal strips

$$\frac{\pi}{2} + 2k\pi < \operatorname{Im} z < \frac{\pi}{2} + (2k+1)\pi$$

are contained in the Fatou set since E_λ maps these strips to $\operatorname{Re} z < 0$ which is contained in $\operatorname{Re} z < p_\lambda$.

We denote by S_k the closed halfstrip given by

$$\operatorname{Re} z \geq p_\lambda \text{ and } -\frac{\pi}{2} + 2k\pi \leq \operatorname{Im} z \leq \frac{\pi}{2} + 2k\pi.$$

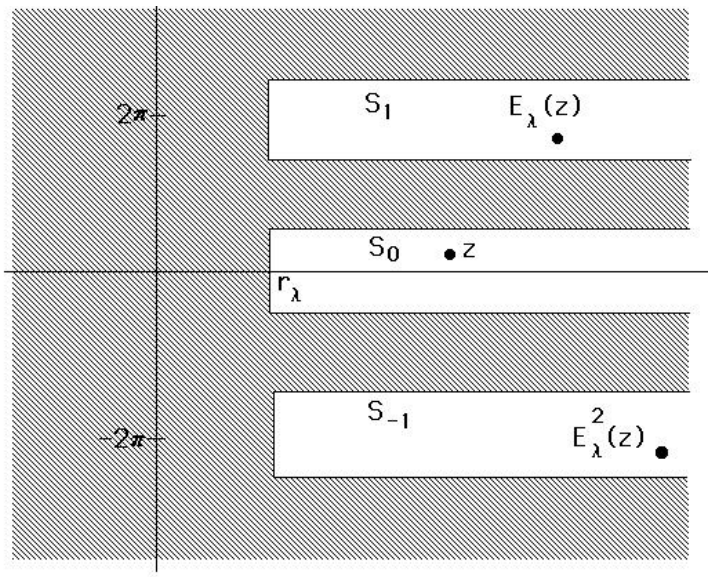

Figure 30: The itinerary of z is $0, 1, -1, \ldots$.

Note that these strips contain the Julia set since the complement of the strips lies in the Fatou set.

Given $z \in J(E_\lambda)$, we define the itinerary of z, $S(z)$, as usual by

$$S(z) = s_0 s_1 s_2 \ldots$$

where $s_j \in \mathbb{Z}$ and $s_j = k$ iff $E_\lambda^j(z) \in S_k$. Note that $S(z)$ is an infinite string of integers that indicates the order in which the orbit of z visits the S_k. We will associate to z the irrational number given by the itinerary of z (and the decomposition of the irrationals described above). This will determine the hair in the straight brush to which z is mapped. See Figure 30. Thus we need only define the y-value along this hair. This takes a little work.

We will construct a sequence of rectangles $R_k(j)$ for each $j, k \geq 0$. The point $E_\lambda^j(z)$ will be contained in $R_k(j)$ for each $k \geq 0$. And we will have $R_{k+1}(j) \subset R_k(j)$ for each j and k. Each $R_k(j)$ will have sides parallel to the axes and be contained in a strip S_α. Finally each $R_k(j)$ will have height π. Since the $R_k(j)$ are nested with respect to k, the intersection $\bigcap_{k=0}^{\infty} R_k(j)$ will be a nonempty rectangle of height π that contains $E_\lambda^j(z)$. We then define $h(z)$ to be the real part of the left hand edge of this limiting rectangle.

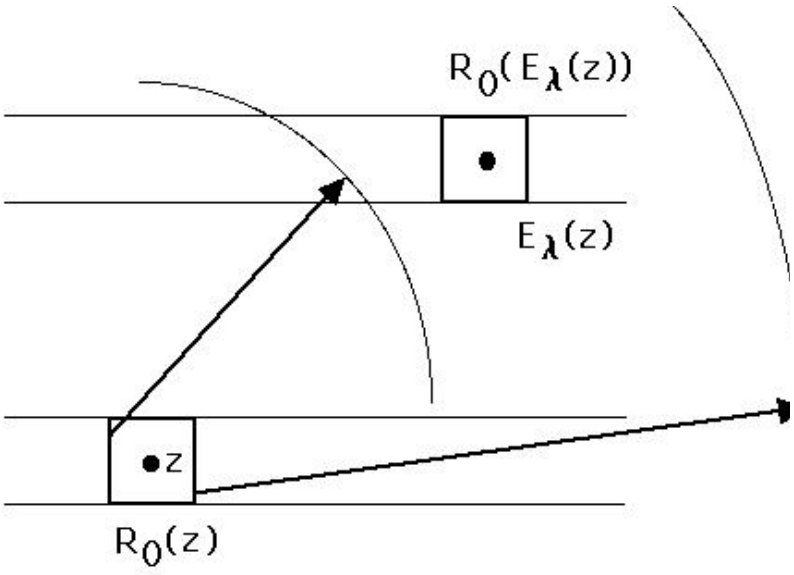

Figure 31: Construction of $R_0(0)$ and $R_0(1)$.

To begin the construction, we set $R_0(j)$ to be the square centered at $E_\lambda^j(z)$ with sidelength π and contained in the appropriate strip S_α. Observe that $E_\lambda(R_0(j)) \supset R_0(j+1)$. Indeed, the image of $R_0(j)$ is an annulus whose inner radius is $e^{-\pi/2}|E_\lambda^{j+1}(z)|$ and outer radius $e^{\pi/2}|E_\lambda^{j+1}(z)|$. Now $e^{\pi/2} > 4$ and $e^{-\pi/2} < 1/4$ so the image annulus is much larger than $R_0(j+1)$. See Figure 31.

It follows that we may find a narrower rectangle $R_1(j)$ strictly contained in $R_0(j)$ having the property that the height of $R_1(j)$ is π and the image $E_\lambda(R_1(j))$ just covers $R_0(j+1)$. That is, $R_1(j)$ is the smallest rectangle in $R_0(j)$ whose image annulus is just wide enough so that $R_0(j+1)$ fits inside. See Figure 32. Note that $E_\lambda^j(z) \in R_1(j)$.

Continue inductively by setting $R_k(j)$ to be the subrectangle of $R_{k-1}(j)$ whose image just covers $R_{k-1}(j+1)$. The $R_k(j)$ are clearly nested for each fixed j.

Example. Suppose $z = p_\lambda$. We have that $R_0(j)$ is the square bounded by $\text{Re } z = p_\lambda \pm \pi/2$ and $\text{Im } z = \pm\pi/2$ for each j. One may check that, for each j, $\bigcap_{k=0}^{\infty} R_k(j)$ is the strip bounded by $\text{Re } z = p_\lambda$ and $\text{Re } z = \zeta$ where the circle of radius λe^ζ passes through $\zeta \pm i\pi/2$. See Figure 33.

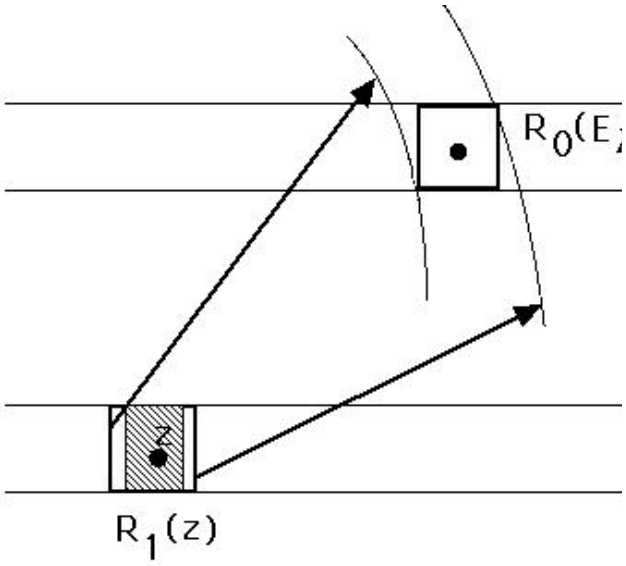

Figure 32: Construction of $R_1(0)$.

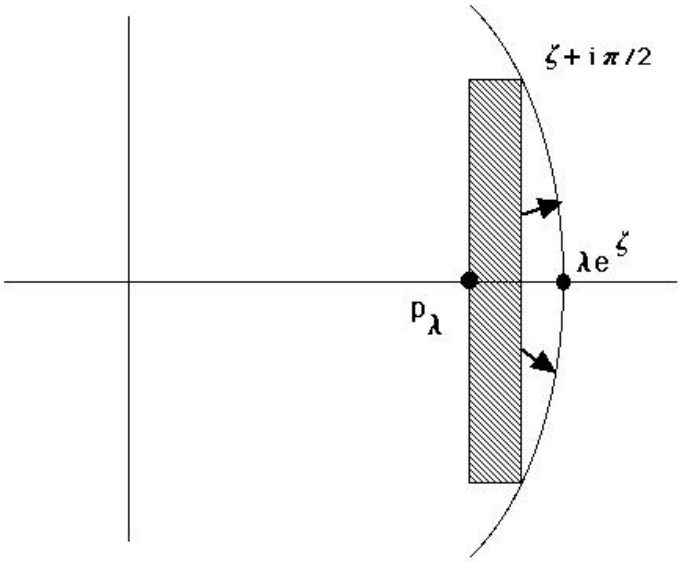

Figure 33: The intersection of $R_j(0)$.

Suppose z has itinerary $S(z) = s_0 s_1 s_2 \ldots$. Let $I(S(z))$ denote the irrational number determined by the sequence $S(z)$ as above. Then set $\phi(z) = (h(z), I(S(z)))$. Then, as shown in [AO], ϕ is a homeomorphism onto a straight brush.

5.4 Connectedness Properties of Cantor Bouquets

We call the set of endpoints of a Cantor bouquet the *crown*. Since a Cantor bouquet is homeomorphic to a straight brush with the points at ∞ coinciding, it follows that any Cantor bouquet has the amazing connectedness property that the crown together with ∞ is connected, but the crown alone is totally disconnected. Note also that the bouquet is nowhere locally connected (except at ∞).

It can be shown that the construction above works for any exponential for which there exists an attracting or neutral periodic point. However, in the general case, some of the hairs in the Cantor bouquet may be attached to the same point in the crown. We will discuss this phenomenon in detail in Section 8.

McMullen [McM] has shown that the Hausdorff dimension of the Cantor bouquet constructed above is 2 but its Lebesgue measure is zero. This accounts for why figures 22 and 23 seem to have open regions in the Julia set. Also, Viana [V] has shown that each of the hairs in the Cantor bouquet is actually a C^∞ curve.

Cantor bouquets arise in many critically finite entire maps. In order to see this, suppose all singular points of F lie in some disk B_r of radius r centered at the origin. Consider the preimage $F^{-1}(\mathbb{C} - B_r)$ and let U be any component of this set. Now F maps U analytically onto $C - B_r$ without singular values, so F must be a universal covering. As such, F acts like an exponential map. If, in fact, U is disjoint from $\mathbb{C} - B_r$ and F has sufficient growth in U, it can be shown (see [DT]) that there is an invariant Cantor bouquet for F in U. For a specific example dealing with the complex standard map $z \mapsto z + \omega + \epsilon \sin z$ we refer to [Fa].

Exercise. Construct a similar Cantor bouquet for the map $S_\lambda(z) = \lambda \sin z$ when $0 < \lambda < 1$. *Hint:* The rectangles will now be arranged vertically and there will be two bouquets: one in the upper half plane and one in the lower.

5.5 Uniformization of the Attracting Basin

The basin of attraction Ω_λ of E_λ is an open, dense, and simply connected subset of the Riemann sphere. Hence the Riemann Mapping Theorem guarantees the existence of a uniformization $\phi_\lambda \colon D \to \Omega_\lambda$. Given such a uniformization, it is natural to ask if the uniformizing map extends to the boundary of D.

In order to extend ϕ_λ to the boundary, we need that the image of a straight ray $re^{i\theta}$ where θ is constant under ϕ_λ converges to a single point as $r \to 1$. It is known that if the boundary of the uniformizing region is locally connected, then in fact ϕ_λ does extend continuously to D. On the other hand, if the boundary of the region is not locally connected, then not all rays need converge (though a full measure set of them must converge). In our case, the boundary of Ω_λ is nowhere locally connected (except at ∞). However, it is a fact that all rays do converge. In fact, they land at precisely the endpoints of the Cantor bouquet. See [DG]. This means that we can induce a map on the set of endpoints, but that map is necesarily nowhere continuous [Pi].

Exercise. Show that if we normalize the Riemann map ϕ_λ so that 0 is mapped to 0, then the induced map $\phi_\lambda^-1 \circ E_\lambda \circ \phi_\lambda$ on the unit disk is given by

$$T_\mu(z) = \exp\left(i\left(\frac{\mu + \overline{\mu}}{1+z}\right)\right).$$

Here μ is a parameter that lies in the upper half plane and depends upon λ.

Exercise. Discuss the dynamics of T_μ on the boundary of the unit disk.

Remark. While the Cantor bouquets constructed in this exercise are homeomorphic to those for E_λ, McMullen has shown [McM1] that the Lebesgue measure of the Cantor bouquet in the exponential case is zero whereas it is infinite in the case of the sine function. The rough reason for this is, in the case of sine, we have two Cantor bouquets, so most orbits tend to infinity by jumping back and forth between these two bouquets. So there are lots of additional itineraries. In the exponential case, orbit that tend to infinity just do so by heading to the right.

We have seen that a Cantor bouquet is a very interesting object from the topological point of view. But there is more to this story. For Karpinska has shown the following remarkable result [Kar]:

Theorem 5.6 *The Julia set of E_λ with $0 < \lambda < 1/e$ divides into two disjoint subsets: the "small" set consisting of the endpoints and the "large" set*

consisting of all the other points, i.e., the stems without the endpoints. The Hausdorff dimension of the set of stems is 1*, but the Hausdorff dimension of the "smaller" set of endpoints is* 2*!*

6 Indecomposable Continua

As we have seen, the Julia set of the exponential function $E_\lambda(z) = \lambda e^z$ is a rich structure from the topological point of view. For many values of λ, the Julia set contains Cantor bouquets. For other values of λ, the Julia set is the entire plane. Now it might appear that this type of Julia set, while quite chaotic dynamically, is "tame" topologically. As we will see in this section, this is far from the truth: There are invariant sets for E_λ that are homeomorphic to complicated sets known as indecomposable continua. Specifically, we will investigate in this section the dynamics of E_λ when λ is real and $\lambda > 1/e$. As we have seen, the Julia set of E_λ is the entire plane in this case.

Consider the horizontal strip

$$S = \{z \,|\, 0 \leq \text{Im } z \leq \pi\}$$

(or its symmetric image under $z \to \overline{z}$). The exponential map E_λ takes the boundary of S to the real axis and the interior of S to the upper half plane. Thus, E_λ maps certain points outside of S while other points remain in S after one application of E_λ. Our goal is to investigate the set of points whose entire orbit lie in S. Call this set Λ. The set Λ is clearly invariant under E_λ. There is a natural way to compactify this set in the plane to obtain a new set Γ. Moreover, the exponential map extends to Γ in a natural way. Our main results in this section include:

Theorem 6.1 Γ *is an indecomposable continuum.*

Moreover, we will see that Λ is constructed in similar fashion to a family of indecomposable continua known as *Knaster continua.*

As we will show in Section 6.2, the topology of Λ is quite intricate. Despite this, we will show that the dynamics of E_λ on Λ is quite tame. Specifically, we will prove:

Theorem 6.2 E_λ *has a unique repelling fixed point* $w_\lambda \in \Lambda$*, and the* α*-limit set of all points in* Λ *is* w_λ*. On the other hand, if* $z \in \Lambda$*,* $z \neq w_\lambda$*, then the* ω*-limit set of* z *is either*

1. *the point at ∞, or*

2. *the orbit of 0 under E_λ together with the point at ∞.*

Thus we see that E_λ possesses an interesting mixture of topology and dynamics in the case where the Julia set is the whole plane. When $J = \mathbb{C}$, the dynamics of E_λ are quite chaotic, but the overall topology is tame. On our invariant set Λ, however, it is the topology that is rich, but the dynamics are tame.

6.1 Topological Preliminaries

In this section we review some of the basic topological ideas associated with indecomposable continua. See [Ku] for a more extensive introduction to these concepts.

Recall that a continuum is a compact, connected space. A continuum is decomposable if it is the union of two proper subcontinua (we emphasize the fact that these subcontinua are not disjoint but rather overlap). Otherwise, the continuum is indecomposable. One famous example of an indecomposable continuum is the Knaster continuum, K. One way to construct this set is to begin with the Cantor middle-thirds set sitting on the real axis in the plane between $x = 0$ and $x = 1$. Then draw the semi-circles lying in the upper half plane with center at $(1/2, 0)$ that connect each pair of points in the Cantor set that are equidistant from $1/2$. Next draw all semicircles in the lower half plane that have, for each $n \geq 1$, centers at $(5/(2 \cdot 3^n), 0)$ and pass through each point in the Cantor set lying in the interval

$$2/3^n \leq x \leq 1/3^{n-1}.$$

The resulting set is partially depicted in Figure 34.

For a proof that this set is indecomposable, we refer to [Ku]. Dynamically, this set appears as the closure of the unstable manifold of Smale's horseshoe map (see [Ba], [Sm]).

Note that the curve passing through the origin in this set is dense, since it passes through each of the endpoints of the Cantor set. It also accumulates everywhere upon itself. Such a phenomenon gives a criterion for a continuum to be indecomposable, as was shown by S. Curry. See his paper [Cu] for a proof.

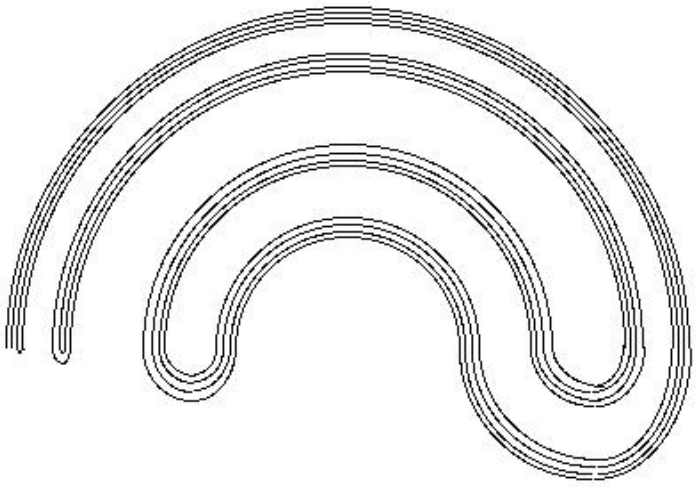

Figure 34: The Knaster Continuum.

Theorem 6.3 *Suppose X is a one-dimensional nonseparating plane continuum which is the closure of a ray that limits upon itself. Then X is indecomposable.*

Another view of the Knaster continuum which is intimately related to our own construction is as follows. Begin with the unit square S_0 in the plane. Next remove a "canal" C_1 from S_0 whose boundary lies within a distance $1/3$ of each boundary point of S_0 as depicted in Figure 2. Call this set S_1. Next remove a new canal C_2 from S_1. This time the boundary of C_2 should be within $1/9$ of the boundary of S_1 as depicted in Figure 35. It is possible to continue this construction inductively in such a way that the resulting set is homeomorphic to the Knaster continuum.

6.2 Construction of Λ

Recall that the strip S is given by $\{z \mid 0 \leq \text{Im } (z) \leq \pi\}$. Note that E_λ maps S in one-to-one fashion onto $\{z \mid \text{Im } z \geq 0\} - \{0\}$. Hence E_λ^{-1} is defined on $S - \{0\}$ and, in fact, E_λ^{-n} is defined for all n on $S - \{\text{orbit of } 0\}$. We will always assume that E_λ^{-n} means E_λ^{-n} restricted to this subset of S.

Define

$$\Lambda = \{z \mid \ E_\lambda^n(z) \in S \text{ for all } n \geq 0\}.$$

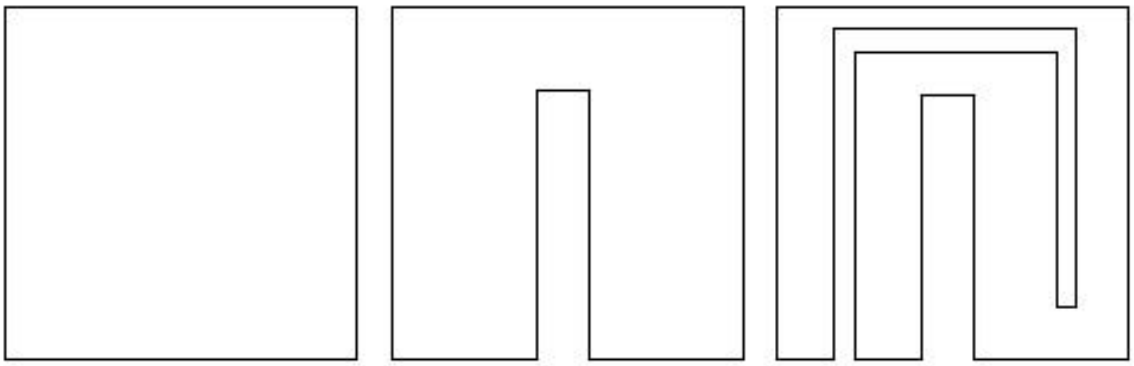

Figure 35: A different construction of the Knaster Continuum.

If $z \in \Lambda$ it follows immediately that $E_\lambda^n(z) \in S$ for *all* $n \in \mathbb{Z}$ provided z does not lie on the forward orbit of 0. Our goal is to understand the structure of Λ. Toward that end we define L_n to be the set of points in S that leave S at precisely the n^{th} iteration of E_λ. That is,

$$L_n = \{z \in S \mid E_\lambda^i(z) \in S \text{ for } 0 \leq i < n \text{ but } E_\lambda^n(z) \notin S\}.$$

Let B_n be the boundary of L_n.

Recall that E_λ maps a vertical segment in S to a semi-circle in the upper half plane centered at 0 with endpoints in $\mathbb{R}$. Either this semi-circle is completely contained in S or else an open arc lies outside S. As a consequence, L_1 is an open, simply connected region which extends to ∞ toward the right in S as shown in Figure 36. There is a natural parametrization $\gamma_1 \colon \mathbb{R} \to B_1$ defined by

$$E_\lambda(\gamma_1(t)) = t + i\pi.$$

As a consequence,

$$\lim_{t \to \pm\infty} \text{Re } \gamma_1(t) = \infty.$$

If $c > 0$ is large, the segment Re $z = c$ in S meets $S - L_1$ in two vertical segments v_+ and v_- with Im v_- > Im v_+. E_λ maps v_- to an arc of a circle in $S \cap \{z \mid \text{Re } z < 0\}$ while E_λ maps v_+ to an arc of a circle in $S \cap \{z \mid \text{Re } z > 0\}$. As a consequence, if c is large, v_+ meets L_2 in an open interval. Since $L_2 = E_\lambda^{-1}(L_1)$, it follows that L_2 is an open simply connected subset of S

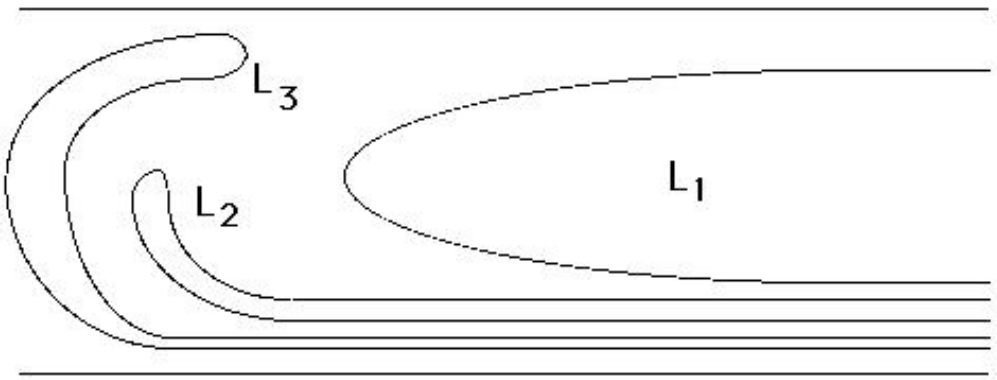

Figure 36: Construction of the L_n.

that extends to ∞ in the right half plane *below* L_1, at least in the far right half-plane.

Continuing inductively, we see that L_n is an open, simply connected subset of S that extends to ∞ toward the right in S. We may also parametrize the boundary B_n of L_n by $\gamma_n\colon \mathbb{R} \to B_n$ where

$$E_\lambda^n(\gamma_n(t)) = t + i\pi$$

as before. Again

$$\lim_{t\to\pm\infty} \text{Re } \gamma_n(t) = \infty.$$

Since each L_n is open, it follows that Λ is a closed subset of S.

Proposition 6.4 *Let $J_n = \bigcup_{i=n}^{\infty} B_i$. Then J_n is dense in Λ for each $n > 0$.*

Proof. Let $z \in \Lambda$ and suppose $z \notin B_i$ for any i. Let U be an open connected neighborhood of z. Fix $n > 0$. Since $E_\lambda^i(z) \in S$ for all i, we may choose a connected neighborhood $V \subset U$ of z such that $E_\lambda^i(V) \subset S$ for $i = 0, \ldots, n$.

Now the family of functions $\{E_\lambda^i\}$ is not normal on V, since z belongs to the Julia set of E_λ. Consequently, $\bigcup_{i=0}^{\infty} E_\lambda^i(V)$ covers $\mathbb{C} - \{0\}$. In particular, there is $m > n$ such that $E_\lambda^m(V)$ meets the exterior of S. Since $E_\lambda^m(z) \in S$, it follows that $E_\lambda^m(V)$ meets the boundary of S. Applying E_λ^{-m}, we see that B_m meets V.

In fact, it follows that for any $z \in \Lambda$ and any neighborhood U of z, all but finitely many of the B_m meet V. This follows from the fact that E_λ has fixed points outside of S (in fact one such point in each horizontal strip of width 2π—see [DK]), so we may assume that $E_\lambda^m(V)$ contains this fixed point for all sufficiently large m. In particular, we have shown:

Proposition 6.5 *Let $z \in \Lambda$ and suppose that V is any connected neighborhood of z. Then $E_\lambda^m(V)$ meets the boundary of S for all sufficiently large m.*

Proposition 6.6 *Λ is a connected subset of S.*

Proof. Let G be the union of the boundaries of the L_i for all i. Since Λ is the closure of G, it suffices to show that G is connected. Suppose that this is not true. Then we can write G as the union of two closed and disjoint sets A and B. One of A or B must contain infinitely many of the boundaries of the L_i. Say A does. But then, if $b \in B$, the previous proposition guarantees that infinitely many of these boundaries meet any neighborhood of b. Hence b belongs to the closure of A. This contradiction establishes the result.

We can now prove:

Theorem 6.7 *There is a natural compactification Γ of Λ that makes Γ into an indecomposable continuum.*

Proof. We first compactify Λ by adjoining the backward orbit of 0. To do this we identify the "points" $(-\infty, 0)$ and $(-\infty, \pi)$ in S: this gives $E_\lambda^{-1}(0)$. We then identify the points (∞, π) and $\lim_{t\to-\infty} \gamma_1(t)$. This gives $E_\lambda^{-2}(0)$. For each $n > 1$ we identify

$$\lim_{t\to\infty} \gamma_n(t)$$

and

$$\lim_{t\to-\infty} \gamma_{n+1}(t)$$

to yield $E_\lambda^{-n-1}(0)$. This augmented space Γ may easily be embedded in the plane. See Figure 37. Moreover, if we extend the B_i and the lines $y = 0$ and $y = \pi$ in the natural way to include these new points, then this yields a curve which accumulates everywhere on itself but does not separate the plane. See the proposition above. By the theorem of S. Curry [Cu], it follows that Γ is indecomposable.

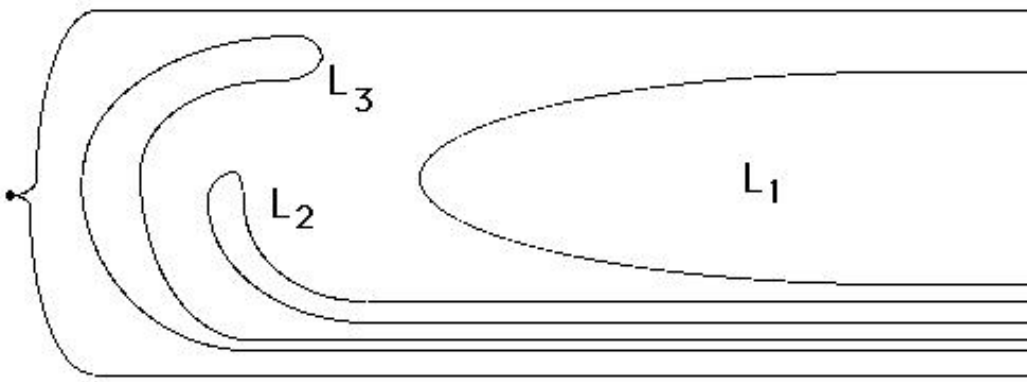

Figure 37: Embedding Γ in the plane.

□

As a consequence of this theorem, Λ must contain uncountably many composants (see [Ku], p. 213). In fact, in [DK] it is shown that Λ contains uncountably many curves.

6.3 Dynamics on Λ

In this section we describe completely the dynamics of E_λ on Λ.

Proposition 6.8 *There exists a unique fixed point w_λ in S if $\lambda > 1/e$. Moreover, w_λ is repelling and, if $z \in S-$orbit of 0, $E_\lambda^{-n}(z) \to w_\lambda$ as $n \to \infty$.*

Proof. First consider the equation

$$\lambda e^{y \cot y} \sin y = y.$$

Since $y \cot y \to 1$ as $y \to 0$ and $\lambda e > 1$, we have $\lambda e^{y \cot y} \sin y > y$ for y small and positive. Since the left-hand side of this equation vanishes when $y = \pi/2$, it follows that this equation has at least one solution y_λ in the interval $0 < y < \pi/2$.

Let $x_\lambda = y_\lambda \cot y_\lambda$. Then one may easily check that $w_\lambda = x_\lambda + iy_\lambda$ is a fixed point for E_λ in the interior of S. Since the interior of S is conformally equivalent to a disk and E_λ^{-1} is holomorphic, it follows from the Schwarz

Lemma that w_λ is an attracting fixed point for the restriction of E_λ^{-1} to S and that $E_\lambda^{-n}(z) \to w_\lambda$ for all $z \in S$.

Remarks.
1. Thus the α-limit set of any point in Λ is w_λ.
2. The bound $\lambda > 1/e$ is necessary for this result, as we have seen that E_λ has two fixed points on the real axis for any positive $\lambda < 1/e$. These fixed points coalesce at 1 as $\lambda \to 1/e$ and then separate into a pair of conjugate fixed points, one of which lies in S.

We now describe the ω-limit set of any point in Λ. Clearly, if $z \in B_n$ then $E_\lambda^{n+1}(z) \in \mathbb{R}$ and so the ω-limit set for z is infinity.

Theorem 6.9 *Suppose $z \in \Lambda$ and $z \neq w_\lambda$, $z \notin B_n$ for any n. Then the ω-limit set of z is the orbit of 0 under E_λ together with the point at infinity.*

We first need a lemma.

Lemma 6.10 *Suppose $z \in \Lambda$, $z \neq w_\lambda$. Then $E_\lambda^n(z)$ approaches the boundary of S as $n \to \infty$.*

Proof. Let h be the uniformization of the interior of S taking S to the open unit disk and w_λ to 0. Recall that E_λ^{-1} is well defined on S and takes S inside itself. Then $g = h \circ E_\lambda^{-1} \circ h^{-1}$ is an analytic map of the open disk strictly inside itself with a fixed point at 0. This fixed point is therefore attracting by the Schwarz Lemma. Moreover, if $|z| > 0$ we have $|g(z)| < |z|$. As a consequence, if $\{z_n\}$ is an orbit in Λ, we have $|h(z_{n+1})| > |h(z_n)|$, and so $|h(z_n)| \to 1$ as $n \to \infty$. This completes the proof of the lemma.

□

The remainder of the proof is essentially contained in [DK] (see pp. 45-49). In that paper it is shown that there is a "quadrilateral" Q containing a neighborhood of 0 in $\mathbb{R}$ as depicted in Figure 5. The set Q has the following properties:

1. If $z \in \Lambda - \bigcup_n B_n$ and $z \neq w_\lambda$, then the forward orbit of z meets Q infinitely often.

2. Q contains infinitely many closed "rectangles" $R_k, R_{k+1}, R_{k+2}, \ldots$ for some $k > 1$ having the property that if $z \in R_j$, then $E_\lambda^j(z) \in Q$ but $E_\lambda^i(z) \notin Q$ for $0 < i < j$.

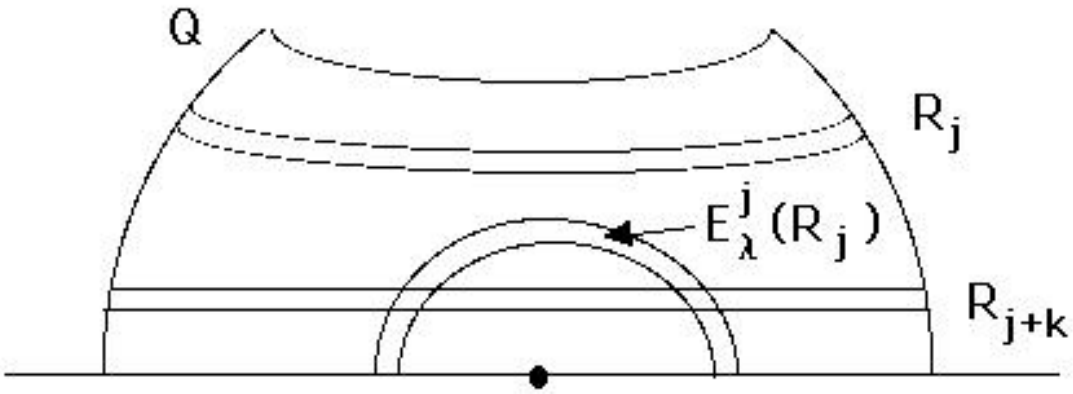

Figure 38: The return map on Q.

3. If $z \notin \bigcup_{j=k}^{\infty} R_j$, then $z \in L_n$ for some n.

4. $E_\lambda^j(R_j)$ is a "horseshoe" shaped region lying below R_j in Q as depicted in Figure 5.

5. $\lim_{j\to\infty} E_\lambda^j(R_j) = \{0\}$.

As a consequence of these facts, any point in Λ has orbit that meets the $\cup R_j$ infinitely often. We may thus define a return map

$$\Phi\colon \Lambda \cap (\cup_j R_j) \to \cup_j R_j \cap \Lambda$$

by

$$\Phi(z) = E_\lambda^j(z)$$

if $z \in R_j$. By item 4, $\Phi(z)$ lies in some R_k with $k > j$. By item 5, it follows that

$$\Phi^n(z) \to 0$$

for any $z \in \Lambda \cap Q$. Consequently, the ω-limit set of z contains the orbit of 0 and infinity.

For the opposite containment, suppose that the forward orbit of z accumulates on a point q. By the Lemma, q lies in the boundary of S. Now the orbit of q must also accumulate on the preimages of q. If q does not lie on the orbit of 0, then these preimages form an infinite set, and some points in

this set lie on the boundaries of the L_n. But these points lie in the interior of S, and this contradicts the Lemma. Thus the orbit of z can only accumulate in the finite plane on points on the orbit of 0. Since the "preimage" of 0 is infinity, the orbit also accumulates at infinity. This completes the proof.

□

6.4 Final Comments and Questions

A very interesting result of Lyubich [Ly] asserts that the exponential map e^z, though quite chaotic, is not ergodic. Indeed, a full measure set of points have orbits that accumulate only on the orbit of 0 together with the point at ∞.

Douady and Goldberg [DoG] have shown that if $\lambda, \mu > 1/e$, then E_λ and E_μ are not topologically conjugate. Each such map possesses invariant indecomposable continua Λ_λ and Λ_μ in S, and the dynamics on each are similar, as shown above. However, we conjecture:

Conjecture: *If $\lambda, \mu > 1/e$, $\lambda \neq \mu$, then Λ_λ and Λ_μ are not homeomorphic.*

We expect that each Λ_λ yields a different Knaster-like continuum (when suitably compactified).

There are many other ways that indecomposable continua arise in the dynamics of the exponential family. For example, in [DJ], it is shown that, for $0 < \lambda < 1/e$, the set of points that correspond to uncountably many other itineraries are also indecomposable continua. These itineraries consist on infinitely many blocks of all zeroes whose length grows quickly. These sets are no longer invariant and all orbits in them accumulate on the orbit of 0 together with ∞.

In [DJM] other kinds of indecomposable continua were shown to exist in the case of a Misiurewicz parameter value, for example, when $\lambda = 2\pi i$. In the Julia set for this map, there are indecomposable continua for which a pair of "hairs" accumulate on one another. There are also other instances where the set of points that share the same itinerary is an indecomposable continuum together with a separate hair that accumulates on this continuum.

7 The Parameter Plane

In this chapter, we continue to paint the picture of the parameter plane for the exponential family. Thus far we have concentrated on the hyperbolic

components C_k in this picture, the λ-values for which E_λ has an attracting cycle of period k. Here we concentrate on the structure of the set of λ-values for which $E_\lambda^n(0) \to \infty$, so that $J(E_\lambda) = \mathbb{C}$. First recall the following facts about the parameter plane from section 4:

1. The attracting fixed point region C_1 is a cardioid-shaped region surrounding the origin.

2. C_2 is a simply connected region filling a large portion of the left half plane.

3. When $k \geq 3$, C_k consists of infinitely many components, each of which is simply connected and extends to ∞ in the right half plane.

4. The portion of the real axis $(1/e, \infty)$ consists of λ-values for which $E_\lambda^n(0) \to \infty$, so that $J(E_\lambda) = \mathbb{C}$.

Thus we have two different types of regions in the parameter plane: the hyperbolic components where the Julia set is a nowhere dense collection of tangled hairs (usually), and the line $(1/e, \infty) \subset \mathbb{R}^+$. Our goal in this section is to showthat there are uncountably many other "hairs" in the parameter plane like $(1/e, \infty)$ on which the Julia set is the entire plane, and that, moreover, these hairs and the hyperbolic components are arranged in a rather interesting manner.

7.1 Structural Instability

In order to underscore the complexity of the parameter plane of λe^z, we first describe the dynamics of E_λ when λ lies off $\mathbb{R}$ but very close to 1. That is, we consider perturbations of e^z within the exponential family. We shall show that, in every neighborhood of $\lambda = 1$, there are parameters for which E_λ has an attracting cycle of period n for infinitely many different values of n, and there are also infinitely many other parameters for which the orbit of 0 is preperiodic of different periods (so $J(E_\lambda) = \mathbb{C}$). As a consequence, the parameter plane for E_λ is extremely complicated near this parameter, and, in particular, e^z is (highly) structurally unstable.

As we have seen, it is the orbit of 0 that determines much of the dynamics of E_λ. If E_λ has an attracting periodic orbit, 0 is attracted to this orbit. If $E_\lambda^n(0) \to \infty$ or if 0 is preperiodic, then $J(E_\lambda) = \mathbb{C}$. So let us consider the orbit of 0 for each $\lambda = e^{i\theta}$ with $\theta > 0$ and small. Intuitively, multiplication

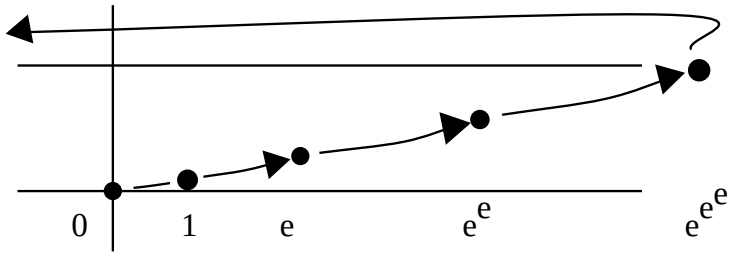

Figure 39: The orbit of 0 under E_λ, $\lambda = e^{i\theta}$.

by $e^{i\theta}$ gives successive points on the orbit of 0 a slight counterclockwise twist after each application of the exponential function. So we expect the orbit of 0 to "climb" in the imaginary direction when $\theta \neq 0$. That being the case, it is entirely possible that, for certain θ's, the orbit of 0 will land on the line Im $z = \pi$. If this occurs, then the next iterate lands in the far left hand half plane, and one more iterate carries 0 back extremely close to itself. See Figure 39.

We emphasize that 0 comes back extremely close to itself, for the real parts of the orbit of 0 form a sequence which is approximately given by

$$0, 1, e, e^e, e^{e^e}, \ldots, E_1^{n-1}(e), -E_1^n(e), e^{-E_1^n(e)}$$

and, of course, $e^{-E^n(e)}$ is extremely small. We also observe that it should be possible to select values θ_n of the parameter with n sufficiently large so that 0 hops to the far left half plane precisely at iteration n.

Let us make all of this a little more more precise. We will write $E_\lambda = E_\theta$, with $0 \leq \theta < \pi/2$. Let S be the strip determined by Re $z \geq 2$, $0 \leq$ Im $z \leq \pi$. Let $z_0 = x_0 + iy_0$. We write

$$z_1 = z_1(\theta) = x_1 + iy_1 = E_\theta(z_0).$$

Lemma 7.1 *There exists θ_1 with $0 < \theta_1 < \pi/2$ such that, if $0 \leq \theta \leq \theta_1$ and both $z_0, z_1 \in S$, then*

1. $x_1(\theta) > 2x_0 + 1$,
2. $y_1(\theta) > 2y_0$.

Proof. First let $\theta = 0$. Then $e^{x_0} \sin y_0 \leq \pi$, so that $\sin y_0 \leq \pi e^{-2}$. Hence $\cos y_0 > 0.8$. Therefore,

$$x_1 = e^{x_0} \cos y_0 > 0.8 e^{x_0} > 2x_0 + 1.5.$$

Also,

$$y_1 = e^{x_0} \sin y_0 > e^{x_0} y_0/2 > y_0 e^2/2 > 3y_0.$$

So (i) and (ii) certainly hold for E_0. Now, for $\theta \neq 0$, we note that $E_\theta(z) = e^{i\theta} E_0(z)$. If $z, E_\theta(z) \in S$, then it follows that $E_0(z) \in S$ as well. Hence it suffices to find θ_1 such that, if $\theta < \theta_1$, then

$$0 < \mathrm{Re}(w - e^{i\theta} w) < 1/2, \tag{1}$$

$$\mathrm{Im}(e^{i\theta} w) > \mathrm{Im}(w) \tag{2}$$

for all $w \in S$ such that $e^{i\theta} w \in S$. (2) clearly holds if $\theta_1 < \pi/2$. For (i), we observe that if $e^{i\theta} w \in S$, then Re $w < \pi / \sin\theta$. Therefore,

$$0 < \mathrm{Re}(w - e^{i\theta} w) < (\mathrm{Re}\ w)(1 - \cos\theta) + \pi \sin\theta$$

$$< \pi(1 - \cos\theta)/\sin\theta + \pi \sin\theta.$$

Since the right side approaches 0 as $\theta \to 0$, we may choose θ_1 small enough so that (i) holds for $\theta < \theta_1$.

□

We remark that there exists $\theta_2 > 0$ such that $E_\theta^2(0) \in S$ for $0 \leq \theta \leq \theta_2$. From now on we assume that $\theta < \min(\theta_1, \theta_2)$.

Define $G_n(\theta) = E_\theta^n(0)$. $G_1(\theta)$ traces out the unit circle, while $G_2(\theta)$ gives a cardioid-like curve, part of which meets S. See Figure 40. Let $\gamma_2(\theta)$ denote the piece of $G_2(\theta)$ in S. Note that $\gamma_2(\theta)$ meets $y = 0$ at $E_0^2(0) = e$. Let $\gamma_n(\theta)$ denote the connected component of $S \cap G_n(\theta)$ that contains $E_0^n(0)$. For n sufficiently large (numerically, $n \geq 3$), $\gamma_n(\theta)$ connects $y = 0$ to $y = \pi$ in S. More precisely, for $n \geq 3$, there exists θ_n such that $\mathrm{Im}\,(\gamma_n(\theta_n)) = \pi$, $\mathrm{Re}\,(\gamma_n(\theta_n)) \geq 2$, and for all θ with $0 \leq \theta < \theta_n$, $\gamma_n(\theta) \in S$. See Figure 10. This can be seen by applying the Lemma repeatedly to $E_\theta(\gamma_2(\theta))$. If $\theta > 0$, there exists $n = n(\theta)$ such that $E_\theta^n(\gamma_2(\theta)) \notin S$.

Clearly, $\exp(\gamma_n(\theta))$ is a curve in the upper half-plane that connects the positive real axis to the negative real axis. Since $0 < \theta < \pi/2$, the curve $E_\theta(\gamma_n(\theta)) = e^{i\theta} \exp(\gamma_n(\theta))$ also meets the negative real axis. When $\theta = \theta_n$,

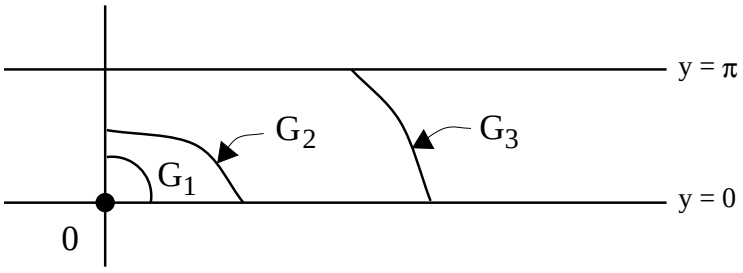

Figure 40: The curves $G_n(\theta)$ for $n = 1, 2, 3$.

the image $E_\theta(\gamma_n(\theta))$ is negative and real. Denote this point by z_{n+1}, so that $z_{n+1} = E_\theta^{n+1}(0)$. Also let $z_j = E_\theta^j(0) = x_j + iy_j$ for $0 \le j \le n+1$. Note that $z_0 = 0, |z_1| = 1$, and $z_j \in S$ for $2 \le j \le n$.

Lemma 7.2 *We have* $\exp(x_n) \ge 2 + \sum_{j=1}^n (x_j + 1)$.

Proof. We have $x_2 \ge x_1 + 1$. Moreover, by the previous Lemma, for $2 \le j \le n-1$, we have $x_{j+1} \ge 2x_j + 1$. Hence,

$$2 + \sum_{j=1}^{n} (x_j + 1) \le \sum_{j=2}^{n-1} (x_{j+1} - x_j) + x_2 + x_n + 3 = 2x_n + 3 < e^{x_n},$$

since $x_n \ge 2$.

□

We now construct a disk about 0 which is contracted inside itself by E_θ^{n+2}. Let $r_{n+1} = 1$ and define $r_k = r_{k+1}/e^{x_k} e$ for $0 \le k \le n$. Note that $r_j < 1$ for $j \le n$ and $r_0 = (e^{n+1} \prod_{j=0}^n e^{x_j})^{-1}$. Let B_j be the disk of radius r_j about z_j.

Proposition 7.3 *If* $z \in B_0$, *then* $E_\theta^j(z) \in B_j$ *for* $j \le n+1$. *Moreover,*

$$\left|(E_\theta^{n+1})'(z)\right| \le e^{n+1} \prod_{j=0}^{n} e^{x_j}.$$

Proof. Suppose $|z - z_j| < r_j$. Let $M_j = \sup |E_\theta'(z)|$. Then, for $j \le n$,

$$|E_\theta(z) - z_{j+1}| \le M_j r_j \le |\lambda e^{x_j + r_j}| r_j \le e^{x_j + r_j} \cdot r_j < e^{x_j} e \cdot r_j = r_{j+1},$$

since $r_j < 1$. Consequently, E_θ maps B_j strictly inside B_{j+1}, and we have $|E_\theta'(z)| \le e^{x_j + 1}$. The result follows immediately.

□

Theorem 7.4 *E_θ has an attracting periodic point of period $n+2$ in B_0.*

Proof. By the preceding proposition, $E_\theta^{n+1}(B_0) \subset B_{n+1}$. We now show that $E_\theta(B_{n+1}) \subset B_0$. Let $z \in B_{n+1}$. Then Re $z \leq x_{n+1} + 1 = -e^{x_n} + 1$. Applying the previous Lemma, we have

$$|E_\theta(z)| \leq \exp(-e^{x_n} + 1) \leq e \exp\Big(-\sum_{j=1}^{n}(x_j + 1) - 2\Big)$$

$$= e^{-1}\Big(\prod_{j=0}^{n} e^{x_j}\Big)^{-1} e^{-n} = r_0,$$

as required. Hence, there exists a periodic point w such that $E_\theta^j(w) \in B_j$ for $0 \leq j \leq n+1$ and $E_\theta^{n+2}(w) = w$.

Finally, observe that $|E_\theta'(z)| < r_0$ if $z \in B_{n+1}$. Combined with the results of Proposition 13, this yields $|(E_\theta^{n+2})'(w)| < 1$.

□

Corollary 7.5 *There is a sequence $\theta_n \to 0$ such that, if n is sufficiently large, E_{θ_n} has an attracting periodic orbit of period n.*

7.2 Other Near-Real Parameters

There is nothing sacred about our using the initial point $\lambda = 1$; one may check easily that the above arguments go through for any $\lambda > 1/e$ and parameter values $\lambda_\theta = \lambda e^{i\theta}$. The result is a sequence of open sets in the λ plane converging to the interval $(1/e, \infty)$. For λ-values in these open sets, E_λ admits an attracting periodic orbit of period n.

As a corollary, we have

Corollary 7.6 *E_λ is not structurally stable if $\lambda > 1/e$.*

See [D2] for more details on the above results. Douady and Goldberg [DoG] have proved that if $\lambda, \mu > 1/e$, then E_λ and E_μ are not topologically conjugate. This is the case despite the fact that $J(E_\lambda) = J(E_\mu) = \mathbb{C}$.

There is much more to the parameter plane picture for E_λ when λ is near 1. Let us consider the functions

$$H_n(\lambda) = E_\lambda^n(0).$$

H_n is a function of the parameter λ and tells where the n^{th} iterate of 0 lands for each λ. As a consequence of our previous work, the family of functions $\{H_n\}$ is not normal at any parameter value $\lambda > 1/e$. Fix $\lambda_0 > 1/e$ and let U be any neighborhood of λ_0 in the λ-plane. Then Montel's Theorem guarantees that the H_n assume all but 2 values in U infinitely often. These 2 omitted values are 0 and ∞, so, for example, there is $\lambda \in U$ such that $H_n(\lambda) = 2\pi i$. But then

$$E_\lambda^{n+1}(0) = E_\lambda(2\pi i) = \lambda = E_\lambda(0).$$

Consequently, for this λ-value, 0 is preperiodic, and so $J(E_\lambda) = \mathbb{C}$. It follows that every $\lambda > 1/e$ is a limit of points for which 0 is preperiodic.

Thus we have

Theorem 7.7 *If $\lambda > 1/e$, there is a sequence $\lambda_n \to \lambda$ such that 0 is preperiodic for E_{λ_n}, so that $J(E_{\lambda_n}) = \mathbb{C}$.*

We will discuss in the next section the fact that each of these λ_n-values also has a "hair" attached in the λ-plane. This hair consists of λ-values for which $E_\lambda^n(0) \to \infty$. Consequently, $J(E_\lambda) = \mathbb{C}$ in this case too.

This means that the picture of the λ-plane near $\lambda > 1/e$ is quite complicated. There are open regions in which E_λ has attracting periodic points as well as preperiodic λ-values with hairs attached for which $J = \mathbb{C}$. Thus we may continue to draw the parameter plane picture for the exponential family that we started in Section 4. In Figure 41 we see the attracting fixed point cardioid to the left. The black regions in this image represent regions where we have an attracting cycle. Note how they accumulate on the real axis, as we showed must be the case.

7.3 Hairs in the Parameter Plane

We now turn our attention to showing that there are infinitely many hairs in the parameter plane on which $E_\lambda^n(0) \to \infty$ so that $J(E_\lambda) = \mathbb{C}$. We recall first the construction of the hairs in the dynamical plane. Given λ and an itinerary $s = (s_0 s_1 s_2 \ldots)$, we considered the family of functions

$$G_s^n(\lambda, t) = L_{\lambda,s}^n \circ E^n(t)$$

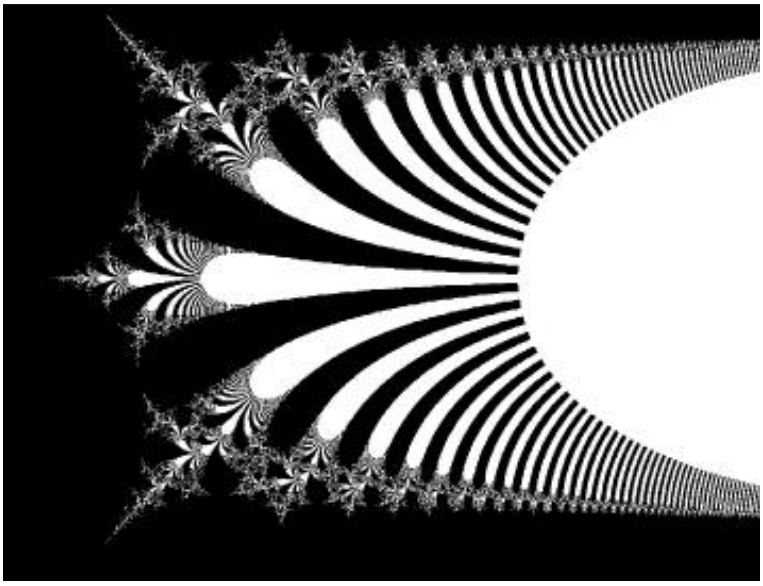

Figure 41: Detail of the parameter plane near $\lambda = 1/e$.The white regions are not open sets; rather, they are collections of hairs in the parameter plane.

where $E(t) = E_{1/e}(t)$ and $t \in [1, \infty)$. That is, $G_s^n(\lambda, t)$ is determined by iterating forward the model map E along the real axis, then puling back by appropriate branches of the inverse of E_λ as determined by the itinerary s. We know that this family of functions converges to a continuous function in t which parametrizes a hair in the dynamical plane, at least if t is large enough. Moreover, this function depends analytically on λ.

The hairs in the parameter plane consist of λ-values for which the orbit of 0 under E_λ tends to ∞ with a specified itinerary. For simplicity, we will restrict attention to sequences in Σ_K, the set of bounded, regular itineraries, i.e., sequences of integers $s_0 s_1 s_2 \ldots$ where $0 < |s_j| \leq K$. So we specifically exclude $s_j = 0$ in this section. The hairs have an endpoint that is given by a λ-value for which the orbit of 0 is bounded. All other λ-values on the hair have the property that the orbit of 0 tends to ∞ with the specified itinerary. As a consequence, $J(E_\lambda) = \mathbb{C}$ for these λ-values.

Definition 7.8 *Let $s = s_0 s_1 s_2 \ldots$. A continuous curve $H_s\colon [1, \infty) \to \mathbb{C}$ is called a hair with itinerary s if H_s satisfies:*

1. *If* $\lambda = H_s(t)$ *and* $t > 1$, *then* $\operatorname{Re} E_\lambda^n(0) \to \infty$ *and the itinerary of* λ *under* E_λ *is* s.

2. *If* $\lambda = H_s(1)$, *then* $E_\lambda(0) = \lambda = z_\lambda(s)$ *where* $z_\lambda(s)$ *is the endpoint of the hair with itinerary* s *in the dynamical plane. Hence, the orbit of* λ *under* E_λ *is bounded and has itinerary* s.

3. $\lim_{t\to\infty} \operatorname{Re} H_s(t) = \infty$.

Remark. We use the term "hair" for curves in both the dynamical plane and parameter plane. When necessary, we use the terms dynamical hair and parameter hair to distinguish between them. Our goal for the remainder of this section is to sketch the proof of the following result.

Theorem 7.9 *Suppose* s *is a bounded sequence with no zeroes. Then there exists a hair in parameter space with itinerary* s. *Moreover, if* s *is periodic or preperiodic, then 0 is preperiodic under* E_λ *for* $\lambda = H_s(1)$.

The proof of the theorem depends upon several technical lemmas so, for simplicity, we merely sketch the main idea of the proof.

Given the itinerary s, we will work in a simply connected region Q_s in parameter space. Q_s will be the union of the horizontal strips $R_\lambda(s_0)$ for $\lambda \in \mathbb{C} - \mathbb{R}^+$. Q_s is an open horizontal strip in $\mathbb{C}$ with height 4π bounded by horizontal lines $\operatorname{Im} z = (2s_0 - 2)\pi$ and $\operatorname{Im} z = (2s_0 + 2)\pi$, so Q_s does not include $\mathbb{R}$ since $s_0 \neq 0$. Given the sequence s, for each t, the dynamical hair $h_{\lambda,s}(t)$ lies in $R_\lambda(s_0) \subset Q_s$. Consider the map $F_t(\lambda) = h_{\lambda,s}(t)$. Note that F_t is a function of λ and assigns to λ the point on the dynamical hair with itinerary s and time parameter t. It can be shown that F_t is an analytic function of λ. Furthermore, F_t maps the closure of Q_s strictly into its interior so therefore F_t has a unique fixed point in Q_s. This fixed point is a λ-value that satisfies $\lambda = h_{\lambda,s}(t)$, so $\lambda = E_\lambda(0)$ lies on the hair in dynamical plane that is attached to $z_\lambda(s)$. We therefore define the point $H_s(t)$ on the hair in the parameter plane as the unique fixed point of F_t for each $t \geq 1$. If $t > 1$ it follows that $E_\lambda^n(0) \to \infty$, whereas, if $t = 1$, 0 maps after one iteration of E_λ onto $z_\lambda(s)$ and so this orbit is bounded. As we vary t, the fixed point of F_t varies, and this curve of fixed points produces the hair in parameter plane.

For further details of the proof, we refer to [Bo1].

7.4 Questions and Problems.

We have shown that there is a unique hair in the parameter plane corresponding to any bounded, regular sequence and that this hair is attached to a λ-value for which the orbit of 0 is bounded. Note that if the itinerary s is periodic, the the orbit of 0 is *preperiodic*. This is true since the itinerary corresponds to the orbit of $E_\lambda(0) = \lambda$, not to the orbit of 0. These are the Misiurewicz points discussed in [DJ].

When the itinerary contains 0's, the situation is much more complicated. We conjecture that some of these are hairs land at bifurcation points in the parameter plane. We also expect that there are many non-regular hairs that land at the same point in the parameter plane, much as happens in the dynamical plane (see Chapter 8.

Problem. Describe where the hairs with non-regular itineraries land in the parameter plane.

Recall that there is a hair in the parameter plane that reaches the saddle-node bifurcation point at $\lambda = 1/e$. This of course in the portion of the real-axis $(1/e, \infty)$. In every other component of C_k with $k > 1$, the multiplier map is a universal covering, so there are infinitely many points on the boundary of a component with multiplier 1. These are the saddle-node points. They are the visible cusps along the boundary of these components.

Problem. Determine an algorithm that describes the set of all hairs that tend to the saddle-node points on the boundary of a component of C_k with $k > 1$.

Problem. Find an algorithm that determines when two different hairs in the parameter plane land on the same parameter value.

In a sense, the hairs in the parameter plane play the same role as the external rays in the exterior of the Mandelbrot set for the quadratic family. Indeed, in each case the singular orbit tends to ∞ with a specific itinerary when the parameter lies on one of these curves. Of course, we have no uniformization of a neighborhood of ∞ for E_λ as we do in the quadratic case, since ∞ is an essential singularity rather than a superstable fixed point. Thus we expect no uniformization near ∞ in parameter space as well. Of course, as we have seen in Chapter 4, all of the hyperbolic components (except C_1) tend to ∞ in the exponential case, whereas they are all bounded for the quadratic family.

8 Untangling Hairs

In this section we discuss the topology of the Julia set for exponential maps for which E_λ has an attracting periodic orbit. As we have seen, there can be at most one attracting periodic orbit. When E_λ has an attracting fixed point, there is a single component of the basin of attraction and the Julia set is a Cantor bouquet. When the attracting orbit has period larger than 1, the topology of the Julia set changes. There are now infinitely many different components in the basin of the cycle. There still are invariant Cantor sets and hairs in the Julia set. However, several of these hairs may actually be attached to the same point in the Cantor set. This is what separates the various components of the basin of the cycle. When this happens, we say that the hairs are *attached* or *tied together*. We present a method in this section for "untangling" these hairs. That is, we provide an algorithm that enables us to read off using symbolic dynamics which hairs are attached to the same point, given the itinerary of 0.

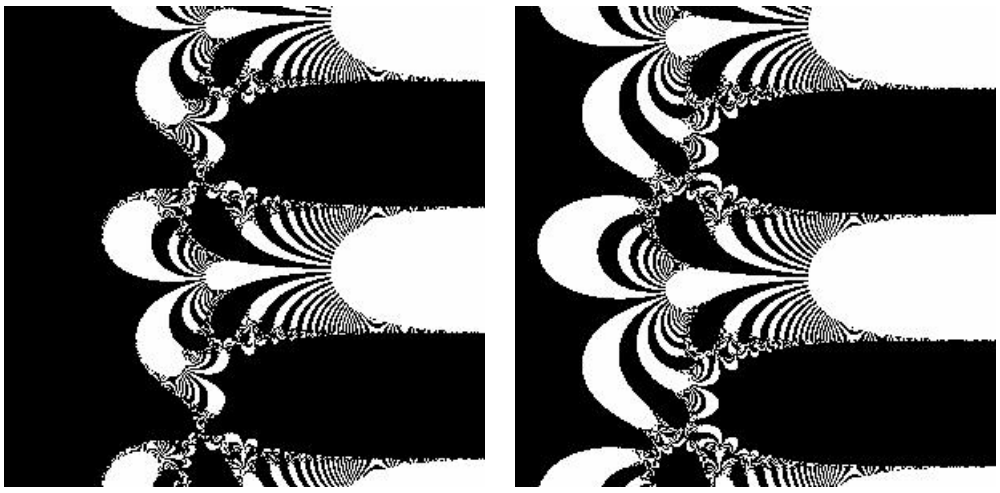

Figure 42: The Julia sets for $\lambda = 5 + \pi i$ and $10 + 3\pi i$.

For example, in Figure 42, we display the Julia set when $\lambda = 5 + i\pi$. As we saw in section 4, this exponential admits an attracting 3-cycle. In this figure we also display the Julia set when $\lambda = 10 + 3\pi i$. This map also has an attracting cycle of period 3. Note that different hairs now seem to be attached to one another. The symbolic dynamics will allow us to

understand the differences between these two cases. In contrast, the Julia set for $\lambda = 3.14i$ (Figure 43) shows that the structure of the attached hairs can be extremely complicated.

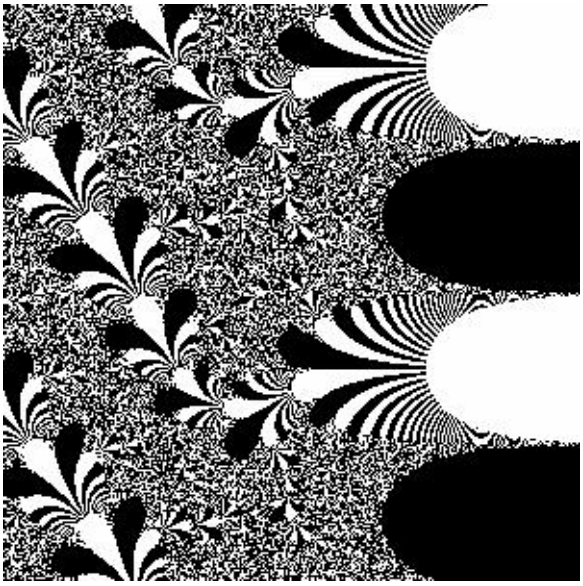

Figure 43: The Julia set for $\lambda = 3.14i$.

Our algorithm will depend on the *kneading sequence* associated to E_λ. The kneading sequence is a sequence of $n-2$ integers that specifies the topology of the basin of attraction of the attracting n-cycle (we assume that $n > 2$ since the period 1 and 2 cases are trivial). It also allows us to codify which hairs land on which points in the Julia set. As an illustration, we will prove that, if the last integer in the kneading sequence is nonzero, then the corresponding exponential must have infinitely many distinct periodic points that have multiple hairs attached.

A similar procedure has been carried out for exponentials for which the orbit of 0 is preperiodic in collaboration with Xavier Jarque. We refer to [DJ] for details. Much of the work in the present chapter is joint with Ranjit Bhattarcharjee [BD]. We refer to this paper for many of the details of this construction.

8.1 The Period Doubling Bifurcation

We begin with a simple example of how two hairs become attached to the same endpoint. As we have seen, the exponential family undergoes a period doubling bifurcation as λ decreases through $-e$. An attracting fixed point becomes neutral when $\lambda = -e$ and then becomes repelling. This is the story on the real axis. In the complex plane, the picture is somewhat different. Before the bifurcation, there is a repelling cycle of period 2 on either side of the real axis, and each of these points has a single hair attached. As λ approaches $-e$, these points approach the attracting fixed point, taking their hairs along with them. When $\lambda = -e$, the repelling 2-cycle collides with the attracting fixed point and produces the neutral fixed point. At this point, the neutral fixed point inherits the two hairs. The hairs lie inside the repelling petal at this fixed point, while portions of the real axis on either side of the fixed point lie in the attracting petals. When $\lambda < -e$, the new attracting 2-cycle splits away, leaving its former hairs attached to the repelling fixed point. This is a *hair transplant*. See Figure 44.

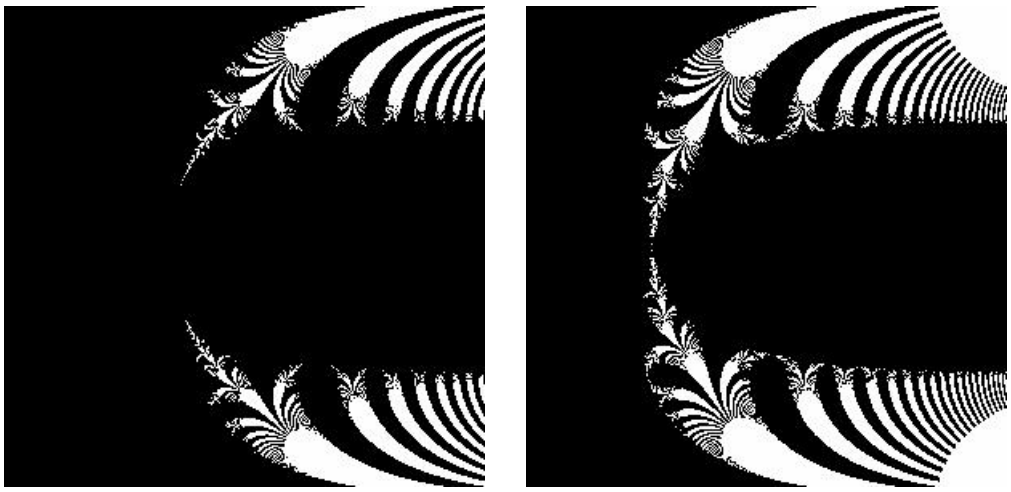

Figure 44: The Julia sets for $\lambda = -2.5$ and $\lambda = -3.5$.

Here's the idea behind how this happens. Suppose first that $-e < \lambda < 0$. Consider a ball B centered at 0 that contains the attracting fixed point z_λ. Then the preimage of B is a half plane that contains B and the second preimage of B is a "glove," as depicted in Figure 45. This is precisely the

picture we obtined in the case where $0 < \lambda < 1/e$ (see section 5), and the arguments there show that the Julia set is a Cantor bouquet.

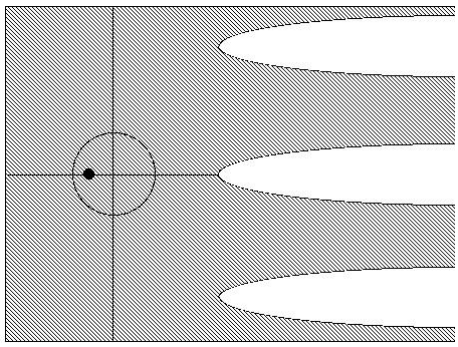

Figure 45: The shaded region is the second preimage of B when $\lambda > -e$.

When $\lambda < -e$ the topology of these preimages changes. The first preimage of B is still a half plane, but this half plane no longer contains B. The second preimage of this half plane is now infinitely many "fingers," one of which necessarily contains B. Call this finger F. See Figure 46. If we then take the preimage of F, we see that this preimage is a glove as depicted in Figure 47. Call this glove G. Then we have $E_\lambda^3(G) = B$.

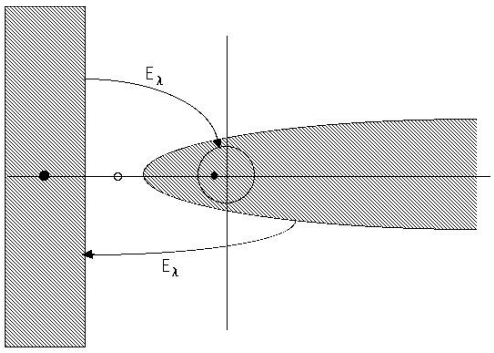

Figure 46: The second preimage of B when $\lambda < -e$. There are actually infinitely many fingers that make up this preimage.

Now the Julia set of E_λ does not meet either F or G. A portion of $J(E_\lambda)$ must be contained between F and G, as we will see below. Actually, this

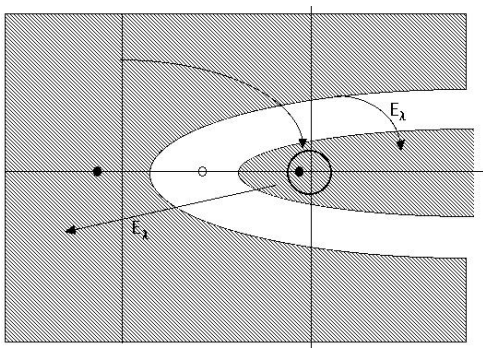

Figure 47: The third preimage of B when $\lambda < -e$ is a glove.

portion contains the pair of hairs that meet at the repelling fixed point.

8.2 Fingers

In this section we generalize the construction of the gloves for the period 2 case. We assume that E_λ has an attracting periodic cycle $z_0, ..., z_n = z_0$ of period n. Throughout we assume that $n \geq 3$.

As we have seen, the asymptotic value 0 lies in the immediate basin of attraction of some point on the cycle. Without loss of generality we will assume that $0 \in A^*(z_1)$ where $A^*(z)$ is the immediate basin of attraction of z. The reason for assuming $0 \in A^*(z_1)$ rather than $0 \in A^*(z_0)$ will become apparent soon. We will define a collection of open sets B_i about each of the z_i. Starting with the point z_1 we first define a set B_{n+1} with the following properties:

1. B_{n+1} is an open and simply connected subset of $A^*(z_1)$;
2. $0, z_1 \in B_{n+1}$;
3. B_{n+1} has compact closure and is also a fundamental domain, i.e., $E_\lambda^n(B_{n+1}) \subset B_{n+1}$.

Next we will obtain a neighborhood of z_0 by considering the preimage of B_{n+1}. Define

$$B_n = E_\lambda^{-1}(B_{n+1}).$$

One checks easily that B_n is simply connected neighborhood of z_0 and B_n contains a half-plane $\mathrm{Re}\, z \leq \xi_1$ and is contained in a half-plane $\mathrm{Re}\, z \leq \xi_2$ for some $\xi_1, \xi_2 \in \mathbb{R}$.

Now we can extend this construction to all the points on the cycle. For $j = 1, ..., n$, let B_{n-j} be the connected component of $E_\lambda^{-1}(B_{n-j+1})$ that contains z_{n-j}. Note that B_1 is contained in the immediate basin of z_1 and $B_1 \supset B_{n+1}$. Indeed, $E_\lambda^n(B_1) = B_{n+1} - \{0\}$. We also have $B_0 \supset B_n$ and $E_\lambda^n(B_0) = B_n$, and, for $j = 1, ..., n-1$, B_j is a simply connected set which is mapped univalently onto B_{j+1} by E_λ.

Note that $E_\lambda : B_0 \to B_1 - \{0\}$ is a universal covering and hence this map is not univalent.

Definition 8.1 *An unbounded, simply connected $F \subset \mathbb{C}$ is called a finger of width c if F is bounded by a simple curve $\gamma \subset \mathbb{C}$ and there exists a $\nu > 0$ such that $F \cap \{z \,|\, Re\, z > \nu\}$ is simply connected, extends to infinity, and satisfies*

$$\{F \cap \{z \,|\, \mathrm{Re}\, z > \nu\}\} \subset \left\{ z \,|\, \mathrm{Im}\, z \in \left[\xi - \frac{c}{2}, \xi + \frac{c}{2}\right] \right\}.$$

Suppose F is a finger of width c and suppose further that $0 \notin F$. Then one checks easily that $E_\lambda^{-1}(F)$ consists of infinitely many disjoint fingers, each of width $d \leq 2\pi$. As a consequence, we have that, for $j = 1, ..., n-1$, B_j is a finger of width $b_j \leq 2\pi$. This construction stops at B_0, since B_0 is not a finger due to the fact that $0 \in B_1$. Indeed, we have that the complement of B_0 consists of infinitely many fingers of width $\leq 2\pi$. In this sense B_0 resembles a "glove", since it contains a left half plane and has infinitely many fingers extending to the right. To summarize:

Theorem 8.2 *Suppose $z_0, ..., z_{n-1}$ is attracting periodic orbit for E_λ with $n \geq 3$. Suppose $0 \in A^*(z_1)$. Then there exist disjoint, open, simply connected sets $B_0, ..., B_{n-1}$ such that*

1. *$z_j \in B_j$, $B_j \subset A^*(z_j)$;*
2. *$E_\lambda(B_j) = B_{j+1}$, $j = 0, ..., n-2$ and $E_\lambda(B_{n-1}) \subset B_0$;*
3. *$B_1, ..., B_{n-1}$ are fingers of width $b_j \leq 2\pi$;*
4. *The complement of B_0 consists of infinitely many disjoint fingers.*

We say that a collection of open subsets $B_0, ..., B_{n-1}$ satisfying the conditions in Theorem 8.2 is a *fundamental set* of attracting domains for the cycle $z_0, ..., z_{n-1}$. The fingers $B_1, \ldots B_{n-1}$ are called *stable fingers*. We remark that we may always assume that, in the far right half-plane, each of the stable fingers is bounded by a curve above and below that is nearly horizontal. See [BD] for the details on this modification.

Example A. Let $\mu = a + i\pi$ where a is sufficiently large. As we saw in section 4, the map E_μ has an attracting cycle of period 3. Let $D(\delta, 0)$ be a disk of radius δ centered at the origin. One can choose δ so that $D(\delta, 0)$ lies in the basin of attraction of a point on the cycle. According to the above construction, we set $B_4 = D(\delta, 0)$. Then the B_j for $j = 0, 1, 2$ form a fundamental set of attracting regions and are as displayed in Figure 48. Note that this picture is again a caricature of the B_j.

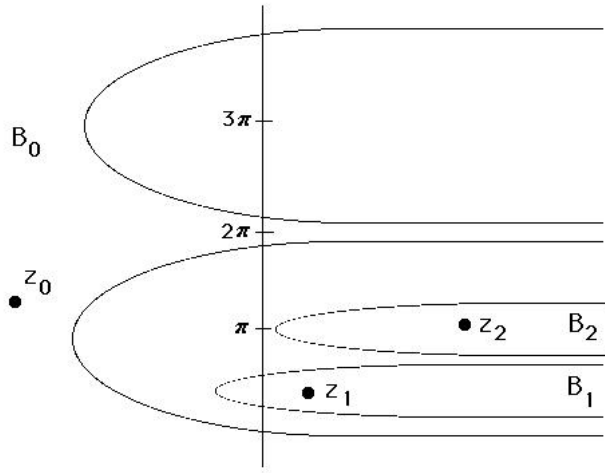

Figure 48: Fingers for E_μ.

Example B. Now let $\nu = a + 3\pi i$ where a is sufficiently large. As we saw in section 4, E_ν also has an attracting cycle of period 3. In Figure 49 we sketch the location of the various B_j for E_ν. Note that the only difference is the placement of B_2 relative to the fingers in the complement of B_0.

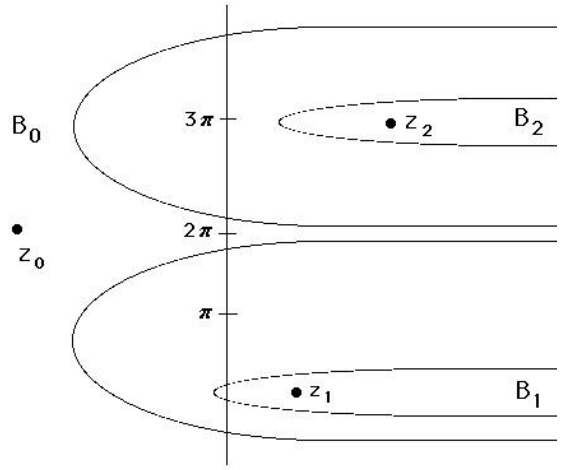

Figure 49: Fingers for E_ν.

8.3 The Kneading Sequence

Using the fundamental set of attracting domains, we can now assign itineraries to each point in the Julia set. Recall that the complement of B_0 consists of infinitely many closed fingers, unbounded in the right half-plane. We denote these fingers by $\mathcal{H}_k$ where $k \in \mathbb{Z}$. We index the $\mathcal{H}_k$ so that $0 \in \mathcal{H}_0$ and so that k increases with increasing imaginary parts. Clearly, $J(E_\lambda)$ is contained in the union of the $\mathcal{H}_k$.

Let $\Sigma = \{(s) = (s_0 s_1 s_2 \ldots) \,|\, s_j \in \mathbb{Z} \text{ for each } j\}$ be the sequence space on infinitely many symbols. As always, the *shift map* σ on Σ is given by

$$\sigma(s_0 s_1 s_2 \ldots) = (s_1 s_2 s_3 \ldots).$$

We then define the *itinerary* $S(z)$ of $z \in J(E_\lambda)$ in the natural manner by setting by

$$S(z) = (s_0 s_1 s_2 \ldots) \text{ where } s_j = k \text{ iff } E_\lambda^j(z) \in \mathcal{H}_k.$$

Note that $S(E_\lambda(z)) = \sigma(S(z))$.

We will be primarily concerned with itineraries whose entries are bounded. Therefore we set

$$\Sigma_N = \{s \in \Sigma \,|\, |s_j| \leq N \text{ for each } j\}.$$

Note that these itineraries are defined slightly differently from those encountered in section 5.

Then, arguing exactly as in section 5, we have:

Theorem 8.3 *For each $N > 0$ there is an invariant subset Γ_N of $J(E_\lambda)$ that is homeomorphic to Σ_N and on which E_λ is conjugate to the shift map.*

So this gives a collection of Cantor sets of bounded orbits for E_λ; now we need to describe how the hairs are attached to these points.

For each B_j with $1 \leq j \leq n-1$, there exists $\mathcal{H}_k$ such that $B_j \subset \mathcal{H}_k$. We define the kneading sequence for λ as follows.

Definition 8.4 *Let E_λ have a attracting cycle of period $n \geq 3$. The kneading sequence as the string of $n-2$ integers*

$$K(\lambda) = k_1 k_2 \dots k_{n-2}$$

where $k_i = j$ iff $E_\lambda^i(0) \in \mathcal{H}_j$.

Note that the kneading sequence gives the location of $E_\lambda(0), \dots, E_\lambda^{n-2}(0)$ relative to the $\mathcal{H}_k$. We do not include the location of 0 since 0 always lies in $\mathcal{H}_0$. Similarly, $E_\lambda^{n-1}(0)$ lies in B_0, which is the complement of the $\mathcal{H}_k$, and so this index is not included in $K(\lambda)$ as well. However, we remark that, in some papers in the literature, these indices are included, so the kneading sequence begins with a 0 and ends with an $*$. Equivalently, the kneading sequence indicates which $\mathcal{H}_k$ contain the points $z_2, \dots z_{n-1}$ on the orbit of the cycle.

For $\tau >> 0$ as defined above, the set

$$\Lambda_\tau = \{z \in \mathbb{C} \,|\, \mathrm{Re}\, z \geq \tau\} - \bigcup_{j=0}^{n-1} B_j$$

consists of infinitely many closed fingers. Each finger in Λ_τ is included in precisely one $\mathcal{H}_j$ since all of the fingers in the glove B_0 which bounds the $\mathcal{H}_k$ are removed with the other B_j. If j is not one of the entries in the kneading sequence, then there is only one finger in Λ_τ that lies in $\mathcal{H}_j$ (namely the far right portion of $\mathcal{H}_j$ itself). We denote this finger in Λ_τ by H_j. However, for j in the kneading sequence, there is more than one finger in Λ_τ that meets $\mathcal{H}_j$ since the B_i separate $\Lambda_\tau \cap \mathcal{H}_j$ into at least two fingers. The fingers that lie in such an $\mathcal{H}_j \cap \Lambda_\tau$ will be denoted H_{j_k} where j_k orders them with ascending

imaginary part beginning with j_0. Note that all of these fingers lie in the half plane $\operatorname{Re} z \geq \tau$.

Example A. Recall the example E_μ where $\mu = a + i\pi$ as described in the previous section. In this case both B_1 and B_2 lie in $\mathcal{H}_0$. Since the kneading sequence only involves the location of B_2 in this case, we have $K(\mu) = 0$. Furthermore, the fingers B_1 and B_2 subdivide $\{\operatorname{Re} z \geq \tau\} \cap \mathcal{H}_0$ into three fingers which we denote by H_{0_0}, H_{0_1}, and H_{0_2}.

Example B. In example B of the previous section, the kneading sequence is now $K(\nu) = 1$, since B_2 lies in $\mathcal{H}_1$. Thus B_1 and B_2 subdivide both $\{\operatorname{Re} z \geq \tau\} \cap \mathcal{H}_0$ and $\{\operatorname{Re} z \geq \tau\} \cap \mathcal{H}_1$ into two subfingers, denoted by H_{0_0}, H_{0_1}, H_{1_0}, and H_{1_1}.

8.4 Augmented Itineraries

We can describe the itinerary of certain points in the Julia set even more precisely by defining an augmented itinerary for $z \in J(E_\lambda) \cap \{z \in \mathbb{C} \mid \operatorname{Re} z \geq \tau\}$. In an augmented itinerary, we specify which of the H_{j_k} the orbit of z visits. More precisely, let $\mathbb{Z}'$ denote the set whose elements are either integers not contained in the kneading sequence, or subscripted integers j_k corresponding to an H_{j_k} if j is an entry in the kneading sequence. Then the *augmented itinerary* of z is

$$S'(z) = (s_0 s_1 s_2 \ldots)$$

where each $s_j \in \mathbb{Z}'$ and s_j specifies the finger in Λ_τ containing $E_\lambda(z)$. Let Σ' denote the set of augmented itineraries. Of course, the augmented itinerary is defined only for points whose orbits remain for all time in Λ_τ.

Definition 8.5 *The deaugmentation map is a map $D : \Sigma' \to \Sigma$ such that if $s_n = j_k$ then $(D(s))_n = j$. If $s_n = j$, then $(D(s))_n = j$.*

That is, D simply removes the subscript from each subscripted entry in a sequence in Σ', and leaves other entries alone.

It turns out that not all augmented itineraries actually correspond to orbits in the far right half plane. In order to describe which augmented itineraries do correspond to points in $J(E_\lambda)$, we introduce the concept of allowable transitions.

Definition 8.6 *Let $s = (s_0 s_1 s_2 \ldots) \in \Sigma'$. A transition is defined as any two adjacent entries (s_i, s_{i+1}) in s. The transition is called allowable if*

$$E_\lambda(H_{s_i}) \cap H_{s_{i+1}} \neq \emptyset.$$

In this case we say $E_\lambda(H_{s_i})$ meets $H_{s_{i+1}}$. An allowable transition will be denoted as $s_i \to s_{i+1}$. An itinerary $s' \in \Sigma'$ will be called allowable if for all s_j it follows that $s_j \to s_{j+1}$. The set of allowable itineraries will be denoted Σ^*.

For the remainder of this section we assume that N satisfies $|k_j| \leq N$ for all entries k_j in the kneading sequence. Let Σ_N^* denote the set of sequences in Σ^* whose deaugmentation is a sequence in Σ_N. Then it can be shown that:

Proposition 8.7 *Let $s \in \Sigma_N^*$. There is a unique tail of a hair in $\Lambda_\tau \cap J(E_\lambda)$ that has augmented itinerary s.*

Thus, for each allowable sequence s' in Σ_N^*, we have a well defined hair in the portion of the Julia set to the right of $\operatorname{Re} z = \tau$ that has itinerary s'. Given the hair $h_{\lambda,\sigma(s)}(t)$, we may pull this curve back into the region $\operatorname{Re} z < \tau$ by applying the appropriate branch of the inverse, L_{λ,s_0}. The result is a curve that extends the hair $h_{\lambda,s}(t)$ into the region $\operatorname{Re} z < \tau$. This follows since $E_\lambda \circ h_{\lambda,s}(t)$ is properly contained in the hair $h_{\lambda,\sigma(s)}(t)$ in the far right half plane. We continue this process by applying

$$L_{\lambda,s_0} \circ \cdots \circ L_{\lambda,s_n}$$

to the hair $h_{\lambda,\sigma^{n+1}(s)}(t)$. Each time we take an inverse, we extend the original hair. The *full hair* corresponding to the sequence $s \in \Sigma_N^*$ is given by

$$\lim_{n\to\infty} L_{\lambda,s_0} \circ \cdots \circ L_{\lambda,s_n} h_{\lambda,\sigma^{n+1}(s)}(t).$$

Then, as in the proof that Γ_N is a Cantor set, these full hairs each tend to a unique point in Γ_N. Now there is only one point in Γ_N that has the same non-augmented itinerary as the hair, namely the point whose deaugmented itinerary is given by $D(s)$. Therefore the full hair with itinerary s must terminate at this point. So we have:

Theorem 8.8 *Let $s \in \Sigma_N^*$. The full hair corresponding to s is a curve in the Julia set that tends to ∞ in the right half plane and limits on $\gamma_{D(s)} \in \Gamma_N$.*

It follows from Theorem 8.8 that hairs that correspond to different sequences in Σ_N^* that have the same deaugmentation must limit on the same point in Γ_N. To go back to our two examples:

Example A. Recall that for E_μ, the kneading sequence is $K(\mu) = 0$ and that the region H_0 contained the only two fingers B_1 and B_2. These fingers subdivide Λ_τ into the three fingers which we denoted by H_{0_0}, H_{0_1}, and H_{0_2}.

Hence there are three full hairs in H_0, one tending to ∞ in each of these three fingers. As we will see in the next section, all of these hairs have deaugmented sequence $(000\ldots)$. Hence, by Theorem 8.3, each of these hairs must be attached to γ_s with $s = (000\ldots)$, which is a fixed point for E_λ. Furthermore, any preimage of γ_s must have three hairs attached, by invariance of the Julia set. These triple attachments are clear in Figure 42, which shows $J(E_\mu)$.

Example B. For the map E_ν, the kneading sequence is $K(\nu) = 1$ and we have two fingers, $B_1 \subset H_0$ and $B_2 \subset H_1$. In H_0 we have two fingers H_{0_0} and H_{0_1}, and there are two in H_1 with indices 1_0 and 1_1. Each of these fingers contains a hair, and we will see that the pair in H_0 is attached to a point of period 2 with itinerary $(010101\ldots)$, while the pair in H_1 is attached to the point with itinerary $(101010\ldots)$. These, as well as many other attachments, are visible in Figure 42. Note the rather obvious difference between $J(E_\nu)$ shown in this figure compared to $J(E_\mu)$.

8.5 Untangling the Hairs

In this section, we show how to determine when two hairs are attached at the same point in the Julia set. By Proposition 8.7, if we have an allowable itinerary in $s' \in \Sigma_N^*$, then there is a unique tail of a hair in $J(E_\lambda)$ with that itinerary. If an augmented sequence is not allowable, then there is no such tail of a hair. Then, using Theorem 8.3, we can pull each of these hairs back until it lands at a point in Γ_N. The landing point is then given by the point whose deaugmented itinerary is $D(s')$. Therefore, to determine whether we have more than one hair attached to a given point, all we need to do is to determine when we have multiple allowable augmented sequences, each of which has the same deaugmentation. This reduces the geometry of the hairs to a combinatorial problem, as we show below.

Our main tool is the following Lemma.

Lemma 8.9 *Let $s_0, s_1, \ldots s_j \in \mathbb{Z}$. Let $s'_j \in \mathbb{Z}'$ with $D(s'_j) = s_j$. Then there is a unique sequence $s'_0, s'_1, \ldots s'_{j-1}$ such that*

1. *$D(s'_i) = s_i$ for $i = 0, 1, \ldots j-1$.*
2. *The transitions*
$$s'_0 \to s'_1 \to \cdots \to s'_j$$
are all allowable.

Proof. Suppose that $i_j \to k_\ell$. Recall that this means that $E_\lambda(H_{i_j})$ meets H_{k_ℓ} in the far right half plane. Equivalently, we must have

$$L_{\lambda,i}(H_{k_\ell}) \cap \Lambda_\tau \subset H_{i_j}.$$

Now if $i_m \to k_\ell$ also, we must have $E_\lambda(H_{i_m})$ meets H_{k_ℓ} in the far right half plane as well. But both H_{i_j} and H_{i_m} are contained in H_i and E_λ is injective on H_i. Hence there can be at most one allowable transition of the form $i_* \to k_\ell$. This shows that the sequence above is unique, if it exists.

To see that there is a transition $i_j \to k_\ell$, recall that $E_\lambda(H_i)$ covers $\mathbb{C} - B_1$. Hence $E_\lambda(H_i)$ meets all of the fingers in Λ_τ. In particular, there is a subfinger in $\Lambda_\tau \cap H_i$ that maps over H_{k_ℓ} in the far right half plane. This proves existence.

□

Thus, according to this lemma, given any $s_j \in \mathbb{Z}'$, we can find one and only one initial portion of an allowable sequence whose j^{th} entry is s_j. Therefore we have:

Corollary 8.10 *Suppose $s \in \Sigma'_N$ contains infinitely many entries that are nonsubscripted. Then there is at most one hair corresponding to this sequence.*

Corollary 8.11 *The only points in Γ_N that can have multiple hairs attached are those*

1. *whose itineraries consist only of subscripted entries in $\mathbb{Z}'$, or*
2. *are preimages of such points.*

Therefore, to determine which hairs are attached to which points in Γ_N, we need only consider allowable sequences that consist entirely of subscripted entries. These allowable sequences together with their preimages are the only sequences that may have multiple hairs attached. So we have reduced the question to: Which sequences $s' \in \Sigma_N^*$ with only subscripted entries have the property that there is a second sequence t' with $D(s') = D(t')$. We will describe the algorithm for determining this after returning to our examples.

Example A. In this case we consider $E_\lambda(z) = \mu e^z$ where $\mu = 5 + i\pi$. We have $K(\mu) = 0$. By the previous corollary, the only points in Γ_N that may have multiple hairs attached are those whose itineraries end $(s_0 \dots s_n\overline{0}\dots)$. That is, only the single (repelling) fixed point in H_0 (and its preimages) can have multiple hairs attached.

We claim that there are exactly three hairs attached to each such point. To determine this, we need to ask which sequences in Σ_N^* have deaugmentation $(000\dots)$. This in turn is determined by the allowable transitions among the 0_j.

For E_μ, the allowable entries in a sequence in Σ_N^* are $0_0, 0_1, 0_2$ and all nonzero integers. The way the corresponding fingers are mapped show that the transition rules among these entries are:

1. $0_0 \to 0_1$;
2. $0_1 \to 0_2, k \geq 1$;
3. $0_2 \to 0_0, k \leq -1$;
4. $j \to k, 0_0, 0_1, 0_2$, for any two nonzero integers j and k.

As a consequence, the only three allowable sequences consisting of only the 0_j are

1. $(\overline{0_0 0_1 0_2})$
2. $(\overline{0_1 0_2 0_0})$
3. $(\overline{0_2 0_0 0_1})$

Hence we have:

Theorem 8.12 *For $\lambda = \mu$, the only points in Γ_N with multiple hairs attached are the fixed point with itinerary $(000\ldots)$ and all of its preimages. Each of these points has exactly three hairs attached. All other points have a single hair attached.*

Notice that we can capture the information about these hairs in matrix form using a *transition matrix*. In this matrix, the (i, j) entry is either 0 or 1 depending on whether $i \to j$ is either not allowed or allowed. Here the rows and columns of the matrix are specified by the subscripted entries in $\mathbb{Z}'$ In this case, the transition matrix involves the entries $0_0, 0_1$, and 0_2 and is given by

$$T_\mu = \begin{pmatrix} 0 & 1 & 0 \\ 0 & 0 & 1 \\ 1 & 0 & 0 \end{pmatrix}.$$

Example B. Now recall the function $E_\lambda(z) = \nu e^z$ where $\nu = a + 3\pi i$ where a is sufficiently large. In this case B_1 lies in H_0 but B_2 now lies in H_1. So $K(\nu) = 1$. Therefore the relevant entries in Σ_N^* are $0_0, 0_1, 1_0$, and 1_1 and we need only consider sequences involving just 0s and 1s. One again checks easily that the transition rules among these entries are:

1. $0_0 \to 0_1, 1_0$;
2. $0_1 \to$ all others;
3. $1_0 \to 0_1, 1_0, 1_2, k > 0$;
4. $1_1 \to$ all others.

Thus the transition matrix now involves the four subscripted entries in Σ_N^* and is given by:

$$T_\nu = \begin{pmatrix} 0 & 1 & 1 & 0 \\ 1 & 0 & 0 & 1 \\ 0 & 1 & 1 & 1 \\ 1 & 0 & 0 & 0 \end{pmatrix}.$$

The hair structure for E_ν is much different from that of E_μ. For example, the period 2 transitions

$$\begin{aligned} 0_0 &\to 0_1 \to 0_0 \\ 0_1 &\to 0_0 \to 0_1 \end{aligned}$$

are both allowable. Also, the transitions

$$\begin{aligned} 0_0 &\to 1_0 \to 0_1 \\ 0_1 &\to 1_1 \to 0_0 \end{aligned}$$

are also allowable. Let α denote the pair $0_0 0_1$ and β the opposite pair $0_1 0_0$. Then we can string together any number of α's, say k, follow it with a 1_1 and then repeat periodically and we obtain an allowable sequence in Σ_N^*. Similarly, the same number of β's followed by a 1_0 and then repeated periodically is also allowable. But both of these sequences have the same deaugmentation, namely

$$\overline{(0 \ldots 01)}$$

with $2k$ 0's in each repeating block. Hence the hairs corresponding to each of these sequences are attached to a periodic point of period $2k+1$.

Now none of these periodic points are preimages of each other. So, unlike the case of E_μ, we have infinitely many distinct periodic points with multiple hairs attached. Of course, each of their infinitely many preimages also has a pair of hairs attached.

Remark. Multiple hairs can be attached to nonperiodic points as well. For example, let $\alpha = 0_0 0_1$ and $\beta = 0_1 0_0$. The we have the following allowable sequences

$$\begin{aligned} &\alpha 1_1 \alpha\alpha 1_1 \alpha\alpha\alpha 1_1 \ldots \\ &\beta 1_0 \beta\beta 1_0 \beta\beta\beta 1_0 \ldots . \end{aligned}$$

Note that each of these sequences has the same nonperiodic deaugmentation.

In analogy with the previous example, one can prove more generally that:

Theorem 8.13 *Suppose that $K(\lambda) = k_1 k_2 \ldots k_{n-2}$ where $k_{n-2} \neq 0$. Then the corresponding exponential has the property that there are infinitely many distinct periodic points that have multiple hairs attached.*

For the proof, we refer to [BD]. This theorem is by no means optimal. A natural problem is to determine exactly which kneading sequences lead to infinitely many attachments.

In the case of the quadratic family, hair attachments are the same as external rays that meet at a common landing point. There are infinitely many such distinct attachments whenever the parameter c is drawn from any portion of the Mandelbrot set that is not connected to the main cardioid by a finite sequence of bifurcations. Perhaps the same is true for the exponential parameter space.

8.6 Back to The Parameter Plane

We can use the kneading sequences described in this section to begin to describe the structure of the parameter plane for E_λ. For it is known that all parameters in a given hyperbolic component have the same kneading sequence. Thus we may associate a string of $n-2$ integers to any hyperbolic component of period n. For technical reasons, in the parameter plane, it is customary to precede this sequence with a 0 (if the period is greater than 1) and to follow it with an asterisk. So the fixed point component has kneading sequence $*$, the period 2 component has kneading sequence $0*$, and the period three components have kneading sequences $0k*$ where $k \in \mathbb{Z}$. Some of these components are displayed in Figure 50.

One of the main results regarding the structure of the parameter plane is the following [DFJ].

Theorem 8.14 *Fix $n \geq 3$ and let $s_1, \ldots, s_{n-2} \in \mathbb{Z}$. There exists a hyperbolic component $\Omega_{0s_1 \ldots s_{n-2}*}$ that extends to ∞ in the right half plane and such that if $\lambda \in \Omega_{0s_1 \ldots s_{n-2}*}$, the map E_λ has an attracting cycle of period n with parameter plane kneading sequence $s = 0s_1 \ldots s_{n-2}*$. Moreover, the components $\Omega_{0s_1 \ldots s_{n-2}*}$ are ordered lexicographically in the far right half plane.*

In particular, it follows that there are infinitely many hyperbolic components of period n for each $n \geq 3$. From the proof of this theorem one obtains the following corollary (see Figure 51).

Corollary 8.15 *Let $\Omega_{0s_1 \ldots s_{n-2}*}$ be as in Theorem A. Then between this hyperbolic component and the hyperbolic component $\Omega_{0s_1 \ldots (s_{n-2}+1)*}$ there exist hyperbolic components $\Omega_{0s_1 \ldots (s_{n-2}+1)\, k*}$ for each $k \in \mathbb{Z}$.*

In this statement the word "between" refers to the ordering given by the imaginary part, since all hyperbolic components of period 3 or higher extend to infinity in the right half plane.

9 Back to Polynomials

At this juncture, there appears to be little similarity between the parameter plane for E_λ and the Mandelbrot set, the parameter plane for the maps $z \to z^2 + c$. It is true that each family is a "natural" one parameter family

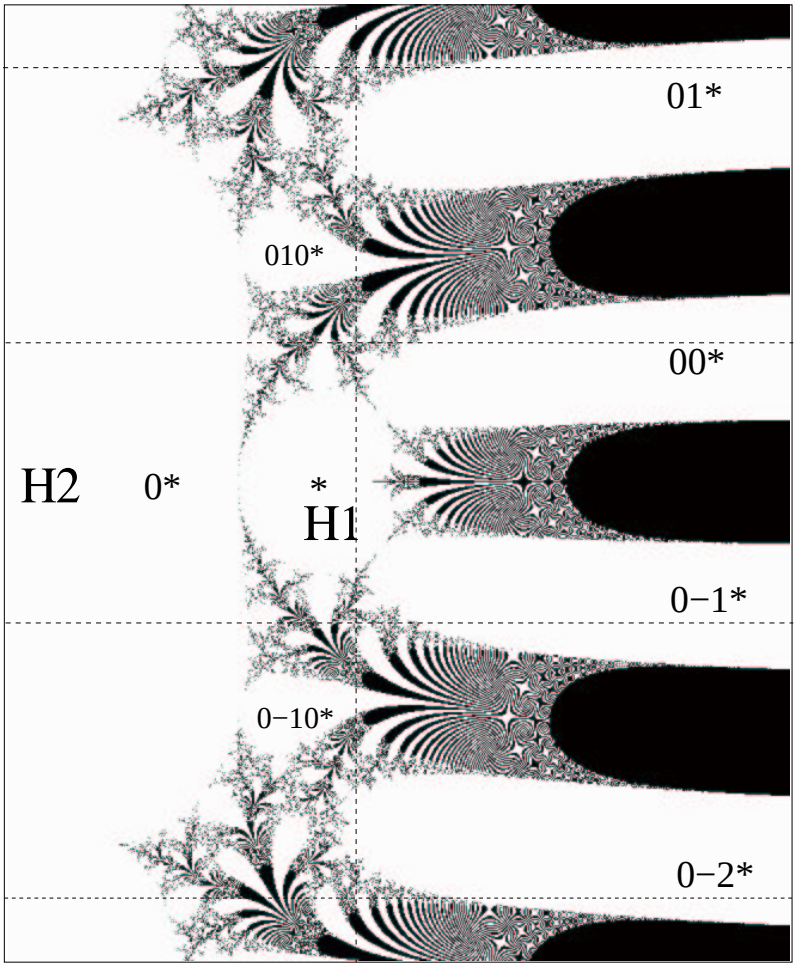

Figure 50: The parameter plane indicating some of the kneading sequences of period 3 and 4 hyperbolic components. $H1$ represents the period 1 region and $H2$ the period 2 component.

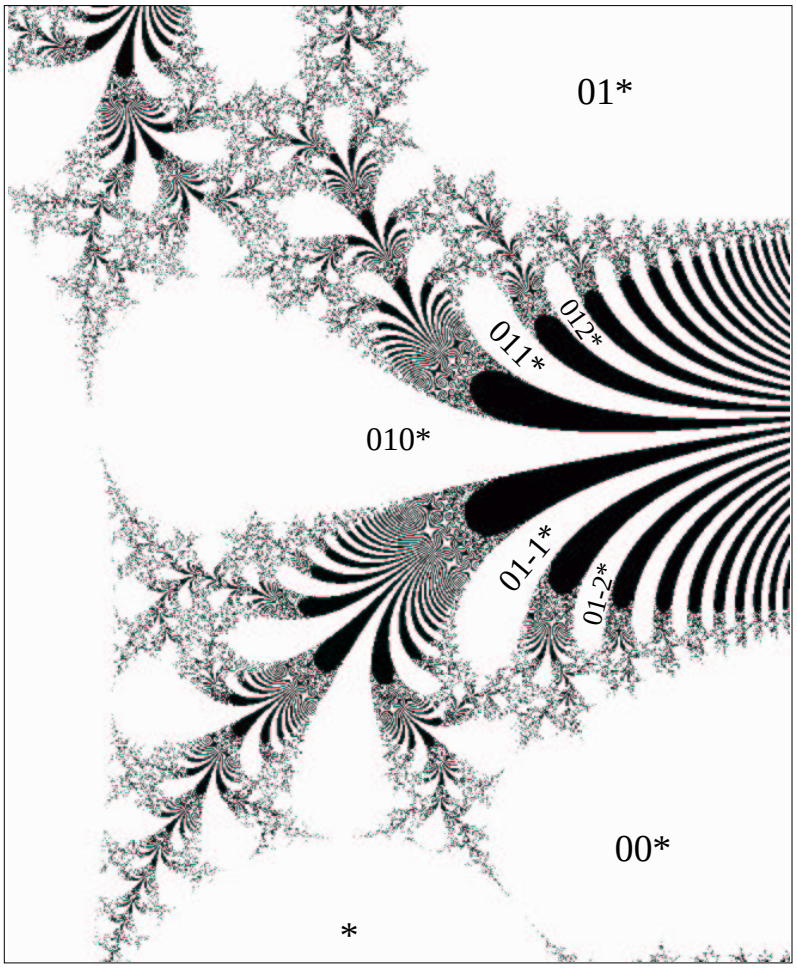

Figure 51: A magnification of the parameter plane showing infinitely many hyperbolic components between two period 3 components.

of maps each of which has a one singular value, and both parameter planes feature a central cardioid-like region in which the associated maps have an attracting fixed point. But there the similarity seems to end. In this section, however, we will show that there is a natural connection between the two sets.

9.1 The Polynomial Family

The connection is given by the family of maps

$$P_{d,\lambda}(z) = \lambda \left(1 + \frac{z}{d}\right)^d .$$

$P_{d,\lambda}$ is a polynomial of degree d which has a single critical point, at $-d$, and a single critical value at 0. Of course, $P_{d,\lambda}$ converges uniformly on compact subsets to E_λ. But the convergence is dynamical as well.

Let $Q_{d,c}(z) = z^d + c$. $Q_{d,c}$ has a single critical point at 0 and critical value c. Hence we may construct the parameter plane for $Q_{d,c}$ just as in the case of the quadratic family (as in [DH]). Define

$$v_c(z) = d\left(\frac{z}{c} - 1\right).$$

Then one may check easily that the affine map v_c conjugates $Q_{d,c}$ to $P_{d,\lambda}$, where c is any of the $d-1$ choices for which $\lambda = dc^{d-1}$, provided $c \neq 0$. Thus v_c gives a ramified covering map from the parameter plane for $Q_{d,c}$ to the parameter plane of $P_{d,\lambda}$. This is a $d-1$-fold covering ramified only at 0. Let B_d denote the parameter plane for the $P_{d,\lambda}$, i.e., the analogue of the Mandlebrot set for these maps. Then, arguing as in [DH] as extended to this case in [PR], we have

Theorem 9.1 *B_d is connected and the complement of B_d in $\overline{\mathbb{C}}$ is an open disk.*

The Fundamental Dichotomy for quadratic maps holds for the $P_{d,\lambda}$ as well. That is, if $\lambda \in B_d$, then the filled Julia set of $P_{d,\lambda}$ is connected, whereas, if $\lambda \in \mathbb{C} - B_d$, then

$$P_{d,\lambda}^n(0) \to \infty$$

and so $J(P_{d,\lambda})$ is a Cantor set. See [Bl].

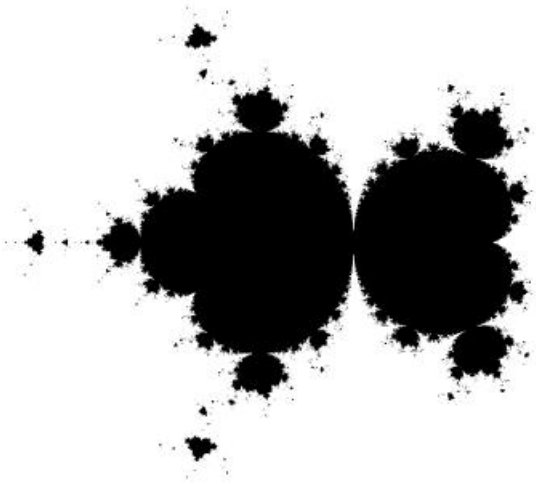

Figure 52: $d = 4$.

In Figures 52–54, we have displayed B_d for $d = 4$ and $d = 8$ and $d = 100$. The size of these images in the parameter plane varies. For example, when $d = 4$, we display a box of sidelength 6, but when $d = 100$, the image is a box of sidelength 200. Each of these images features a main cardioid of roughly the same size (it is hardly visible on the right in Figure 54, so we have magnified this region in Figure 55). Note that in this magnification, the large protruberances heading to the right are the period three regions that tend to the period three regions straddling the lines $\operatorname{Im} z = \pm\pi$ in the exponential parameter plane.

Note also how the period 2 region just to the left of the main cardioid also grows with d. Similarly, the number of cusps on the "decorations" attached to the basic cardioid grows with d. Indeed, as $d \to \infty$, these figures "converge" to the parameter plane of E_λ. This is what provides the link between the quadratic and exponential families.

Exercise. Suppose $\lambda \in C_k$ for the exponential family. Show that there is d_0 such that, if $d > d_0$, then $P_{d,\lambda}$ has an attracting cycle of period k.

Note that there is a fundamental difference between the B_d and the parameter plane for E_λ which we now write as B_∞. For each d, B_d is compact

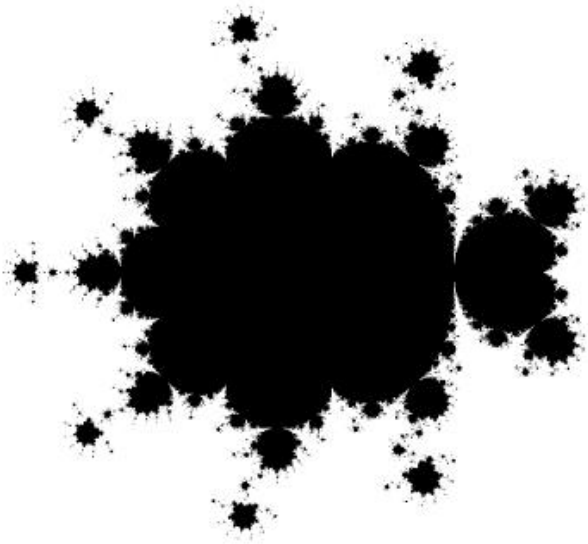

Figure 53: $d = 8$.

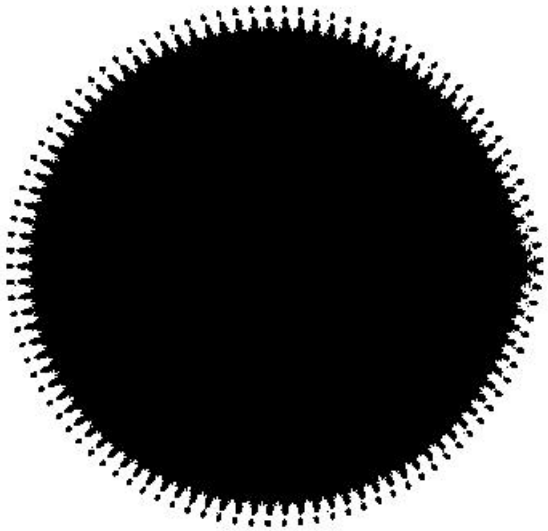

Figure 54: $d = 100$.

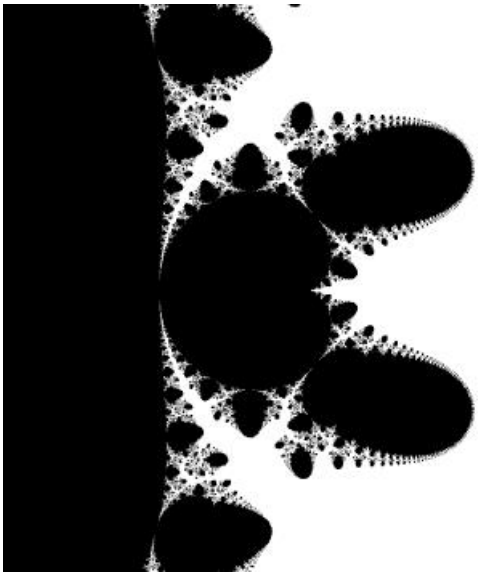

Figure 55: A magnification of the main cardioid in B_λ when $d = 100$.

and its exterior is isomorphic to the unit disk. It is easier to work with the family $z^d + c$ to prove this, but then the parameter plane for this family of maps is a ramified cover (ramified $d-1$ times over 0) of that of $P_{d,\lambda}$. On the other hand, as we showed in 4, each component of C_k, $k \geq 2$, in B_∞ is non-compact, and the "exterior" of B_∞ contains the hairs described above. (Actually, the exterior of B_∞ is not defined since any hair in the λ-plane is a limit of components of the C_k). For more information about the convergence of hyperbolic components, we refer to [KK].

9.2 External Rays

One natural question is what happens to the external rays of Douady and Hubbard which foliate the disk in complement of B_d. In [Bo2], it is shown that certain of these rays have a limit as $d \to \infty$, and that this limit is precisely one of the hairs in B_∞.

How do we identify the hairs which are limit curves of the external rays? The precise answer is spelled out in [Bo2], but we will give some special cases here. The external arguments of Douady and Hubbard are given by rational numbers between 0 and 1. For example, for each d, the external argument

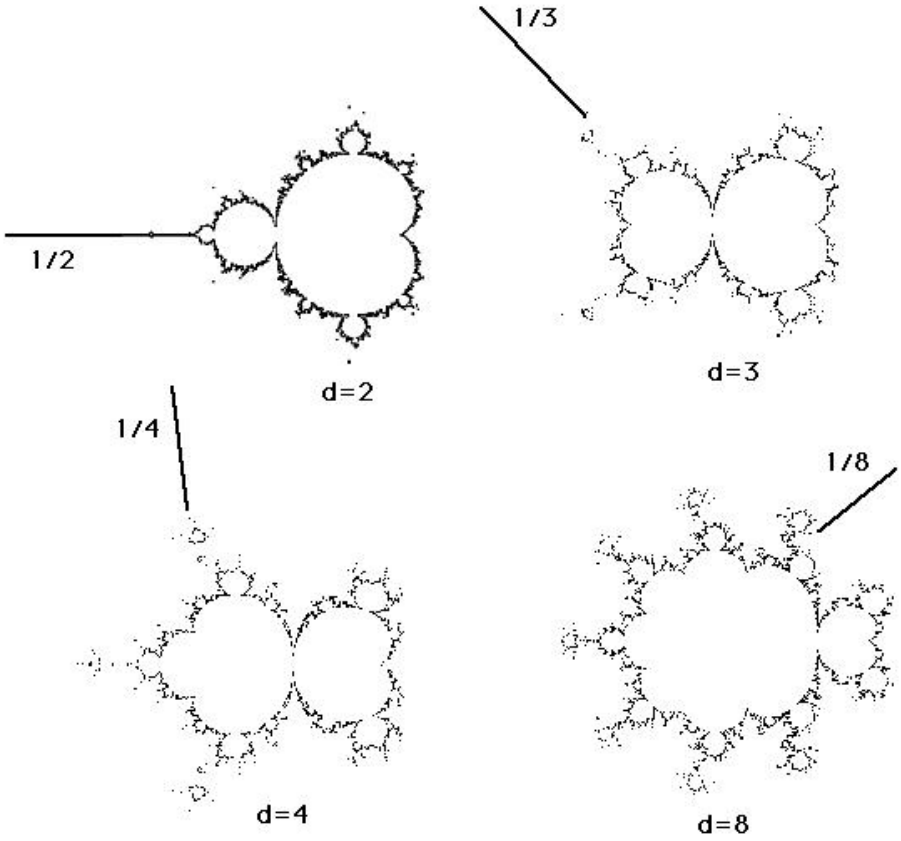

Figure 56: The external ray corresponding to angle $1/d$ for $d = 2, 3, 4, 8$.

of angle $1/d$ converges to a preperiodic λ-value in B_d which is attached to the first "bulb" of the large period 2 region. These angles are depicted in Figure 56.

Note that, in base d, we may write

$$\frac{1}{d} = (d-1)\sum_{i=1}^{\infty} \frac{1}{d^{i+1}}.$$

The result in [Bo2] is that this ray converges as $\lambda \to \infty$ to the hair on which λ has itinerary (111...) (This is the hair which terminates at 2π.)

In general, if for each d, $p(d)$ is the angle given by in base d

$$p(d) = (d-1)\sum_{i=1}^{\infty} \frac{s_i}{d^{i+1}}$$

where the s_i form a repeating, regular sequence, then the rays with angle $p(d)$ in B_d converge as $d \to \infty$ to the hair on which all λ's have itinerary $(s_1 s_2 s_3 \ldots)$.

It is an open question as to just how generally this result holds. For example, we conjecture that if $s = (s_0 s_1 s_2 \ldots)$ is a repeating sequence with $s_0 = 0$, then the corresponding hair converges to a bifurcation point in the parameter plane with external angle

$$p(d) = (d-1)\sum_{i=0}^{\infty} \frac{s_i}{d^{i+1}}.$$

In particular, the hairs corresponding to itineraries of the form $(0j0j0j\ldots)$ should have external angle $j/(d+1)$. See Figure 57.

Problem. Determine the rays in B_∞ that land at bifurcation points on the boundaries of the C_k. How are they related to the external rays in B_n.?

10 Other Families of Maps

Thus far, except for some brief excursions into the land of polynomials, we have concentrated mostly on the exponential family. Of course, there are many other complex analytic maps whose dynamics are rather intriguing. Among entire functions that have been studied, we single out the trigonometric functions and the complex standard family $z \mapsto z + \omega + \beta \sin z$ [Fa] as having received the most attention. More recently, the class of meromorphic functions has received considerable attention. In this section, we describe a few families of such families, paying special attention to how their dynamics differ from that of the exponential. For an excellent survey of these maps, we refer to [Be].

One of the principal differences arising in the iteration of meromorphic (non-rational) functions is the fact that, strictly speaking, iteration of these maps does not lead to a dynamical system. Infinity is an essential singularity for such a map, and so the map cannot be extended continuously to infinity. Hence the forward orbit of any pole terminates, and, moreover, any preimage

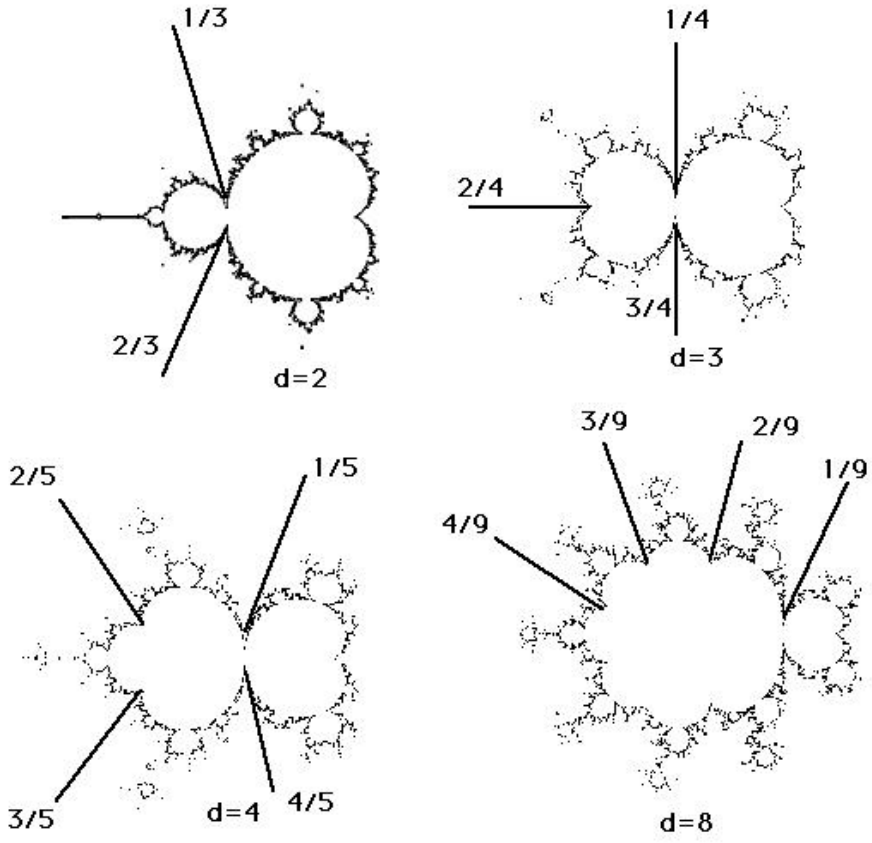

Figure 57: The external ray corresponding to angle $1/d$ for $d = 2, 3, 4, 8$.

of a pole also has a finite orbit. All other points have well defined forward orbits.

Despite the fact that certain orbits of a meromorphic map are finite, the iteration of such maps is important. For example, the iterative processes associated to Newton's method applied to entire functions often yields a meromorphic function as the root-finder. See [CGS], [Be1].

10.1 Maps with Polynomial Schwarzian Derivative

In this section we will deal exclusively with a very special and interesting class of meromorphic functions, namely, those whose Schwarzian derivative is a polynomial. This class of maps includes a number of dynamically important families of maps, including $\lambda \tan z$ and $\lambda \exp z$.

The Schwarzian derivative has played a role in the analysis of dynamical systems in other settings. For example, if the Schwarzian derivative of two C^3 maps of the interval is negative, the same is true for their composition. Singer [Si] has used this to show that the class of functions satisfying these conditions share many of the special properties of complex analytic maps.

The main property of maps with polynomial Schwarzian derivative that makes this class special was noted first by Nevanlinna [N]. These maps are precisely the maps that have only finitely many asymptotic values and no critical values. As we have seen, the fate of the asymptotic values and critical values under iteration plays a crucial role in determining the dynamics. A further important fact about these maps concerns the covering properties of the map itself. Hille [H] has shown that the plane may be decomposed into exactly p sectors of equal angle (when the Schwarzian derivative has degree $p-2$) each of which is associated to one of the asymptotic values. This structure theorem allows us to say much about the Julia set of the map.

Definition 10.1 *If $F(z)$ is a meromorphic function, its Schwarzian derivative is defined by*

$$S(F(z)) = \frac{F'''(z)}{F'(z)} - \frac{3}{2}\left(\frac{F''(z)}{F'(z)}\right)^2.$$

Associated to the Schwarzian differential equation

$$S(F(z)) = Q(z) \qquad (*)$$

is a linear differential equation obtained by setting

$$g(z) = (F'(z))^{-\frac{1}{2}}.$$

The resulting equation is

$$g'' + \frac{1}{2}Q(z)g = 0. \qquad (**)$$

If g_1, g_2 are linearly independent (locally defined) solutions of $(**)$, their Wronskian is a non-zero constant k. Since

$$\left(\frac{g_1}{g_2}\right)' = \frac{k}{g_2^2},$$

it follows that $F(z) = g_1(z)/g_2(z)$ is a solution of $(*)$. Conversely, each solution of $(*)$ may be written locally as a quotient of independent solutions of $(**)$.

There is a wide class of maps whose Schwarzian derivatives are polynomials. These include such maps as $\lambda \tan z$ and $\lambda \exp z$, for which the Schwarzian derivative is a constant, and $\int^z \exp(R(u))du$ where R is a polynomial.

Results of Nevanlinna [N] and Hille [H] allow us to describe the asymptotic properties of the solutions to $(**)$ when Q is a polynomial of degree $p-2$. There are exactly p special solutions, $G_0 \ldots G_{p-1}$, called *truncated* solutions, which have the following property: in any sector of the form

$$\left|\arg z - \frac{2\pi\nu}{p}\right| < \frac{3\pi}{p} - \epsilon$$

with $\epsilon > 0$, $G_\nu(z)$ has the asymptotic development

$$\log G_\nu(z) \sim (-1)^{\nu+1} z^{p/2}.$$

Each G_ν is an entire function of order $p/2$. It follows that each G_ν tends to zero as $z \to \infty$ along each ray in a sector W_ν of the form

$$|\arg z - \frac{2\pi\nu}{p}| < \frac{\pi}{p}.$$

Moreover, $G_\nu(z) \to \infty$ in the adjacent sectors $W_{\nu+1}$ and $W_{\nu-1}$. Note that G_ν and $G_{\nu+1}$ are necessarily linearly independent. However, G_ν and $G_{\nu+k}$ for $|k| \geq 2$ need not be independent.

Any solution of the associated Schwarzian equation may therefore be written in the appropriate sector in the form

$$\frac{AG_\nu(z) + BG_{\nu+1}(z)}{CG_\nu(z) + DG_{\nu+1}(z)} = F(z) \qquad (\dagger)$$

with $AD - BC \neq 0$. Note that $F(z)$ tends to A/C along any ray in the interior of $W_{\nu+1}$ and to B/D in W_ν. Recall that an asymptotic (or critical) path for a function $F(z)$ is a curve $\alpha : [0, 1) \to \mathbb{C}$ such that

$$\lim_{t\to 1} \alpha(f) = \infty$$

and

$$\lim_{t\to 1} F(\alpha(t)) = \omega.$$

The point ω is called an asymptotic value of F. Thus A/C and B/D are asymptotic values.

Example. Let $G_0(z) = e^{z/2}$ and $G_1(z) = e^{-z/2}$. Then we may write

$$e^z = \frac{g_0(z) + 0 \cdot G_1(z)}{0 \cdot G_0(z) + G_1 z}.$$

So $A/C = \infty$ and $B/D = 0$. If W_0 is the left half plane and W_1 is the right half plane, then e^z tends to 0 along rays in W_0 and to ∞ in W_1. So, as we have seen, both 0 and ∞ are asymptotic values for the exponential.

Asymptotic values can be classifed. Nevanlinna's results show that the assumption that Q is a polynomial implies that F has only finitely many asymptotic values. They are therefore all isolated. Let B be a neighborhood of the asymptotic value ω that contains no other asymptotic values. Consider the components of $F^{-1}(B - \omega)$. Since the only points at which F is not a covering of its image are the asymptotic values, F is a covering map on these components. Hence these components are either disks or punctured disks. If some component is a disk, then the asymptotic value ω is called a *logarithmic singularity.*

Example. Let $F(z) = \tan z$. Then i and $-i$ are logarithmic singularities. F maps the half plane $\operatorname{Im} z > y_0 > 0$ onto a punctured neighborhood of i. The image of any path $\alpha(t)$ such that $\lim_{t\to 1} \operatorname{Im} \alpha(t) = \infty$ is a path $\beta(t)$ such that $\lim_{t\to 1} \beta(t) = i$. Similarly the image of a lower half plane $\operatorname{Im} z < v_1 < 0$

is mapped onto a punctured neighborhood of $-i$. The point at ∞ is an accumulation point of the poles; it is not an asymptotic value.

Since a map with a polynomial Schwarzian derivative assumes the special form (†) in each sector W_ν, it follows that such a map has exactly p asymptotic values. Two or more of these values may coincide, but in this case, non-adjacent sectors of asymptotic paths correspond to this value. Also, F has no critical points since

$$F'(z) = \frac{k}{g_2^2(z)}$$

where k is a constant and g_2 is entire. We summarize these facts in a theorem originally proved by Nevanlinna [N].

Theorem 10.2 *Functions whose Schwarzian derivatives are degree $p-2$ polynomials are precisely the functions that have p logarithmic singularities, $a_0, \ldots, a_{p-1}$. The a_i need not be distinct. There are exactly p disjoint sectors $W_0, \ldots, W_{p-1}$, at ∞, each with angle $2\pi/p$ in which F has the following behavior: there is a collection of disks B_i, one around each of the a_i, satisfying $F^{-1}(B_i - a_i)$ contains a unique unbounded component $U_i \subset W_i$ and $F : U_i \to B_i - a_i$ is a universal covering.*

The U_i are called *exponential tracts*. Since the truncated solutions tend to 0 or ∞ in adjacent sectors, it follows that the boundary curve of each U_i has as asymptotic directions the pair of rays which bound the sectors W_i. A ray β is called a *Julia ray* for F if, in any angle about β, F assumes all (but at most one) values infinitely often. See Figure 1. It is an immediate consequence of (†) that the ray β_i bounding a pair of adjacent sectors W_{i-1} and W_i for F is a Julia ray. See Figure 58.

Example. The positive and negative imaginary axes are Julia rays for e^z. Similarly, the rays

$$\arg\, z = \frac{(2k+1)\pi}{2p}$$

for $k \in \mathbb{Z}$ are Julia rays for $\exp(z^p)$.

When F is meromorphic, the arguments of the poles of F accumulate on the argument of the Julia rays. Therefore, except for finitely many poles,

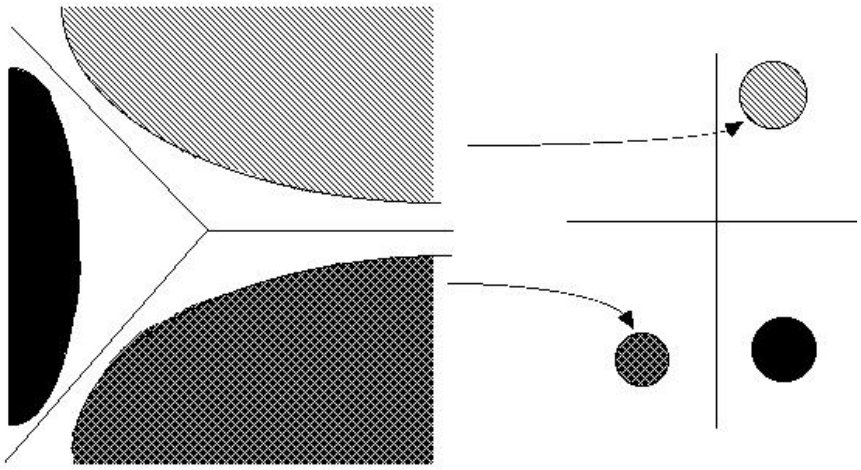

Figure 58: Exponential tracts and Julia rays.

it is possible to associate to a given pole p, that particular Julia ray, $\beta_{i(p)}$, such that the pole lies in a small angle about $\beta_{i(p)}$. We also associate two asymptotic values to each pole; $\nu_1(p)$ is the asymptotic value corresponding to $U_{i(p)-1}$ and $\nu_2(p)$ is the asymptotic value corresponding to $U_{i(p)}$.

Example. The positive and negative axes are Julia rays for $\tan z$, the poles are contained in these rays and $\nu_1(p) = i$, $\nu_2(p) = -i$ for each of the positive poles while $\nu_1(p) = -i$, $\nu_2(p) = i$ for each of the negative poles.

10.2 The Tangent Family

Consider the equation

$$S(F(z)) = k \qquad (**)$$

where $k \in \mathbb{R} - \{0\}$. The truncated solutions of $(**)$ are given by

$$e^{\pm\sqrt{-k/2}\,z}$$

and the general solution is

$$\frac{Ae^{\sqrt{-k/2}\,z} + Be^{-\sqrt{-k/2}\,z}}{Ce^{\sqrt{-k/2}\,z} + De^{-\sqrt{-k/2}\,z}}$$

with $AD - BC \neq 0$. Two of these parameters can be fixed by affine conjugation. We will consider one parameter subfamilies of this family in this and the next two sections.

Let

$$T_\lambda(z) = \lambda \tan z = \frac{\lambda}{i} \frac{e^{iz} - e^{-iz}}{e^{iz} + e^{-iz}}$$

where $\lambda > 0$. We have $S(T_\lambda(z)) = 2$. As we have seen, T_λ has asymptotic values at $\pm\lambda i$, and T_λ preserves the real axis.

To define the Julia set of this map (and other maps in this class), we adopt the usual definition: $J(T_\lambda)$ is the set of points at which the family of iterates of the map is not a normal family in the sense of Montel. As in the case of entire functions, $J(T_\lambda)$ is also the closure of the set of repelling periodic points. But there is also a new equivalent formulation of the Julia set: $J(T_\lambda)$ is also the closure of the set which consists of the union of all of the preimages of the poles of T_λ.

Exercise. Prove that all the poles and their preimages are dense in the Julia set.

Usually, when the Julia set is not the entire plane, this set is a "fractal." Some exceptions are the quadratic maps $z \mapsto z^2$ whose Julia set is the unit circle, and $z \mapsto z^2 - 2$, whose Julia set is the interval $[-2, 2]$. For all other values of c, the Julia set of $z^2 + c$ is a fractal. The tangent family provides another example of a map whose Julia set is a smooth submanifold of $\mathbb{C}$.

Proposition 10.3 *If $\lambda \in \mathbb{R}$, $\lambda > 1$, then $J(T_\lambda)$ is the real line and all other points tend asymptotically to one of two fixed sinks located on the imaginary axis.*

Proof. Write $T_\lambda(z) = L_\lambda \circ E(z)$ where

$$\begin{aligned} E(z) &= \exp(2iz) \\ L_\lambda(z) &= -\lambda i \left(\frac{z-1}{z+1} \right). \end{aligned}$$

E maps the upper half plane onto the unit disk minus 0 and L_λ maps the disk back to the upper half plane. Both E and L_λ preserve boundaries, so T_λ maps the interior of the upper half plane into itself. Now T_λ also preserves the imaginary axis and we have

$$T_\lambda(iy) = i\lambda \tanh(y).$$

The graph of $\lambda \tanh y$ shows that T_λ has a pair of attracting fixed points located symmetrically about 0 if $\lambda > 1$. By the Schwarz Lemma, all points in the upper (resp., lower) half-plane tend under iteration to one of these points.

Hence neither the upper nor the lower half plane is in $J(T_\lambda)$. The real line is in $J(T_\lambda)$. This follows from the facts that the real line satisfies $T_\lambda^{-1}(\mathbb{R}) \subset \mathbb{R}$ and $T_\lambda(\mathbb{R}) = \mathbb{R} \cup \infty$, and that $T'_\lambda(x) > 1$ for all $x \in \mathbb{R}$ if $\lambda > 1$ ($T'_\lambda(x) \geq 1$ if $\lambda = 1$). Each interval of the form

$$\left(\frac{2k-1}{2}\pi,\ \frac{2k+1}{2}\pi\right)$$

is expanded over all of $\mathbb{R}$. If U is any open interval in $\mathbb{R}$, then there is an integer k such that $T_\lambda^k(U)$ covers one of these intervals of length π. Hence $T_\lambda^{k+1}(U)$ covers U. It follows that there exist repelling fixed points and poles of T_λ^{k+1} in U.

□

Remarks.

1. If $\lambda = 1$, then $J(T_\lambda) = \mathbb{R}$, and all points with non-zero imaginary parts tend asymptotically to the neutral fixed point at 0.

2. When $\lambda < -1$, the dynamics of T_λ are similar to those for $\lambda > 1$, except that T_λ has an attracting periodic cycle of period two. Points in the upper and lower half-planes hop back and forth as they are attracted to the cycle. Since $|T'_\lambda(x)| > 1$ for $x \in \mathbb{R}$, it follows as above that $J(T_\lambda) = \mathbb{R}$ for $\lambda < -1$.

For $0 < |\lambda| < 1$, 0 is an attracting fixed point for T_λ. In this case, the Julia set of T_λ breaks up into a Cantor set, as we show below. We will as usual employ symbolic dynamics to describe the Julia set in this case. Let Γ denote the set of one-sided sequences whose entries are either integers or the symbol ∞. If ∞ is an entry in a sequence, then we terminate the sequence at this entry, i.e., Γ consists of all infinite sequences $(s_0, s_1, s_2, \ldots)$ where $s_j \in \mathbb{Z}$ and all finite sequences of the form $(s_0, s_1, \ldots, s_j, \infty)$ where $s_i \in \mathbb{Z}$.

The topology on Γ was described in [Mo]. For completeness, we will recall this topology here. If $(s_0, s_1, s_2, \ldots)$ is an infinite sequence, we choose as a neighborhood basis of this sequence the sets

$$U_k = \{(t_0, t_1, \ldots) \,|\, t_i = s_i \text{ for } i \leq k\}.$$

If, on the other hand, the sequence is finite $(s_0, \ldots, s_j, \infty)$, then we choose the U_k as above for $k \leq j$ as well as sets of the form

$$V_\ell = \{(t_0, t_1, \ldots) \mid t_i = s_i \text{ for } i \leq j \text{ and } |t_{j+1}| \geq \ell\}$$

for a neighborhood basis.

There is a natural shift map $\sigma : \Gamma \to \Gamma$ which is defined as usual by $\sigma(s_0 s_1 s_2 \ldots) = (s_1 s_2 \ldots)$. Note that $\sigma(\infty)$ is not defined. In Moser's topology, σ is continuous and Γ is a Cantor set. Γ provides a model for many of the Julia sets of maps in our class, and $\sigma \mid \Gamma$ is conjugate to the action of F on $J(F)$. One such instance of this is shown in the following proposition.

Proposition 10.4 *Suppose $\lambda \in \mathbb{R}$ and $0 < |\lambda| < 1$. Then $J(T_\lambda)$ is a Cantor set in $\hat{\mathbb{C}}$ and $T_\lambda | J(T_\lambda)$ is topologically conjugate to $\sigma | \Gamma$.*

Proof. Since $0 < |\lambda| < 1$, 0 is an attracting fixed point for T_λ. Let B denote the immediate basin of attraction of 0 in $\mathbb{R}$. B is an open interval of the form $(-p, p)$ where $T_\lambda(\pm p) = \pm p$. (The points $\pm p$ lie on a periodic orbit of period two if $-1 < \lambda < 0$.) The preimages $T_\lambda^{-1}(B)$ consist of infinitely many disjoint open intervals. Let I_j, $j \in \mathbb{Z}$, denote the complementary intervals, enumerated left to right so that I_0 abuts p. Then $T_\lambda : I_j \to (\mathbb{R} \cup \infty) - B$ for each j, and $|T_\lambda'(x)| > 1$ for each $x \in I_j$. Standard arguments [Mo] then show that

$$\Lambda = \{x \in \mathbb{R} \cup \{\infty\} \mid T_\lambda^j(x) \in \cup I_j \text{ for all } j\}$$

is a Cantor set and $T_\lambda | \Lambda$ is conjugate to $\sigma | \Gamma$.

Now Λ is invariant under all branches of the inverse of T_λ. It therefore contains preimages of poles of all orders and is closed. Hence Λ is the Julia set of T_λ. The classification of stable regions tells us that all other points lie in the basin of 0.

□

Remarks.

1. The basin of 0 is therefore infinitely connected. This contrasts with the situation for polynomial or entire maps in which *finite* attracting fixed points always have a simply connected immediate basin of attraction.

2. In fact, the Julia set of T_λ is a similar Cantor set for all λ with $|\lambda| < 1$. See [DKe]

3. A full picture of the parameter plane for the tangent family may be found in [KKo]

10.3 Asymptotic Values that are Poles.

As we have seen, entire transcendental functions of finite type often have Julia sets which contain analytic curves. Indeed, for a wide class of these maps (see [DT]), all repelling periodic orbits lie at the endpoints of invariant curves which connect the orbit to the essential singularity at ∞.

In this section we give an example of a family of maps with constant Schwarzian derivative for which certain of the repelling fixed points lie on analytic curves in the Julia set, but for which many of the other periodic points do not. This lack of homogeneity in the Julia set is caused by the fact that one of the asymptotic values is a pole.

Consider the family of maps

$$F_\lambda(z) = \frac{\lambda e^z}{e^z - e^{-z}}$$

with $\lambda > 0$. We have $S(F(z)) = -2$ and F_λ is periodic with period πi. These maps have asymptotic values at 0 and λ, and 0 is also a pole.

The graph of F_λ restricted to $\mathbb{R}$ shows that F_λ has two fixed points in $\mathbb{R}$ at p and q with $p < 0 < q$. We note that $F_\lambda(z) = L_\lambda \circ E(z)$ where $E(z) = \exp(-2z)$ and L_λ is the linear fractional transformation

$$L_\lambda(z) = \frac{\lambda}{1 - z}.$$

F_λ has poles at $k\pi i$ where $k \in \mathbb{Z}$ as well as the following mapping properties:

1. F_λ preserves $\mathbb{R}^+$ and $\mathbb{R}^-$.

2. F_λ maps the horizontal lines Im $z = \frac{1}{2}(2k+1)\pi$ onto the interval $(0, \lambda)$ in $\mathbb{R}$.

3. F_λ maps the imaginary axis onto the line Re $z = \lambda/2$, with the points $k\pi i$ mapped to ∞.

4. F_λ maps horizontal lines onto circular arcs passing through both 0 and λ.

5. F_λ maps vertical lines with Re $z > 0$ to a family of circles orthogonal to those in 4 which are contained in the plane Re $z > \lambda/2$.

6. F_λ maps vertical lines with Re $z < 0$ to a family of circles orthogonal to those in 4 which are contained in the plane Re $z < \lambda/2$.

As a consequence of these properties, we have

Proposition 10.5 *If $\lambda > 0$, then the fixed point q is attracting. Moreover, if Re $z > 0$, then $F_\lambda^n(z) \to q$ as $n \to \infty$. Hence $J(F_\lambda)$ is contained in the half plane Re $z \leq 0$.*

To see this, just compute $|F_\lambda'(q)| < 1$. Then use property 5 above and the Schwarz Lemma.

Proposition 10.6 *$J(F_\lambda)$ contains $\mathbb{R}^- \cup \{0\}$.*

Proof. The fixed point p is repelling. This follows from the fact that F_λ has negative Schwarzian derivative: if $|(F_\lambda)'(p)| \leq 1$, then it follows that p would have to attract a critical point or asymptotic value of F_λ on $\mathbb{R}$. This does not occur since q attracts λ and 0 is a pole.

Let $x \in (-\infty, p)$. One may check easily that

$$|(F_\lambda^2)'(x)| > 1.$$

Moreover,

$$|(F_\lambda^{2n})'(x)| \to \infty$$

as $n \to \infty$. This again follows from the fact that F_λ^2 has negative Schwarzian derivative on $\mathbb{R}^-$. Let U be a neighborhood of x in $\mathbb{C}$. Note that F_λ^{2n} expands U until some image overlaps the horizontal lines $y = \pm\pi/2$. By the above properties, these points are in the basin of q. Hence the family $\{F_\lambda^{2n}\}$ is not normal at x, and so $(-\infty, p) \subset J(F_\lambda)$. The image of this interval under F_λ is $(p, 0)$, so $\mathbb{R}^- \subset J(F_\lambda)$.

□

Thus some points in the Julia set lie on analytic curves; for example, $\mathbb{R}^-$ and all of its preimages. But not all points in the Julia set lie on smooth invariant curves:

Proposition 10.7 *There is a unique repelling fixed point p_1 in the half strip*

$$\pi/2 < \text{Im } z < 3\pi/2$$

and this point does not lie on any smooth invariant curve in $J(F_\lambda)$.

Proof. Let R be the rectangle $\pi/2 < \operatorname{Im} z < 3\pi/2,\ \nu < \operatorname{Re} z < 0$ where ν is chosen far enough to the left in $\mathbb{R}$ so that

$$|F_\lambda(\nu + iy)| < \pi/4.$$

Then $F_\lambda(R)$ is a "disk" which covers R and $F_\lambda|R$ is 1-1. So, F_λ^{-1} has a unique attracting fixed point p_1 in R. Since this argument is independent of ν for ν large enough negative, the first part of the Proposition follows.

Now suppose that p_1 lies on a smooth invariant curve γ in $J(F_\lambda)$. Since $J(F_\lambda)$ is invariant under F_λ^{-1}, we may assume that γ accumulates on the boundary of the strip $\pi/2 < \operatorname{Im} z < 3\pi/2,\ \operatorname{Re} z < 0$ by taking iterates of F_λ^{-1} as above. The upper and lower boundaries of the strip are stable by property 2; hence γ cannot meet $y = \pi/2$ or $y = 3\pi/2$. Similarly, γ cannot meet the line $x = 0$ (except possibly at $i\pi$). So γ can only accumulate at ∞ or $i\pi$. If γ accumulates at ∞, then γ must also accumulate at $i\pi$, since $F_\lambda(i\pi) = \infty$. Since all points on γ leave the strip under iteration, it follows that γ must contain $i\pi$. Now γ cannot have a tangent vector at $i\pi$, for if so, γ would enter the region $\operatorname{Re} z \geq 0$, $\operatorname{Im} z \neq i\pi$, which lies in the Fatou set. □

Remark. There is a continuous invariant curve which lies in the Julia set and accumulates on p_1. Indeed, the horizontal line ℓ_0 given by $y = \pi,\ x \leq 0$ lies in $J(F_\lambda)$ since it is mapped onto $\mathbb{R}^-$ by F_λ. Consider the successive preimages $\ell_n = F_\lambda^{-n}(\ell_0)$, where F_λ^{-1} is the branch of the inverse of F_λ whose image is $\pi/2 < \operatorname{Im} z < 3\pi/2$. Then ℓ_1 meets ℓ_0 at $i\pi$, ℓ_2 meets ℓ_1 at $F_\lambda^{-1}(i\pi)$, and so forth. Since p_1 is an attracting fixed point for F_λ^{-1}, the curve ℓ formed by concatenating the ℓ_i is invariant and accumulates on p_i as $i \to \infty$. Note that this curve is considerably different from a dynamical point of view from the invariant curve $\mathbb{R}^-$ through p.

10.4 Bifurcation to an entire function.

Most maps with polynomial Schwarzian derivatives are bona fide meromorphic functions, but occasionally they are entire functions. In this section we give an example of an "explosion" in the Julia set which occurs when a member of a meromorphic family suddenly becomes an entire function. An *explosion* occurs at a parameter value for a family of functions whenever the Julia sets of the functions in the family change suddenly, when the parameter is reached, from a nowhere dense subset of $\mathbb{C}$ to all of $\mathbb{C}$.

Consider the family

$$F_\lambda(z) = \frac{e^z}{\lambda e^z + e^{-z}} = \frac{1}{\lambda + e^{-2z}}.$$

When $\lambda = 0$, the corresponding element of this family is the entire function $F_0(z) = \exp(2z)$ whose dynamics are well understood. Indeed, e^{2z} is linearly conjugate to $2e^z$, and so $J(F_0) = \mathbb{C}$, since the orbit of the asymptotic value 0 tends to ∞.

When $\lambda > 0$, $J(F_\lambda) \neq \mathbb{C}$. This follows since F_λ has a unique attracting fixed point p_λ on the real line. In fact, we can say much more about $J(F_\lambda)$.

Proposition 10.8 *For all $\lambda > 0$, the Julia set of F_λ is a Cantor set in $\mathbb{C}$ and $F_\lambda \,|\, J(F_\lambda)$ is the shift map on infinitely many symbols.*

Proof. First note that the entire real axis lies in the basin of attraction of p_λ. This follows since F_λ has negative Schwarzian derivative and maps $\mathbb{R}$ diffeomorphically onto the interval bounded by the asymptotic values, $(0, 1/\lambda)$. In particular, both asymptotic values lie in the immediate basin of p_λ and so there are disks about these points which lie in the basin. Taking preimages of these disks, it follows that there are half planes of the form Re $z < \nu_1$ and Re $z > \nu_2$ with $\nu_1 < p_\lambda < \nu_2$ which lie in the immediate basin of p_λ.

We may find a strip S_μ surrounding the interval $[\nu_1, \nu_2]$ of the form

$$\{z \,|\, |\text{Im } z| < \mu, \nu_1 \leq \text{Re } z \leq \nu_2\}$$

which is mapped inside itself. Now let B denote the "ladder-shaped" region consisting of the two half planes together with S_μ and all of its πi translates. See Figure 59. Clearly, F_λ maps B inside itself as long as the ν_i are chosen large enough.

The complement of B consists of infinitely many congruent rectangles R_j where $j \in \mathbb{Z}$ and the R_j are indexed according to increasing imaginary part. F_λ maps each R_j diffeomorphically onto $\mathbb{C} - F_\lambda(B)$. In particular, $F_\lambda(R_j)$ covers each R_k and ∞. It follows that there exists at least one point z corresponding to any sequence $(s_0, s_1, \ldots)$ in the sequence space which has the property that $F_\lambda^n(z) \in R_{s_n}$ for each n. Then our usual arguments show that this point is unique, lies in the Julia set, and $J(F_\lambda)$ therefore is a Cantor set modeled on the sequence space with infinitely many symbols as described in Section 2. .

□

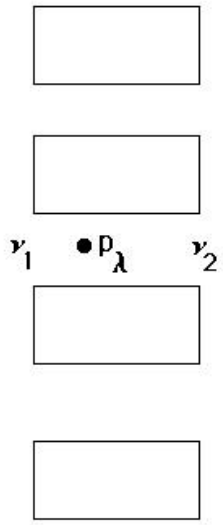

Figure 59: The region B.

10.5 Cantor Bouquets and Cantor Sets

Our goal in this section is to describe the topology of the Julia set for a general meromorphic map F with Schwarzian derivative that is a polynomial $P(z)$. By Nevanlinna's Theorem, each such map F has p asymptotic values $a_0, \ldots, a_{p-1}$. To each a_i there corresponds a sector W_i with angle $2\pi/p$ in which F has the following behavior: We may choose a small disk B_i about a_i such that, if U_i is the component of $F^{-1}(B_i)$ meeting W_i, then $F : U_i \to B_i - a_i$ is a universal covering map. The sectors are separated by the Julia rays β_i. Almost all poles p have associated Julia rays, $\beta_{i(p)}$, and asymptotic values $\nu_1(p)$ and $\nu_2(p)$.

Note that all of the a_i need not be distinct, but it follows from the linear-independence of the truncated solutions G_ν and $G_{\nu+1}$ that a_i corresponding to adjacent W_i are distinct. Thus the basic mapping properties of F are as depicted in Figure 60.

Let us assume that all of the a_i are finite. We may choose R sufficiently large so that $D_R = \{z \,|\, |z| \leq R\}$ contains all of the B_i in its interior. Let Γ_R

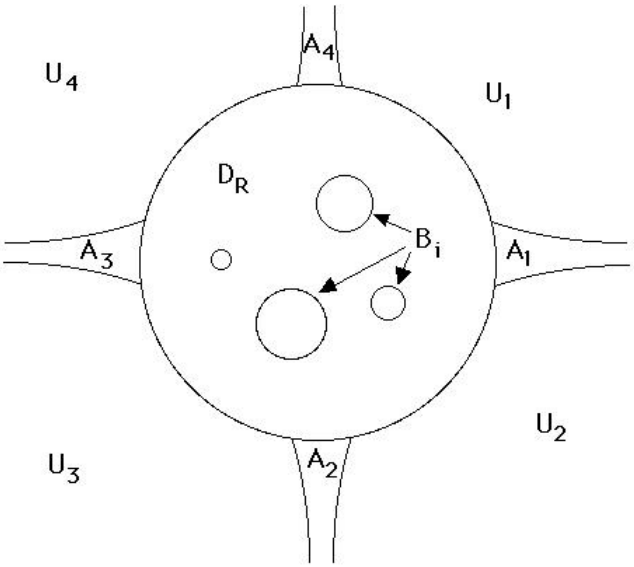

Figure 60: Exponential tracts and Julia rays.

denote the disk in $\hat{\mathbb{C}}$ which is the complement of D_R. Let

$$\tilde{\Gamma}_R = \Gamma_R - \bigcup_{i=0}^{p-1} U_i.$$

If R is large enough, $\tilde{\Gamma}_R$ consists of exactly p "arms" which extend to ∞ in Γ_R and which separate the U_i. Let A_i denote the arm between U_i and U_{i+1}. A_i contains the Julia ray β_i. See Figure 60.

Since $F \mid A_i$ is a covering map that covers $\hat{\mathbb{C}} - (B_i \cup B_{i+1})$ infinitely often, it follows that $F^{-1}(\Gamma_R) \cap A_i$ consists of infinitely many disks, each of which is mapped by F in a one-to-one fashion over Γ_R. These disks accumulate only at ∞. This is similar to the situation in the previous section.

Proposition 10.9 *Suppose all of the asymptotic values of F are finite. Let $\Lambda_R = \{z \mid F^j(z) \in \Gamma_R \text{ for all } j\}$. If R is chosen large enough, then Λ_R is a closed, forward invariant subset of $J(F)$. Moreover, Λ_R is homeomorphic to a Cantor set that is modeled on the shift space with infinitely many symbols.*

Proof. As there are only countably many disks in $F^{-1}(\Gamma_R) \cap A_i$ for each arm A_i, we may choose an indexing of these disks by the natural numbers. Say

$F^{-1}(\Gamma_R) \cap (\cup A_i) = \cup_{j=0}^{\infty} D_j$. Thus each $D_j \subset \Gamma_R$ and F maps each D_j onto Γ_R. In particular, $F \mid D_j$ covers each other D_k and ∞. Standard arguments as described in §2 then yield the result.

□

Thus the set of points whose orbits remain in a neighborhood of ∞ form a closed forward invariant subset of the Julia set which is homeomorphic to a Cantor set. We may apply these ideas on a global level if we can guarantee that all of the asymptotic values lie in a single immediate attracting basin of a fixed point.

Corollary 10.10 *Suppose each of the a_i lie in the immediate attracting basin of an attracting fixed point. Then $J(F)$ is a Cantor set and $F|J(F)$ is conjugate to the shift map on infinitely many symbols.*

Proof. Our assumption allows us to choose a simple closed curve in $\mathbb{C}$ which bounds an open set in the immediate attractive basin, and which contains all of the B_i. The Julia set is contained in the complement of this set. Applying the above argument to this curve instead of Γ_R yields the result.

□

Recall that the Julia set of a rational map is also a Cantor set under this hypothesis so that these meromorphic maps are dynamically similar to rational maps. By contrast, there are no entire transcendental functions whose Julia sets are Cantor sets [Ba1]. On the other hand, if one or more of the asymptotic values is the point at ∞, then the Julia set contains Cantor bouquets.

Theorem 10.11 *Suppose $F(z)$ has polynomial Schwarzian derivative with degree $p-2$. Suppose that F has an asymptotic value a_i which is also a pole. Let W_i be the sector containing the exponential tract corresponding to a_i. Then for each $N > 0$, $J(F)$ contains a Cantor N-bouquet in W_i which is invariant under F^2.*

The proof may be found in [DKe].

References

[AA] Arnold, V.I., Avez, A. *Ergodic Problems of Classical Mechanics.* New York: Benjamin (1968).

[Ahl] Ahlfors, L. *Lectures on Quasiconformal Mappings.* American Mathematical Society, 2006.

[AB] Ahlfors, L. and Bers, L. The Riemann Mappings Theorem for Variable Metrics, *Annals of Math.*, **72** (1960), 385-404.

[A] Atela ,P. Bifurcations of Dynamic Rays in Complex Polynomials of Degree Two. *Ergod. Th. & Dynam. Sys.* **12** (1991), 401-423.

[AO] Aarts, J. and Oversteegen, L. The Geometry of Julia Sets. *Trans. Amer. Math. Soc.* **338** (1993),897-918.

[B] Branner, B. The Mandelbrot Set. In *Chaos and Fractals: The Mathematics Behind the Computer Graphics.* Amer. Math. Soc. (1989) 75-106.

[Ba] Barge, M. Horseshoe Maps and Inverse Limits. *Pacific J. Math.* **121** (1986),29-39.

[Ba1] Baker, I.N., Wandering Domains in the Iteration of Entire Functions, *Proc. London Math. Soc.* **49** (1984), 563-576.

[Ba2] Baker, I. N. The Domains of Normaility of an Entire Function. *Ann. Acad. Sci. Fenn. Ser. A Math* **1** (1975), 277-283.

[Ba3] Baker, I. N. An Entire Function which Has Wandering Domains. *J. Australian Math. Society.* **22** (1976), 173-176.

[Ba4] Baker, I. N. The Iteration of Polynomials and Transcendental Entire Functions. *J. Australian Math. Society.* **30** (1981), 483-495.

[BKL] Baker, I. N., Kotus, J., and Lü, Y. Iteration of Exponential Functions. *Ann. Acad. Sci. Fenn.* **9** (1984), 49-57.

[Bar1] Baranski, K. Hausdorff Dimension of Hairs and Ends for Entire Maps of Finite Order. Preprint.

[Bar2] Baranski, K. Trees and Hairs for Some Hyperbolic Entire Maps of Finite Order. Preprint.

[BD] Bhattacharjee, R. and Devaney, R. L. Tying Hairs for Structurally Stable Exponentials. Preprint.

[Be] Berweiler, W. Iteration of Meromorphic Functions. *Bull. Amer. Math. Soc.* **29** (1993), 151-188.

[Be1] Bergweiler, W. et. al. Newton's Method for Meromorphic Functions. *Complex Analysis and its Applications.* Pitman Res. Notes Math. **305** (1994), 147-158.

[Bea] Beardon, A. *Iteration of Rational Functions.* Cambridge University Press, 1994.

[BF] Baranski, K. and Fagella, N. Univalent Baker Domains. *Nonlinearity.* **14** (2001), 411-429.

[BK] Baranski, K. and Karpińska, B. Coding Trees for Entire Maps. Preprint.

[Bl] Blanchard, P. Complex Analytic Dynamics on the Riemann Sphere, *B.A.M.S.* **2** (1984),85-141.

[Bo1] Hairs for the Complex Exponential Family (C. Bodelón, R. L. Devaney M. Hayes, L. Goldberg, J. Hubbard and G. Roberts). *International Journal of Bifurcation and Chaos.* **9** (1999), 1517-1534.

[Bo2] Dynamical Convergence of Polynomials to the Exponential C. Bodelón, R. L. Devaney, M. Hayes, L. Goldberg, J. Hubbard and G. Roberts). *Journal of Difference Equations and Applications.* **6** (2000), 275-307.

[BR] Baker, I. N. and Rippon, P. Iteration of Exponential Functions, *Ann. Acad. Sci. Fenn.*, Series 1A Math. **9** (1984),49-77.

[CG] Carleson, L. and Gamelin, T. *Complex Dynamics.* Springer-Verlag, 1994.

[CGS] Curry, J., Garnett, L., and Sullivan, D. On the Iteration of a Rational Function. *Comm. Math. Phys.* **91** (1983), 267–277.

[Cu] Curry, S. One-dimensional Nonseparating Plane Continua with Disjoint ϵ-dense Subcontinua. *Topol. and its Appl.* **39** (1991),145-151.

[D1] Devaney, R. L. Se^x: Dynamics, Topology, and Bifurcations of Complex Exponentials. *Topology and its Applications.* **110** (2001), 133-161.

[D2] Devaney, R. L. Structural Instability of Exp(z). *Proc. A.M.S.*, **94** (1985),545-548.

[D3] Devaney, R. L. Julia Sets and the Bifurcation Diagrams for Exponential Maps. *Bull. Amer. Math Soc.* **11** (1984), 167-171.

[D4] Devaney, R. L. e^z: Dynamics and Bifurcations. *Int'l. J. Bifurcation and Chaos.* **1** (1991), 287-308.

[Dev] Deville, R. E. L. Itineraries of Entire Functions *J. Diff. Eq. Appl.* **7** (2001), 193-214.

[Dev2] Brjuno Numbers and the Symbolic Dynamics of the Complex Exponential. *Qual. Theory Dyn. Sys.* **1** (1999), 71-82.

[DFJ] Devaney, R. L., Fagella, N. and Jarque, X. Hyperbolic Components the Complex Exponential Family. *Fundamenta Mathematicae.* **174** (2002), 193-215.

[DG] Devaney, R. L. and Goldberg, L. Uniformization of Attracting Basins for Exponential Maps. *Duke Mathematics Journal.* **55** (1987), 253-266.

[DH] Douady, A. and Hubbard, J. Étude Dynamique des Polynôme Complexes, *Publications Mathematiques d'Orsay.*

[DH1] Douady, A. and Hubbard, J. Itération des Polynômes quadratiques complexes, *C.R. Acad. Sci. Paris*, t.29, Serie I-1982, 123-126.

[DH2] Douady, A. and Hubbard, J. On the Dynamics of Polynomial-like Mappings, *Ann. Scient., Éc. Norm. Sup.* 4^e *séries*, t.18, 1985, 287.

[DJ] Devaney, R. L. and Jarque, X. Misiurewicz Points for Complex Exponentials *Int. J. Bifurcation and Chaos* **7** (1997), 1599-1616.

[DJ1] Devaney, R. L. and Jarque, X. Indecomposable Continua in Exponential Dynamics. *Conformal Geom. Dyn.* **6** (2002), 1-12.

[DJM] Devaney, R. L., Jarque, X, and Moreno Rocha, M. Indecomposable Continua and Misiurewicz Points in Exponential Dynamics. *Int'l. J. Bifurcation and Chaos* **10** (2005), 3281-3293.

[DK] Devaney, R. L. and Krych, M. Dynamics of Exp(z), *Ergodic Theory and Dynamical Systems* **4** (1984), 35-52.

[DKe] Devaney, R. L. and Keen, L. Dynamics of +Meromorphic Maps: Maps with Polynomial Schwarzian Derivative. (with Linda Keen.) *Annales Scientifiques de l'Ecole Normale Supérieure.* **22**(1989), 55-79.

[DM1] Devaney, R. L. and Moreno Rocha, M. Geometry of the Antennas in the Mandelbrot Set. *Fractals.* **10** (2002), 39-46.

[DoG] Douady, A. and Goldberg, L. The Nonconjugacy of Certain Exponential Functions. In *Holomorphic Functions and Moduli.* MSRI Publ., Springer Verlag (1988), 1-8.

[DT] Devaney, R. L. and Tangerman, F. Dynamics of Entire Functions Near the Essential Singularity, *Ergodic Thy. Dynamical Syst.* **6** (1986), 489-503.

[Du] Durkin, M. B. The Accuracy of Computer Algorithms in Dynamical Systems. *Internat. J. Bifur. Chaos.* **1** (1991), 625-639.

[EL] Eremenko, A. and Lyubich, M. Yu. Iterates of Entire Functions. *Dokl. Akad. Nauk SSSR* **279** (1984), 25-27. English translation in *Soviet Math. Dokl.* **30** (1984), 592-594.

[EL1] Eremenko, A. and Lyubich, M. Yu. Dynamical Properties of Some Classes of Entire Functions. *Ann. Inst. Fourier (Grenoble)* **42** (1992), 989-1020.

[F] Farey, J. On a curious property of vulgar fractions. *Phil. Mag. J. London* **47** (1816), 385-386.

[Fa] Fagella, N. Limiting Dynamics for the Complex Standard Family. *Intern. J. Bifur. chaos Appl. Sci. Engrg.* **5** (1995), 673-679.

[FH] Fagella, N. and Henriksen, C. Deformation of Entire Functions with Baker Domains. *Discrete and Continuous Dynamical Systems.* **15** (2006), 379-394.

[FG] Fagella, N. and Garijo, A. Capture Zones of the Family of FUnctions $\lambda z^m e^z$. *Int'l. J. Bifurcation and CHaos.* **13** (2003), 2623-2640.

[Fat] Fatou, P. Sur l'Itération des Fonctions Transcendantes Entiéres *Acta. Math.* **47** (1926), 337-370.

[GGS] Ghys, E., Goldberg, L., and Sullivan, D. On the Measurable Dynamics of $z \mapsto e^z$, *Ergodic Theory and Dyn. Sys.* **5** (1985), 329-335.

[GK] Goldberg, L. R. and Keen, L. A Finiteness Theorem For A Dynamical Class of Entire Functions, *Ergodic Theory and Dynamical Systems* **6** (1986), 183-192.

[GT] Goldberg,L. and Tresser, C. Rotation orbits and the Farey tree. *Ergod. Thy. & Dynam. Sys.* **16** (1996), 1011-1029.

[H] Hille, E. On the Zeroes of the Functions of the Parabolic Cylinder, *Ark. Mat. Astron. Fys.* **18** No. 26 (1924).

[Kar] Karpinska, B. On the Accessible Points in the Julia Sets of Some Entire Functions. *Fund. Math.* **180** (2003), 89-98.

[KK] Krauskopf, B. and Kriete, H. Kernel Convergence of Hyperbolic Components. *Ergodic Theory and Dyn. Sys.* **17** (1997), 1137–1146.

[KKo] Keen, L. and Kotus, J. Dynamics of the family $\lambda \tan z$. *Conform. Geom. Dyn.* **1** (1997), 28-57.

[Ku] Kuratowski, K. *Topology* Vol. 2. Academic Press, New York, 1968.

[KU] Kotus, J. and Urbanski. M. Conformal, Geometric, and Expanding Measures for Transcendetal Expanding Functions. *Math. Ann.* **324** (2002), 619-656.

[Lav] LaVaurs,P. Une Description Combinatoire de l'involution definie par M sur les rationelles a denominateur impaire. *C. R. Acad. Sci. Paris Sér. I Math.* **303** (1986), 143-146.

[Lee] Lee, E. The Structure and Topology of the Brjuno Numbers. *Proc. 1999 Topology and Dynamics Conference.* **24** (1999), 189-201.

[LS] Lau, E. and Schleicher, D. Internal Addresses in the Mandelbrot Set and Irreducibility of Polynomials. *SUNY Stony Brook Institute for Mathematical Sciences* Preprint #1994–19.

[Ly] Lyubich, M. Measurable Dynamics of the Exponential, *Soviet Math. Dokl.* **35** (1987), 223-226.

[Ma] Mayer, J. An Explosion Point for the Set of Endpoints of the Julia Set of $\lambda \exp(z)$. *Erg. Thy. and Dyn. Syst.* **10** (1990), 177-184.

[Mil] Milnor, J. Dynamics in One Complex Variable. Princeton University Press, 2006.

[McM] McMullen, C. Complex Dynamics and Renormalization. Princeton University Press, 1994.

[McM1] McMullen, C. Area and Hausdorff Dimension of Julia Sets of Entire Functions. *Trans. A.M.S.* **300** (1987), 329-342.

[Mo] Moser, J. Stable and Random Motions in Dynamical Systems. Princeton: Princeton University Press, 1973.

[MR] Mayer, J. and Rogers, J. T. Indecomposable Continua and the Julia Sets of Polynomials. Preprint.

[N] Nevanlinna, R. Über Riemannsche Flächen mit endlich vielen Windungspunkten. *Acta Math.* **58** (1932).

[Pi] Piranian, G. The Boundary of a Simply Connected Domain. *Bull. Amer. Math. Soc.* **64** (1958), 45-55.

[PM] Pomeau, Y. and Manneville, P. Intermittent Transition to Turbulence in Dissipative Dynamical Systems. *Commun. Math. Phys.* **74**, 189-197 (1980).

[PR] Petersen, C. and Ryd, Convergence of Rational Rays in Parameter Spaces, *The Mandelbrot set: Theme and Variations*, London Mathematical Society, Lecture Note Series 274, Cambridge University Press, 161-172, 2000.

[Prz] Przytycki, F. Riemann Map and Holomorphic Dynamics *Invent. Math.* **85** (1986), 439-455.

[Re] Rees, M. The Exponential Map is Not Recurrent. *Math. Zeit.* **191** (1986), 593-598.

[Si] Singer, D. Stable Orbits and Bifurcations of Maps of the Interval, *SIAM J. Appl. Math.* **35** (1978), 260-267.

[SZ] Schleicher, D. and Zimmer, J. Escaping Points of Exponential Maps. *J. London Math. Soc.* **67** (2003), 380-400.

[Sc] Schleicher, D. Hyperbolic Components in Exponential Parameter Space. Preprint.

[Sm] Smale, S. Diffeomorphisms with Many Periodic Points. *Differential and Combinatorial Topology.* Princeton University Press, 1964, 63-80.

[Sta] Stallard, G. The Hausdorff Dimension of Julia Sets of Entire Functions. *Ergodic Theory and Dyn. Sys.* **11** (1991), 769-777.

[Sta1] Stallard, G. Entire Functions with Julia Sets of Zero Measure. *Math. Proc. Cambridge Philos. Soc.* **108** (1990), 551-557.

[Ste] Steinmetz, N. Rational Iteration: Complex Analytic Dynamical Systems. De Gruyter, Berlin, 1993.

[Su] Sullivan, D., Quasiconformal Maps and Dynamical Systems I, Solutions of the Fatou-Julia Problem on Wandering Domains. *Ann. Math.* **122** (1985), 401-418.

[V] Viana, M. The Differentiability of the Hairs of $\exp(z)$. *Proc. Amer. Math. Soc.* **103** (1988), 1179-1184.